Vol. 29 No. 8 August 1978

Journal of the Society of Cosmetic Chemists

Contents

ORIGINAL PAPERS

DEPARTMENTS

the Fragrance Achievers

Let our 85 years of experience and modern technology create a wondrous fragrance for you.

Write for free informative booklet: "The Language of Perfumery." Ungerer & Company, 161 Avenue of the Americas, New York, N.Y. 10013.
ATLANTA • BOSTON • CHICAGO • LOS ANGELES • PHILADELPHIA • SAN FRANCISCO • ST. LOUIS • LONDON, ENGLAND • MEXICO CITY

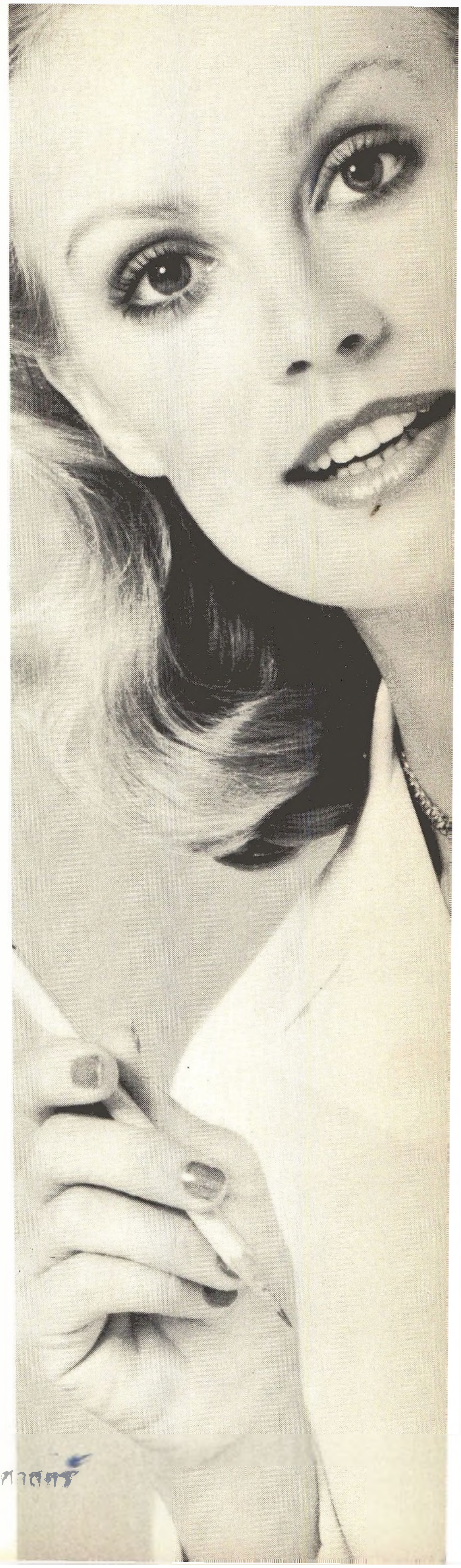

Journal of the Society of Cosmetic Chemists®
VOLUME 29 • NUMBER 8
AUGUST 1978
Published by the Society of Cosmetic Chemists

Editor: **John J. Sciarra**, Arnold and Marie Schwartz College of Pharmacy and Health Sciences, Long Island University, 75 DeKalb Ave. at University Plaza, Brooklyn, NY 11201
Associate Editor: **Leszek J. Wolfram**, Clairol, Inc., 2 Blachley Rd., Stamford, CT 06902
Editorial Assistant: **Susan W. Cole**, 50 E. 41st St., New York, NY 10017
Publications Committee Chairman: **Ralph Sorrentino**, Onyx Chemical Co., 190 Warren St., Jersey City, NJ 07302
Business Manager: **Hamilton C. Carson**, 26 Lake St., Box 555, Ramsey, NJ 07446
Advertising Manager: **Robert E. Doris**, 76 Ninth Ave., New York, NY 10019
Business Administrator: **David B. Martin**, 50 E. 41st St., New York, NY 10017
British Editorial Office: Society of Cosmetic Chemists of Great Britain, 56 Kingsway, London, WC2 B 6 DX, Great Britain
German Editorial Office: **Otto Salzmann**, Loewen Strasse 52, D-2000 Hamburg 20, West Germany
Editorial Committee: **John J. Sciarra, Chairman, Gabriel Barnett, Carl W. Bruch, John H. Butala, Robert T. Connor, Roger K. Curtis, Kenneth I. Damer, Jr., Maison G. de Navarre, Chester de Zeih, Carl Felger, Paul Finklestein, Terry Gerstein, Laurence Greenspan, Eric Jungerman, E. J. Karolyi, Albert M. Kligman, Winthrop E. Lange, Irving Levenstein, Edward F. Levy, O. J. Lorenzetti, Robert Marchisotto, Francis N. Marzulli, John Menkart, R. A. Parent, Gerald S. Roye, Hosny Y. Saad, Paul A. Sanders, Harry C. Saunders, Ralph Shangraw, Frank Tranner, Charles O. Ward, Alfred Weissler, Richard H. Wildnauer, Ann M. Wolven, John H. Wood**

OFFICERS FOR 1978

President: **Phyllis J. Carter**, ICI Americas Inc., Wilmington, DE 19897
Chairman of the Board: **Dr. Karl Laden**, Carter Products Div., Half Acre Road, Cranbury, NJ 08512
President-Elect: **Dr. John J. Sciarra**, Arnold and Marie Schwartz College of Pharmacy and Health Sciences, Long Island University, 75 DeKalb Ave. at University Plaza, Brooklyn, NY 11201
Secretary: **Virginia R. Kickertz**, Avon Products, Inc., 1 Division Street, Suffern, NY 10901
Treasurer: **Dr. Carl B. Felger**, Gillette Res. Labs., 1413 Research Blvd., Rockville, MD 20850

Subscriptions: JOURNAL OF THE SOCIETY OF COSMETIC CHEMISTS is published seven times per year, in February, March, May, August, September, November and December, in the U.S.A., with additional issues published in Great Britain. Yearly subscription price is $60.00.

© Copyright 1978 by the Society of Cosmetic Chemists.

JOURNAL OF THE SOCIETY OF COSMETIC CHEMISTS is a registered trademark of the Society of Cosmetic Chemists.

Missing Numbers: Because of uncertain and hazardous conditions, claims for missing numbers can be entertained only from subscribers in the country of origin of the particular issue and must be made within 30 days from date of issue.

Change of Address: Members and subscribers are urged to give notice of change of address to the office of the Society, 50 E. 41st St., New York, NY 10017.

Responsibility for Statements Published: The Society of Cosmetic Chemists, the Committee on Publications and the Board of Directors assume no responsibility for statements or opinions advanced by contributors to this Journal.

Editors and Publishers: Abstracts or digests of articles not exceeding 400 words may be published, duly credited to the author and JOURNAL OF THE SOCIETY OF COSMETIC CHEMISTS. Reprinting or more extensive copying (whole pages or articles) are forbidden, except by special permission, in writing, from the Chairman of the Publications Committee.

Authors: When using illustrations or quotations taken from copyrighted publications, authors must get written permission from the copyright holder to reproduce the same.

Manuscript: Manuscripts should be prepared in accordance with the "Directions for the Preparation of Manuscripts," copies of which are available from Dr. John J. Sciarra, Arnold and Marie Schwartz College of Pharmacy and Health Sciences, Long Island University, 75 DeKalb Avenue at University Plaza, Brooklyn, NY 11201.

Second-class postage paid at New York, New York and additional mailing offices.

Publication Office: 50 E. 41st St., New York, NY 10017

ห้องสมุด กรมวิทยาศาสตร์
21 [illegible]

INNOVATORS

ou know them.

he **first** with
e **freshest**
fashions.
he women
nd the men
ho set the
ace and style
e others
mulate.

ou know other
novators.

erry Fragrances.

reators of
ew and
xciting nuances
at start
riginal trends,
deas and fashions.

PERRY

MEMBER RIFM

PERRY BROTHERS
FRAGRANCES
creators & manufacturers
61-12 32nd AVENUE • WOODSIDE, NEW YORK 11377 • (212) 932-1200
Offices in Principal Cities

Division of
Mallinckrodt ®

Mirapol A-15 polymer with amphoteric-anionic surfactants

Mirapol A-15 is the highest active cationic polymer available that is pourable. In shampoos it acts as a coupling agent between fatty anionic surfactants and the hair. It is a moisturizer for skin and hair as well as being easier and more economical to use than other polymers.

Mirapol A-15 confers excellent hair manageability, reduction of static, wet and dry combability and, like all Miranol products, is safe, non-toxic and non-irritating.

We invite you to send for our Technical Data Sheet.

Miranol
CHEMICAL COMPANY, INC

277 COIT STREET • IRVINGTON, N. J. 07111
PHONE: Area Code 201 • 399-7000
Agents in principal cities throughout the world

MIRANOL CHEMICAL COMPANY
277 COIT STREET • IRVINGTON, N.J. 07111

Please send your Technical Data Sheet on
Mirapol A-15 ....
....
NAME ....
TITLE ....

Please attach to your letterhead

Substitutes are a sad excuse for Dowicil 200 preservative.

It's downright sad how a fresh face can be ruined by cosmetics gone stale. There's far less chance of that happening with proper use of DOWICIL* 200 preservative. Effective at low concentrations, too? You bet. It's two to eight times more effective than almost any other shelf preservative. This means pseudomonas and other microorganisms won't be making your well-designed makeup old before its time.

DOWICIL 200 is compatible with common formulation components also, including nonionic emulsifiers. And it has a favorable toxicity profile, supported by tox data, and is fully registered. (EPA-464-375 and on FDA Master File).

Where else can you use DOWICIL 200? Glad you asked. Hand creams, face creams and hair dressing. Shaving products, suntan products, shampoos, dermatologicals and waterless hand cleansers. Surgical scrubs and topical steroid ointments, too.

So come on. Help those who buy your cosmetics put on a happy face. Talk to your Dow representative soon. Designed Products Department, Midland, MI 48640.

DOW

DOW CHEMICAL U.S.A.

*Trademark of The Dow Chemical Company

Why top brands use Sonneborn white oils and petrolatums.

List the leaders for any drug or cosmetic product category using white oils or petrolatums. Chances are overwhelming that the Sonneborn Division of Witco will be a major supplier to all.

Total commitment.

We lead the industry in our complete dedication to these products. For example, we already have the world's largest capacity for white oils and petrolatums, and have a major expansion under way.

Exceptional purity.

Purchasing these products to a standard specification is not enough. There are major reliability factors to consider. For white oils it's the ability to deliver exceptional purity along with a total absence of odor and color again and again. For petrolatums absence of odor plus rich emollience and smooth velvety texture must be part of the buy. Again and again. For both products Sonneborn has a longer record of reliability than anyone.

The best service.

Witco has a team in place whose major concern is these products alone. So we can be most responsive when you need help with handling or technical aspects of product quality or development.

Sonneborn Division.

For more details contact:
Witco Chemical Corporation,
Sonneborn Division, Dept. D5,
277 Park Ave., New York, N.Y.
10017. Or call (212) 644-6498.

Witco

SCC Employment Service

As a service to its members, the Society of Cosmetic Chemists will accept and keep on file the detailed resume of any member looking for a position. We also provide, upon request, a listing of positions available.

If you are looking for a new job, or know of an opening in your company, please contact

Constance Hamilton
Society of Cosmetic Chemists
50 East 41st Street
New York, NY 10017
(212) 539-8611

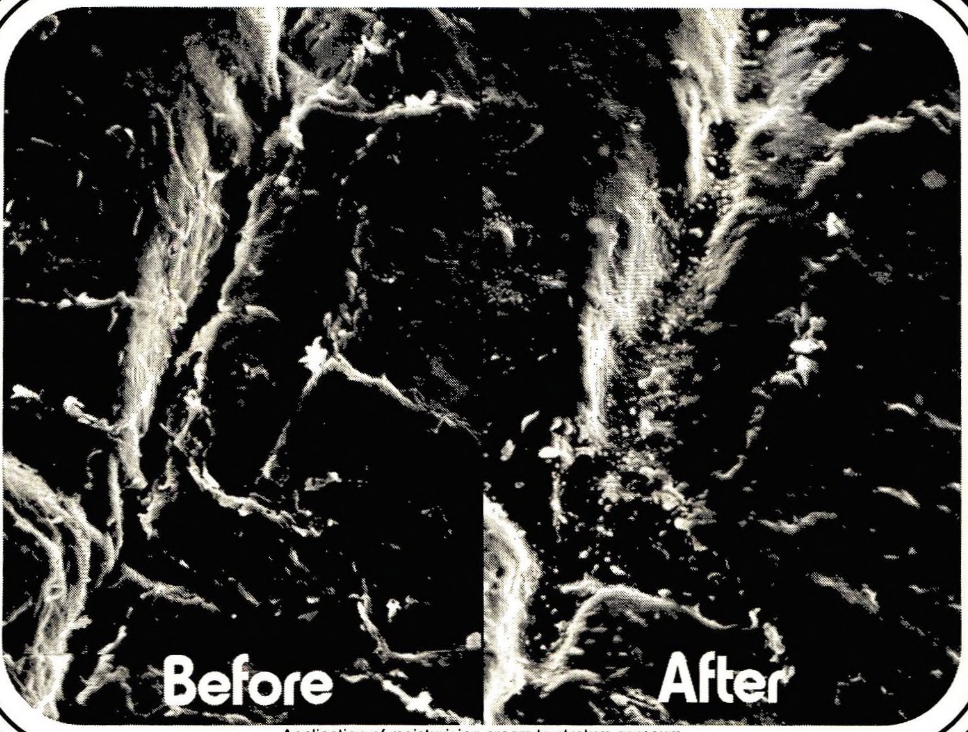
Before
After

SOCIETY OF COSMETIC CHEMISTS ANNUAL SCIENTIFIC MEETING

November 30
and
December 1, 1978
The Waldorf-Astoria Hotel
New York, New York

Program will feature:

- 14 Scientific Papers covering research on Nitrosamines, Hair Care, Skin Care and Microbiology/Preservation
- A simultaneous educational workshop, "Over the Counter Review—Its Impact on New Product Development"
- Frontiers of Science Lecture
- Recipients of SCC Scholarships will present papers
- Medal Award Dinner Dance

Program Co-Chairmen
Robert L. Raymond
Dr. Peter Sgaramella

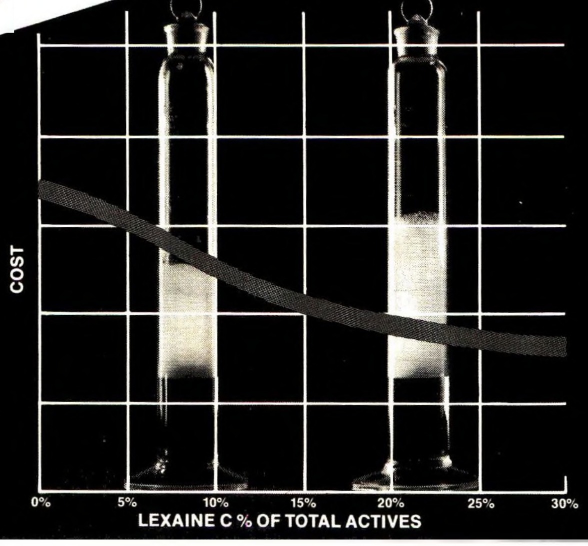
COST
0%
5%
10%
15%
20%
25%
30%
LEXAINE C % OF TOTAL ACTIVES

HYDROLYZED ANIMAL PROTEIN. YOU'RE SEEING IT MORE AND MORE...

...because protein's moisture binding, film forming, stabilizing and conditioning effects are real!

In today's competitive market place, product claims must match consumer perception. The FTC just won't have it any other way.

It's our contention that the inclusion of protein in your shampoos, conditioners and skin treatment products is one of the easiest ways to provide *perceptible* performance. This is why hydrolyzed animal protein is appearing on the ingredient listing of so many cosmetics and toiletries...and pretty high up at that.

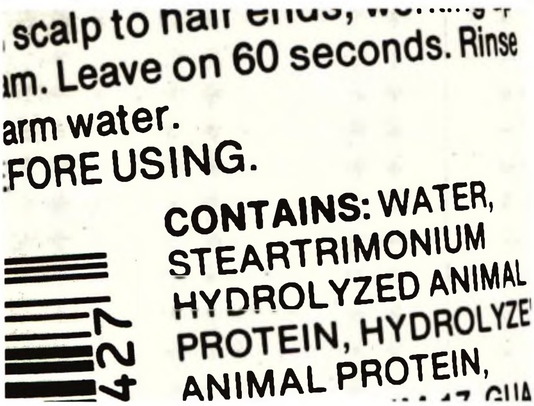

scalp to hair ends,
m. Leave on 60 seconds. Rinse
arm water.
FORE USING.
CONTAINS: WATER,
STEARTRIMONIUM
HYDROLYZED ANIMAL
PROTEIN, HYDROLYZE
ANIMAL PROTEIN,

Crotein Q. Croda's advanced protein research has created a unique molecule by grafting a quaternary ammonium group directly on a functional protein skeleton. The quat groups that have been added are more intensely cationic than the amino groups they replace, so that Crotein Q will bind more tightly anionic groups such as the carboxyl groups of skin and hair. Most importantly, Crotein Q retains its positive charge even at alkaline pH's at which amino groups will have lost their substantivity.

But you don't have to be a post-doctoral fellow in organic chemistry to specify protein performance, just remember these names for the broadest range of these versatile materials: **CROTEIN, CRODYNE AND COLLASOL** from Croda—of course!

Croda

Crotein SPC, SPA, SPO (molecular weight 10,000—1,000), Crodyne BY-19 (molecular weight 25,000), Crotein H CAA Amino Acid Mixtures (molecular weight 100), Collasol Whole Soluble Collagen (molecular weight 300,000)

Croda Inc., 51 Madison Avenue, New York, New York 10010 (212) 683-3089

SYNOPSES FOR CARD INDEXES

The following synopses can be cut out and mounted on 3 x 5 index cards for reference, without mutilating the pages of the Journal.

Fractography of human hair: G. H. Henderson, G. M. Kay and J. J. O'Neill. *Journal of the Society of Cosmetic Chemists* 29, 449 (August 1978)

Synopsis—Scanning electron microscopy and optical microscopy show that when human hair is extended in water the cuticle usually suffers multiple circumferential fracture with local separation from the cortex before the latter fractures. The cortex fracture is typically smooth and perpendicular to the fiber axis. In the dry state the fracture is more irregular indicating axial splitting of the cortex before or during fracture without prior failure of the cuticle. Except for the cuticle—cortex separation which occurs in wet extension, fracture surfaces do not show a strong tendency to follow cell boundaries.

Stiffness of human hair fibers: G. V. Scott and C. R. Robbins. *Journal of the Society of Cosmetic Chemists* 29, 469 (August 1978)

Synopsis—The stiffness of component fibers is known to be important to the behavior of a fiber mass, but measurements are lacking in the cosmetic literature probably because of experimental difficulties with published methods. Recognizing this, we devised a simple method to compare fibers for stiffness. A fiber with a small weight on each end is draped over a wire and the distance ("D") between the vertical legs is measured. Fibers with a wide range of thicknesses clearly showed that values of "D" relate linearly to cross-sectional areas, as expected of "stiffness." This prompted a theoretical study which yielded equations in terms of "D" for calculating, e.g., elastic bending moduli and shapes of hanging fibers. Empirical and theoretical guides are given for selection of wire diameter and fiber weights. The average elastic modulus for bending fibers, assumed round in cross section, is approximately equal to that for stretching the same fibers. Fiber stiffness is affected by humidity and chemical treatments but is relatively unaffected by shampoos.

Über die beeinflussung der anaeroben bakterienflora im talgdrüsenausführungsgang durch eine äthyllactatund äthanolhaltige filmmaske und eine antimikrobielle tensidlösung: M. Gloor, W. Wolf and M. Franke. *Journal of the Society of Cosmetic Chemists* 29, 487 (August 1978)

Synopsis—A group of 15 healthy male subjects was treated with a face mask containing 1% ethyl lactate and 50% ethanol, while a matched group was treated with an antimicrobial surfactant solution with Aromox DMMCDW and Elfan NS242. The left side of the forehead was used as the test area, and a similar active agent free mask and a non-antimicrobial surfactant solution was applied to the right side of the forehead of each individual. Before the start of the treatment and 24 hours after the treatment the number of saprophytic bacteria in the pilosebaceous ducts was analyzed with the aid of a special anaerobic technique. The mask containing ethyl lactate and ethanol caused a significant reduction in the total bacteria and in the propionibacteria counts. The antimicrobial surfactant solution effected a significant decrease in the total bacteria count but did not alter the propionibacteria count. The results indicate that the test mask is an effective acne treatment. The efficacy of the treatment with the surfactant solution has not yet been determined.

Cosmetic properties and structure of fine-particle synthetic precipitated silicas: S. K. Wason. *Journal of the Society of Cosmetic Chemists* 29, 497 (August 1978)

Synopsis—Submicron-fine particle, synthetic silicas are of three types: fumed silicas, silica gels and precipitated silicas. Recent research has led to the synthesis of a wide variety of new controlled-structure, functional-precipitated silicas which exhibit unique cosmetic and dentifrice properties. The end-use applications of the precipitated silicas can be controlled by controlling their structure. It is now possible to make predictions regarding the thickening, viscosity building, humectant demand index, dentifrice abrasive and polishing characteristics of the new class of synthetic, precipitated products. The methods of preparation, the chemistry, the structure and the new cosmetic applications of the precipitated products are discussed.

J. Soc. Cosmet. Chem., **29**, 449–467 (August 1978)

Fractography of human hair

G. H. HENDERSON, G. M. KARG and J. J. O'NEILL
Avon Products, Inc., Suffern, NY 10901.

Received July 30, 1976. Presented at 9th IFSCC International Congress, June 1976, Boston, Massachusetts.

Synopsis

Scanning electron microscopy and optical microscopy show that when HUMAN HAIR is extended in water the cuticle usually suffers multiple circumferential FRACTURE with local separation from the cortex before the latter fractures. The cortex fracture is typically smooth and perpendicular to the fiber axis. In the dry state the fracture is more irregular indicating axial splitting of the cortex before or during fracture without prior failure of the cuticle. Except for the cuticle–cortex separation which occurs in wet extension, fracture surfaces do not show a strong tendency to follow cell boundaries.

INTRODUCTION

Scanning electron microscopy has been applied extensively to the study of human hair topography. Applications have ranged from studies of pathological conditions (1–3) to assessment of the effects of normal weathering and grooming (4) and of cosmetic treatments (5, 6). More recently there have been reports of direct observation of the response of hair to mechanical stresses applied by means of apparatus specially designed to manipulate hair in the specimen chamber of the microscope in modes simulating a variety of grooming operations such as brushing and backcombing (7, 8).

In this paper we report results of a more conventional study of the topography of hair after tensile strain in different environments and after different pretreatments. We discuss our observations with reference to the known histology and chemistry of hair and the expected response to factors such as hydration and age.

MATERIALS AND METHODS

Natural brown European hair was obtained from DeMeo Brothers, New York, New York. With the single exception of the study of fracture type versus age, this hair was used throughout. For the latter study, hair samples were obtained from a young woman with long (approximately 50 cm), light brown virgin hair. The hairs were plucked or snipped at a distance not exceeding 1 cm from the scalp.

Bleaching with potassium persulfate/hydrogen peroxide was done in alternating 1- and 2-hr intervals to give 3- and 6-hr bleached hair. Fresh solution was introduced at the end of each interval. Hairs fractured in solvents were soaked a minimum of 16 hr before Instron testing. Variation in pH was accomplished by addition of acetic acid or ammonium hydroxide. It was noted after 16 hr that the pH of these systems was not affected by the hair. Relative humidities other than 50 ± 1% (room condition) were obtained for 20, 71, 79 and 90% by using saturated salt systems (9) in capped jars containing sample hanging racks and a fixed post. Samples to be fractured were equilibrated for a minimum of three days at 21 ± 1°C in these chambers. A glycerin/water mixture equivalent to a water activity of 50% RH was prepared using 22.5% water and 77.5% anhydrous glycerin by weight.

Stress/strain measurements on hairs were made on a Model TT-B Instron Tester. Hairs were mounted in special holders of stainless steel with chamfered holes and secured with tapered Teflon plugs. The working length was 12.7 mm and most experiments were done at a constant rate of extension of 200%/min. Some determinations were made at one-tenth this speed (20%/min).

Hairs run in the humidity chambers were fixed between small screw clamps to provide the desired working length and suspended between a hook on the Instron and the fixed post in the chamber. The hook extended down through a small hole in the cover. The screw clamp subjected the hair to a 2- to 3-g stress during the conditioning period which was ignored since the resulting extension is negligibly small.

The hairs were viewed in a Coates and Welter Cwik Scan Model 100-2 Field Emission Scanning Electron Microscope. Prior to viewing, the hairs were sputter coated with gold/palladium in a Denton DV-515 Evaporator equipped with a Model DSM-1 Sputtering Module. The sputtering was done at 10 mA and 150 millitorr for 1.5 min in intervals of 30 sec.

For SEM viewing the hairs were mounted perpendicular to the surface of a standard Coates and Welter specimen stub. The length of hair exposed below the fracture varied but was generally of the order of 1 mm. Both sides of the fracture were examined in all cases.

The optical microscopy was carried out on hairs immersed in a dish of water on the stage of a Zeiss Universal Photomicroscope. The hairs were mounted on a Hoffmann hose clamp modified to permit use of the screw-driven bearings to stretch the specimen.

RESULTS

WET FRACTURE

The fracture surfaces of virgin hairs broken under water are often quite flat as shown in Figure 1. Here it appears that the fracture started at a small zone on the edge of the fiber and radiated from there in a plane perpendicular to the axis. Such detailed evidence of fracture propagation is seldom seen but, in general, the new surface is remarkably devoid of evidence of the cellular and subcellular fibrous structure of hair; the fracture pattern is much more similar to the brittle fractures of glass or carbon (10) than to the fracture patterns of other natural fibers such as cotton (11).

The cuticle fracture is also planar and perpendicular to the fiber axis and again evidence of cellular structure is lacking; there is little sign of delamination or axial slippage of the

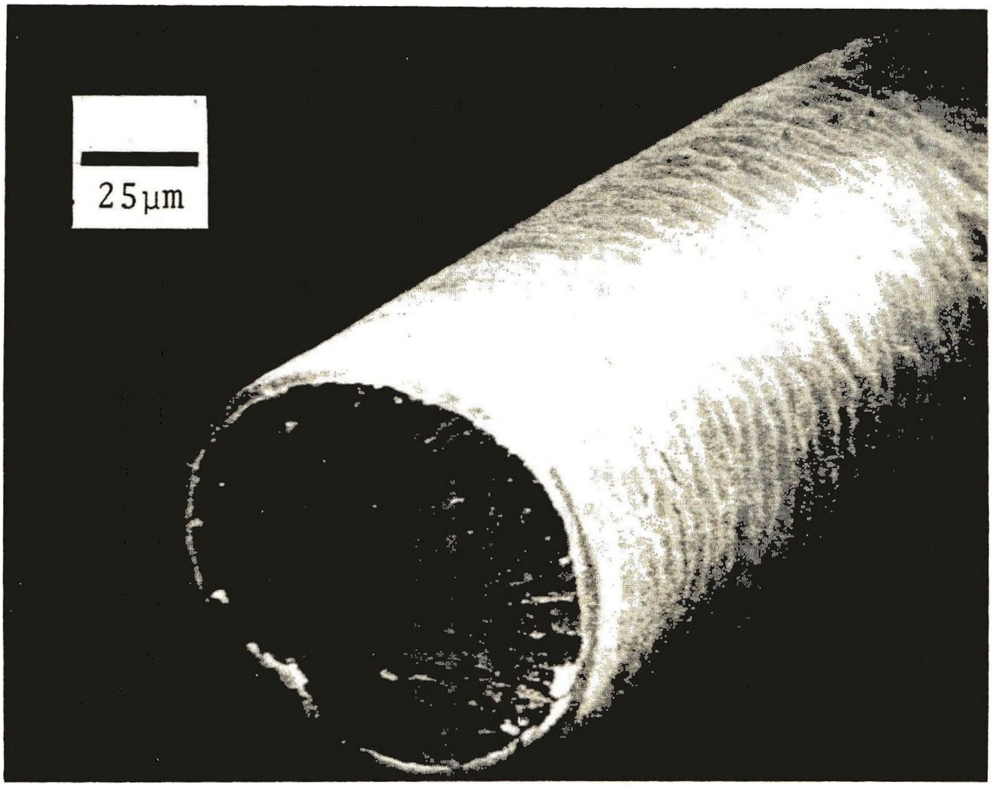

Figure 1. Fracture of natural brown hair in water

cuticle cells. At about a quarter of the fiber diameter from the fracture plane it can be seen that the cuticle has cracked circumferentially; this too is typical of the wet fracture pattern.

In Figure 1 the break fits Brown and Swift's description (7) "almost as if cut with a knife." In a few cases, however, we observed wet fractures like that in Figure 2a where there is a gross mismatch of the fracture planes of the cuticle and cortex. A gap between cuticle and cortex can be seen in Figure 2b. Figure 2c is the opposing fracture surface which is complementary to the first. Here there is much clearer evidence of another circumferential failure of the cuticle far from the fracture surface. Such fractures of the cuticle were frequently observed several diameters from the fracture surface, as seen in Figure 3.

Although such cuticle fractures might have occurred at the instant of failure, the more intriguing possibility is that the cuticle fails well before the cortex. Two types of experiment proved that this is indeed the case. First, hairs that were extended in water to just short of failure, relaxed in water and then dried and examined in the SEM showed many cracks like those in Figure 3. Second, when hairs were extended incrementally in water and examined in the polarizing microscope it was evident in some cases, as shown in Figure 4, that at least part of the cuticle had ruptured. In Figure 4a the rupture lines are clearly seen in top focus against the bright corticle matter between slightly uncrossed polars. In Figure 4b at edge focus in the same view it can be seen that


2a
25µm

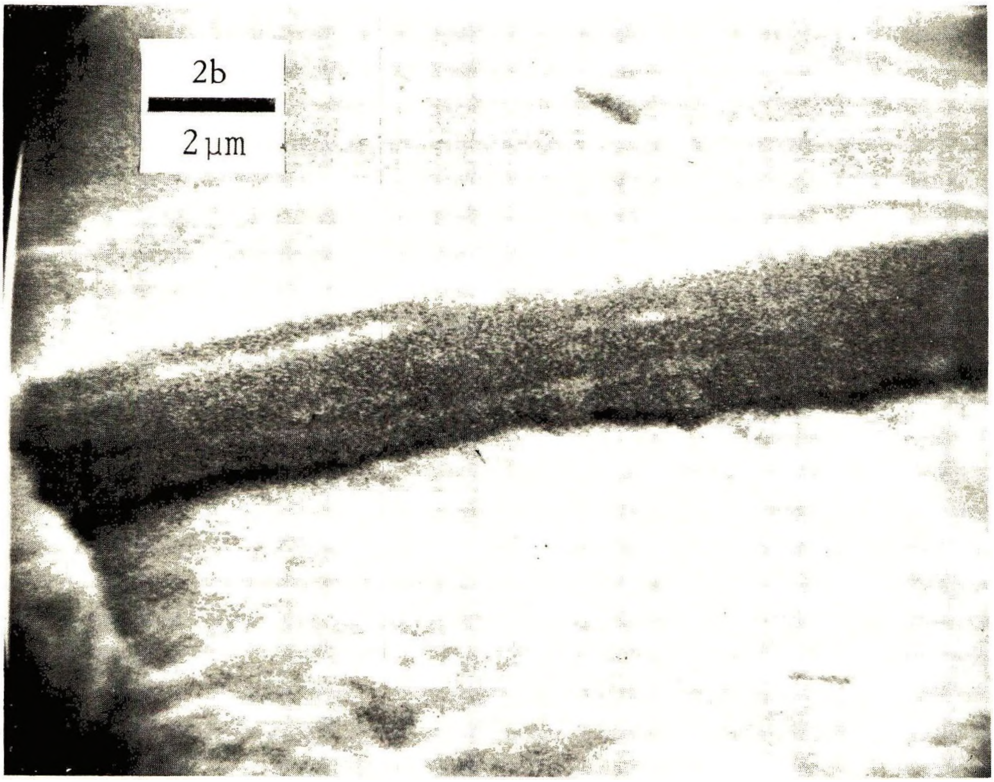
2b
2µm

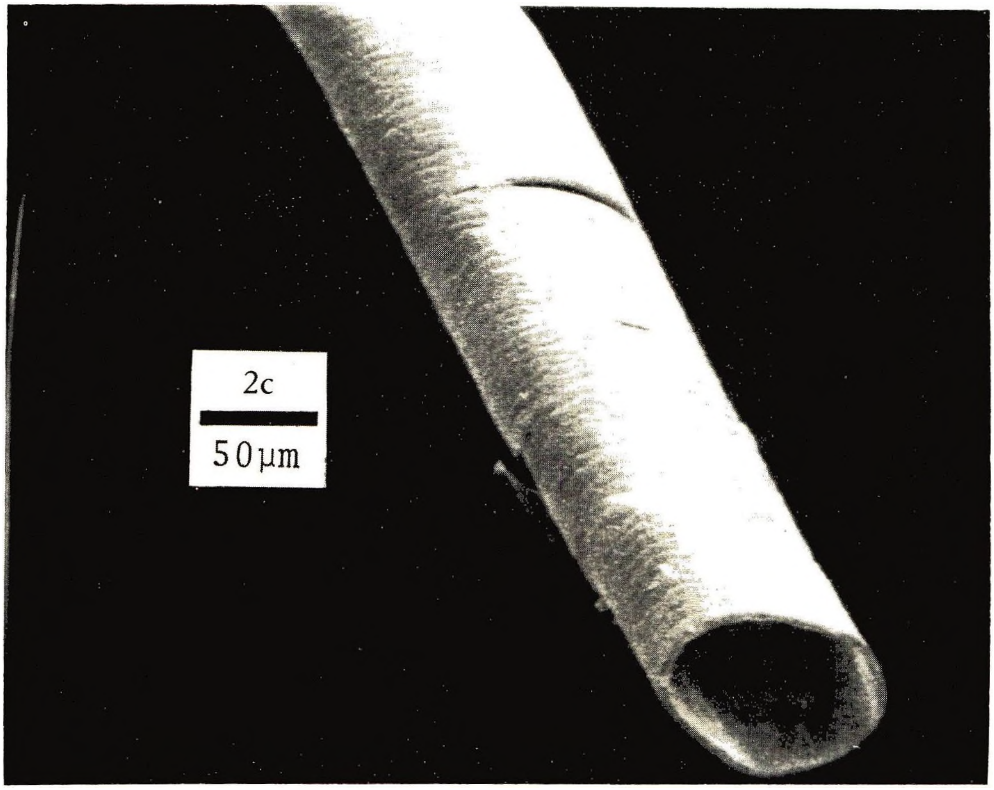

Figure 2. Sleeve-type break of natural brown hair in water showing (a) cortical plug, (b) cuticle fracture on plug showing separation from cortex and (c) cuticle sleeve

near the fracture lines the broken cuticle is flaring away from the fiber; this is seen more clearly in Figure 4c.[1]

Figure 5a is an electron micrograph of the hair in Figure 4c after drying in the extended state. The cuticle flaring is seen again as well as grossly degenerated subcellular cuticle fragments which seem to be barely attached to their substrate. Figure 5b at higher magnification shows that the cortex is exposed between the flares and it also shows details of the spongy surface of the disrupted scales lying on what would seem to be an otherwise normal cuticle surface.

DRY FRACTURE

The fracture surfaces of hairs broken in air at 50% RH are generally more ragged than those of hairs broken in water. Figures 6a and 6b show two of the many types of breaks

---

[1] Although the lower extensibility of cuticular tissue was reported in Alexander and Hudson, "Wool, Its Chemistry and Physics," Chapman & Hall, London, 1954, pp 7 and 12 with prior reference to Reumuth, Klepzig, *Textil-Z.*, 45, 288 (1942), we find that Reumuth in turn cites E. Lehmann, *Melliand Textilber.*, 22, 145 (1941). The Lehmann paper, however, does not contain the attributed illustration contained in Reumuth as well as in Alexander and Hudson. Two other Lehmann papers (in 1943 and 1944) likewise do not. Therefore, we cannot authenticate either the illustration or the experimental conditions under which it was obtained.

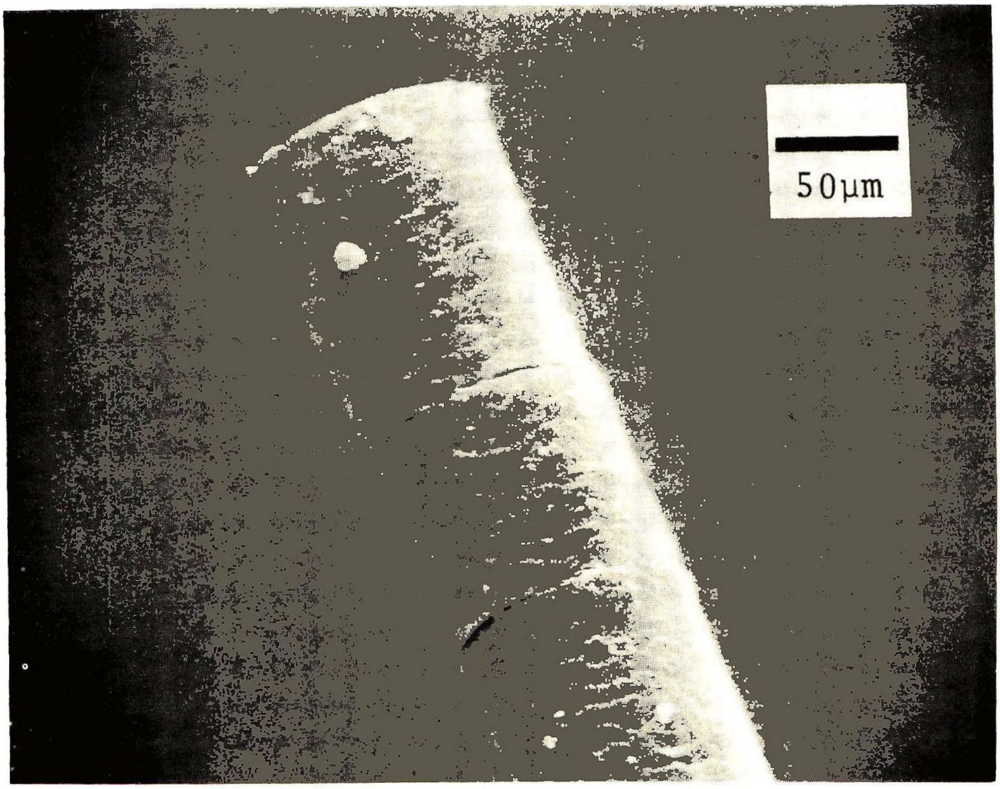

Figure 3. Cracking and buckling of cuticle on natural brown hair broken in water

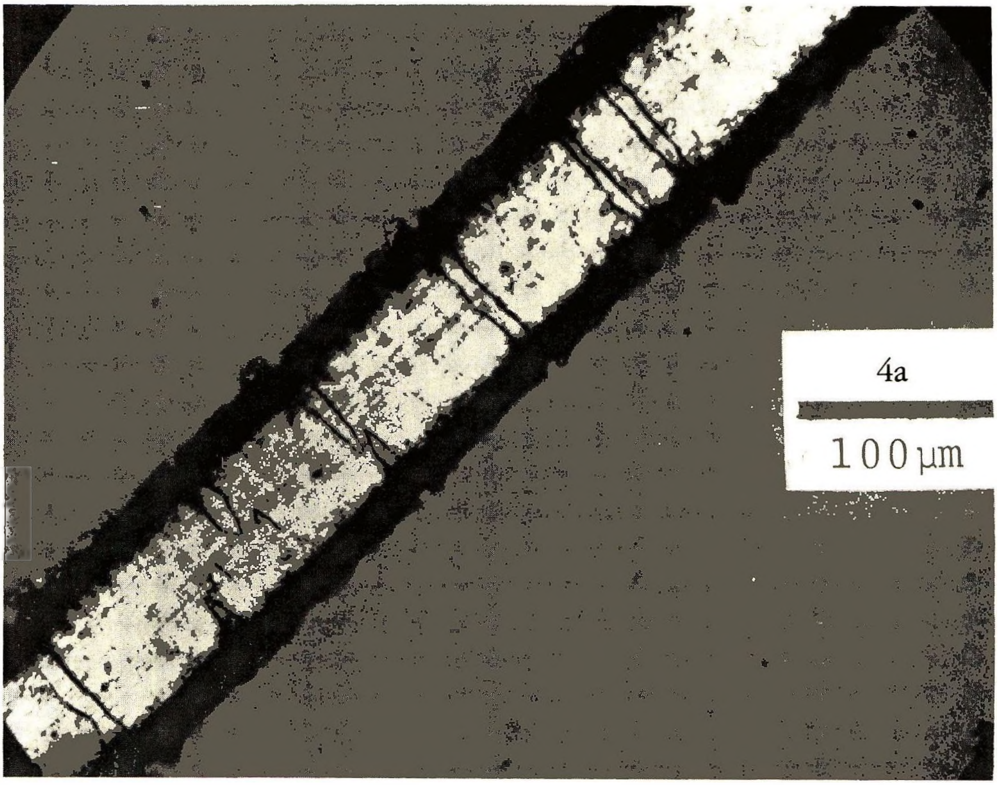

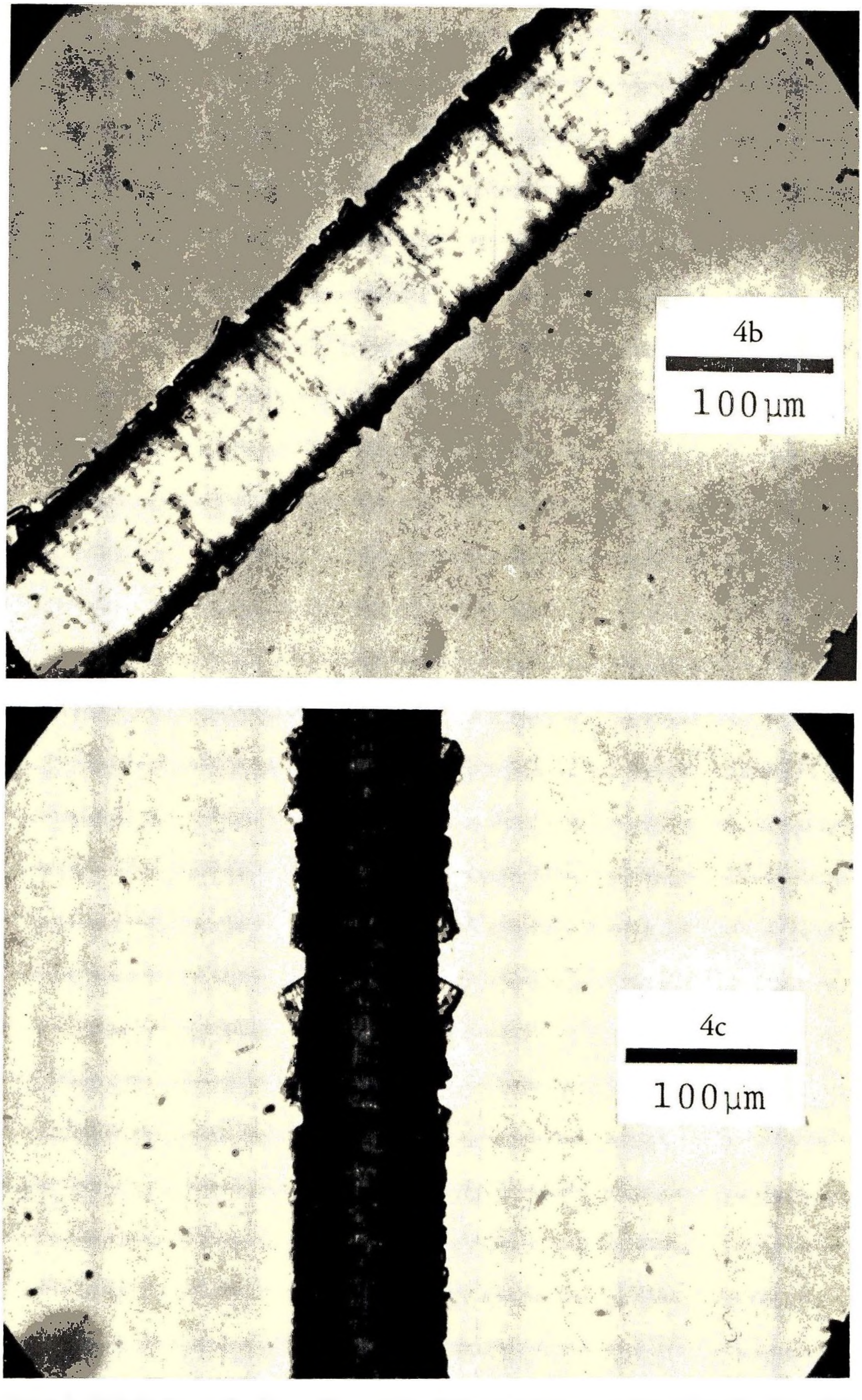

Figure 4. Optical micrographs of natural brown hair at high extension in water, (a) top focus showing cuticle cracks, (b) edge focus showing flaring and (c) extreme flaring at higher extension

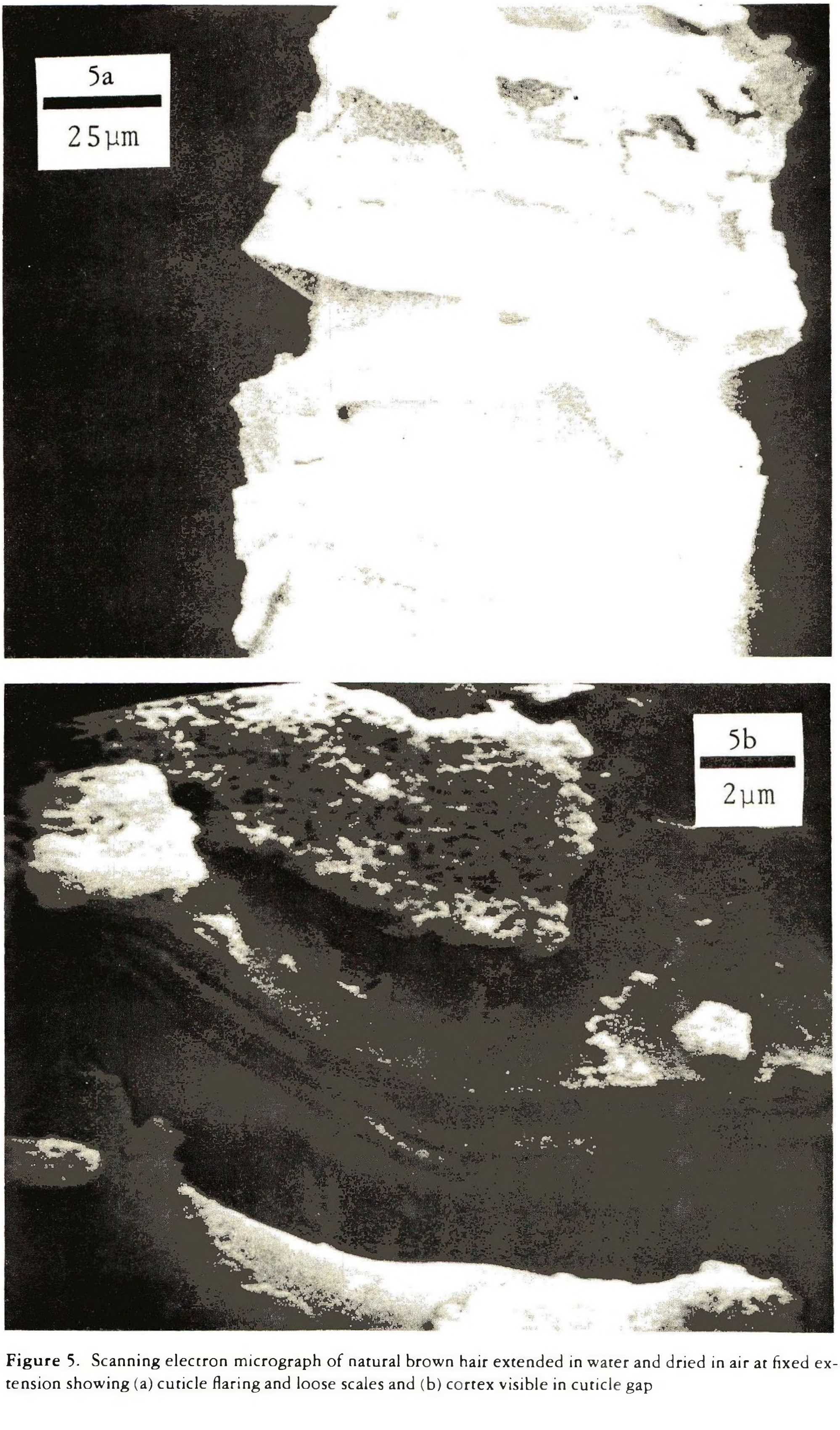

Figure 5. Scanning electron micrograph of natural brown hair extended in water and dried in air at fixed extension showing (a) cuticle flaring and loose scales and (b) cortex visible in cuticle gap

observed with virgin hair under these conditions. A feature common to most dry breaks is that the corticle fracture surfaces are of two kinds: first, flat, smooth surfaces perpendicular to the fiber axis just as in the wet breaks; and second, very rough surfaces in the axial direction revealing details of fibrillation finer than the lateral dimensions of individual corticle cells. Because of the step-like arrangement of the flat radial surfaces these are referred to as step fractures.

In Figure 6b there is an axial crack in the cuticle and more extreme examples of this are shown in Figures 7a and 7b. In dry breaks there is no evidence that the cuticle behaves as a mechanically independent entity; in particular, the cuticle does not split circumferentially as it does in a wet break. Optical examination of a few hairs extended in air revealed no change in the cuticle except possibly a slight uplifting of the distal edges of the scales as the breaking strain was approached.

AGE OF HAIR

Hairs 45 to 50 cm in length, taken from the crown of the scalp of a young woman who had not bleached, dyed or chemically waved her hair, were sampled near the root, the middle and the tip. As expected from observations such as those of Bottoms, Wyatt and Comaish (4), many of the tip sections were found to be partially or totally devoid of cuticle while the mid- and root-section specimens were covered with cuticle and resembled the commercial virgin hair.

Specimens from each section were broken in air at 50% RH and in water. The root- and mid-hair specimens of these hairs behaved very much like the commercial virgin hair; flat breaks with circumferential cuticle cracks were obtained in water, step fractures in air at 50% RH.

The tip sections broke more irregularly under both conditions. In air at 50% RH two out of five specimens were fibrillated completely at the cellular level, the flat step feature being absent altogether as shown in Figure 8. In water, seven out of ten fractures were flat, but three were more like the step fractures typical of dry air breaks.

Although the number of observations is too small to establish a correlation at a high level of confidence, it appears that hairs with more extensively damaged cuticle yield more jagged breaks.

PRE-STRESSED HAIRS

To further study the role of the cuticle in determining fracture type, five virgin hairs that had been hydrated and stretched in water almost to fracture were dried under tension in air and fractured at 50% RH. All five fractures were flat and typical in all respects of a wet break. Hairs pre-stressed almost to break at 50% RH and then broken in water also gave flat fractures.

ENVIRONMENTAL EFFECTS

Virgin hairs conditioned and broken in air at 20, 71 and 79% RH yielded step fractures similar to those obtained at 50% RH, as described above. At 90% RH in air there was a transition to the flat-break pattern obtained in water although circumferential cuticle cracking was absent.

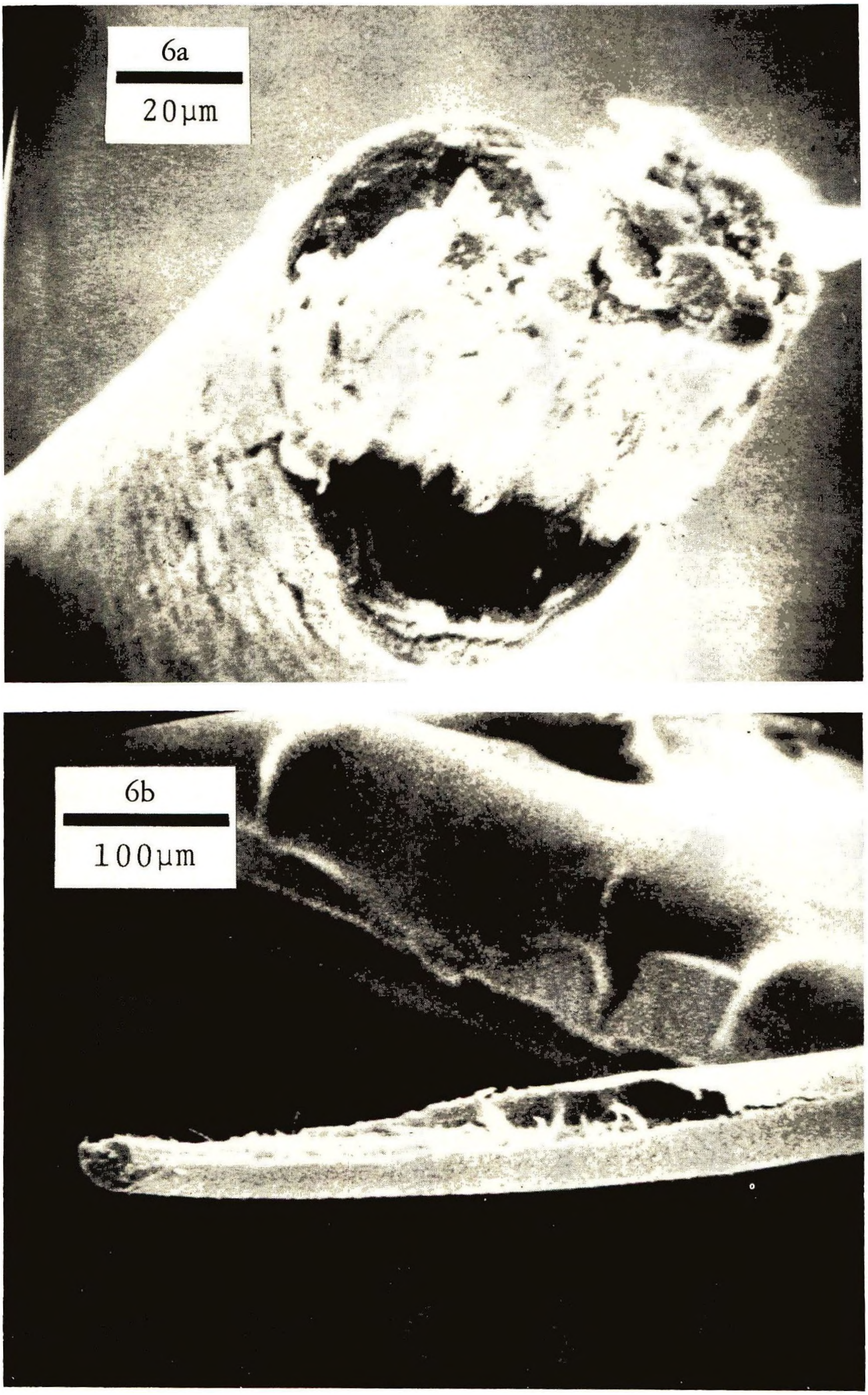

Figure 6. Fractures of natural brown hair at 50% RH in air

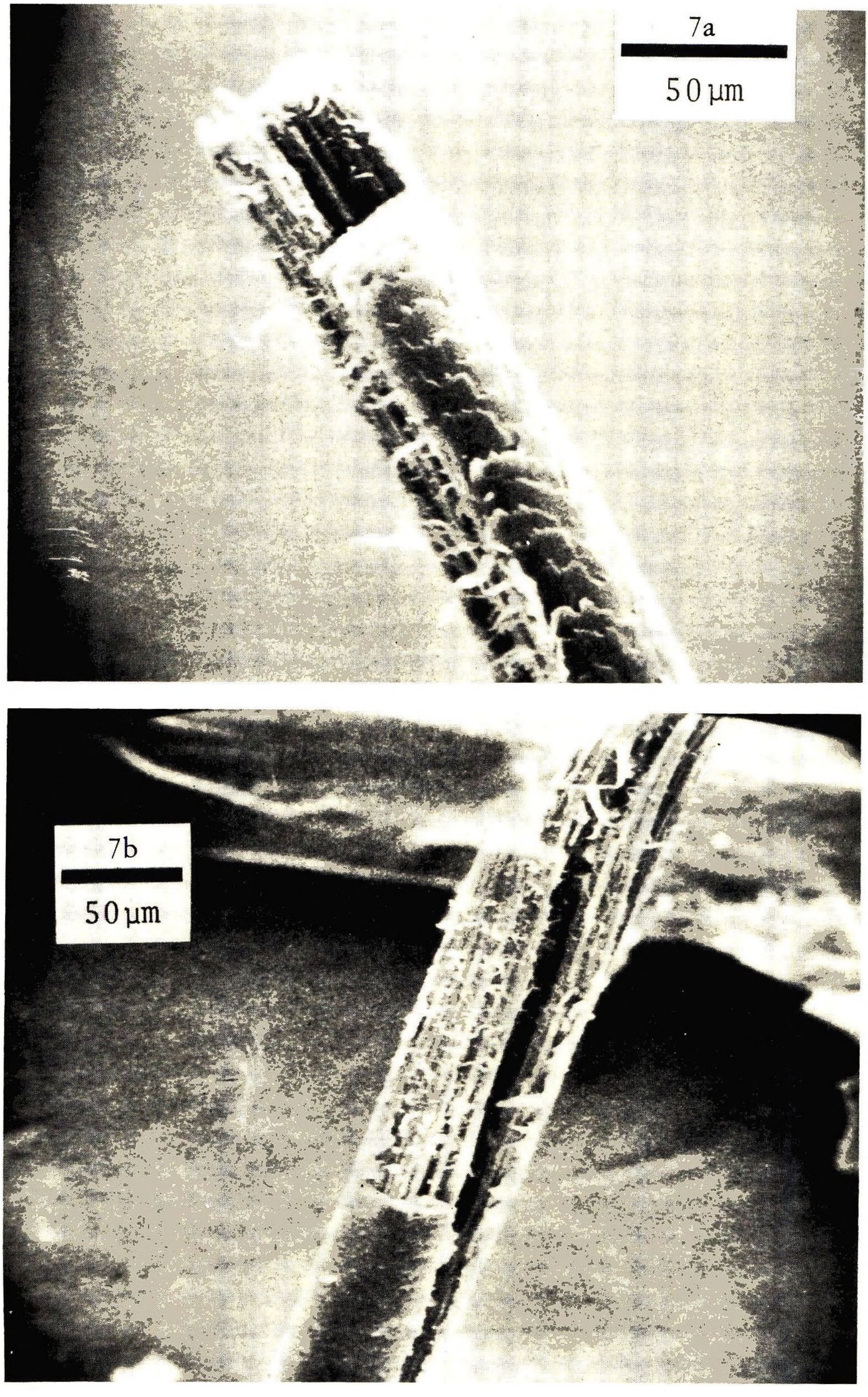

Figure 7. Fractures of natural brown hair at 50% RH in air showing lateral shredding of cortex and axial splits through cuticle

Figure 8. Fracture of aged hair at 50% RH in air illustrating tip-end cortical fibrillation

Hair broken in a water/glycerin mixture equivalent to 50% RH gave flat breaks and this pattern was also obtained in anhydrous glycerin. In anhydrous ethanol and in ethyl acetate the fracture pattern was also more like that obtained in water than in air at 20 to 79% RH in spite of the fact that the hair was not hydrated and gave, as expected, a stress-strain curve like that of dry hair. The sleeve-type break, somewhat like that shown in Figure 2, occurred more frequently than in water but with the significant difference that the annular fracture surface (the surface seen on the protruding plug) was within the cortex, not at the cuticle–cortex junction; this is shown in Figure 9 where it can be seen that the plug tapers into the cortex. The fracture patterns obtained in solvents also differ from those in water in the fact that circumferential cracks in the cuticle do not occur. Although they are superficially similar to breaks in water, breaks in solvents are qualitatively different in detail.

Sodium lauryl sulfate at 3% had no noticeable effect on the fracture pattern relative to that in water, nor did adjustment of pH to 3, 9 and 11.

PRETREATMENTS

Fractographs of hairs bleached for 3 hr and broken in water are shown in Figure 10. The flat-fracture surface of the cortex is like that of virgin hair in water, but the cuticle disruption is much more extensive. Similar results were obtained with hair bleached for 6 hr. At 50% RH in air bleached hair yields step fractures not noticeably

Figure 9. Fracture of natural brown hair in ethyl acetate

different from those of virgin hair. Defatting virgin hair by soaking overnight in 2:1 chloroform/methanol had little or no effect on the fracture pattern in either water or air at 50% RH.

STRESS/STRAIN BEHAVIOR VS. RELATIVE HUMIDITY

Force and elongation measurements were made on natural brown hairs at several relative humidities from 20 to 90%, and also immersed in water. To avoid introducing the variable of hair diameter, the dimensionless ratio of the force at the end of the Hookean region (plateau force) to the break force has been used for comparison of behavior at different relative humidities. This ratio was found to decrease continuously as relative humidity increased, as shown in Figure 11. Also shown is the increase in percentage of elongation at break. The trend is opposite that of the plateau force/break force ratio. Instead of the steady decline exhibited by the ratio data, the percentage-of-elongation trend indicates a change in fracture mechanism above about 80% RH, where a sharp increase in extensibility begins.

DISCUSSION

These studies indicate that there are qualitatively distinct mechanisms involved in the tensile fracture of wet and dry virgin hair. In wet fracture we have observed the cuticle

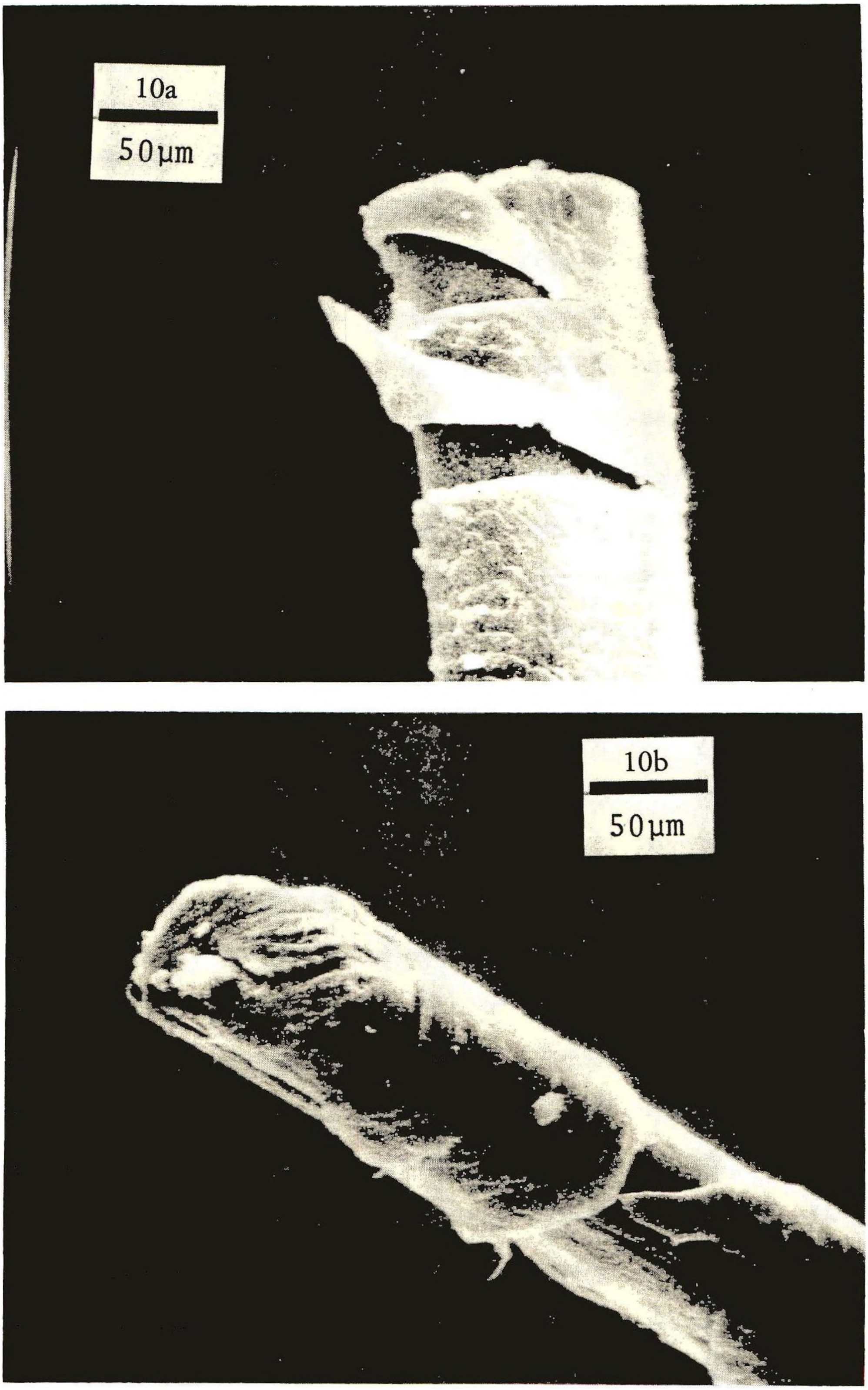

Figure 10. Fractures of 3-hr bleached hair in water showing cuticle peeling

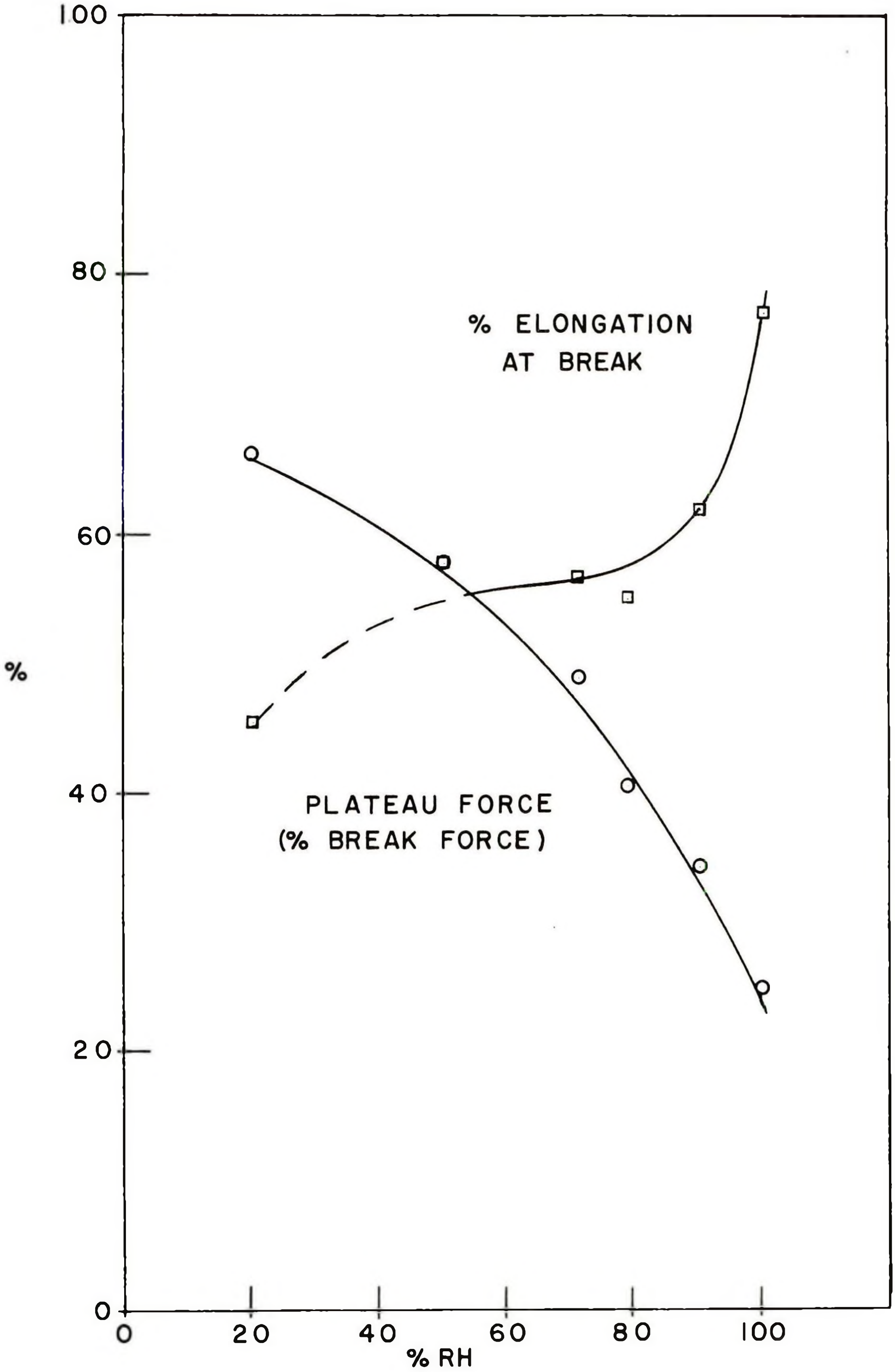

Figure 11. Stress/strain parameters vs. relative humidity

being gradually torn apart circumferentially before the catastrophic failure of the cortex. In air at relative humidities of 80% or less the cortex appears to have split axially into two or more mechanically independent subunits which failed in different radial planes, probably in rapid sequence, yielding a step fracture; in this case it appears that the cuticle fails in a pattern largely determined by that of the underlying corticle elements to which it remains firmly attached.

At 90% RH in air the cuticle and cortex fracture planes coincide as though the fiber were homogeneous. There is no evidence of prior failure of the cuticle as invariably occurs in wet breaks.

From these observations we infer that in the wet state the cortex is more extensible than the cuticle as has been reported on the basis of swelling experiments on animal hair (12, 13), but that in air at less than 90% RH the opposite is true; dry cortex is less extensible than dry cuticle. At 90% RH the extensibilities appear to be equal. Although at 50% RH the cuticle fracture seems to follow that of the cortex, its role may not be entirely passive. The fact that prior wet fracture of the cuticle leads to flat fracture of the cortex at 50% RH indicates that the cuticle is involved in the generation of the compressive or shear forces that crack the cortex axially, producing step fractures.

It is known that if hairs are stressed in water to an extension greater than their elongation at break in 50% RH air and allowed to dry under tension, they do not break until more stress is applied.

As stated above, when they are then broken, flat breaks are obtained as though the fracture had occurred in water. On the other hand, if hairs are extended almost to break at 50% RH, then hydrated and broken in water, flat breaks are also obtained. Apparently the hairs "remember" the pre-stress in water, but not the pre-stress at 50% RH. We interpret this as confirmation of the proposed mechanism, i.e. during the pre-stress in water, the cuticle fails and subsequently the cotex therefore breaks flat even in 50% RH air. The pre-stress in air did not cause failure of either the cuticle or the cortex, and the hairs therefore exhibit the normal flat break when subsequently hydrated and broken. Jagged breaks, then, are the product of failure of the cortex under conditions of intact and attached cuticle, which leads to the tearing and shredding observed.

The experiments in which hairs were pre-stressed at 50% RH, then hydrated and broken in water, provide a confirmation that wet hair is weaker than dry hair. When hairs were extended to 58% elongation (which at 50% RH is virtually the breaking point) and then hydrated, the break force is at least 15% lower than the force required during the pre-stress in air. Experimentally, this is almost equivalent to breaking the same hair segment twice—once at 50% RH and once in water, thereby eliminating sample variation.

It is remarkable how little evidence of the cellular structure of hair is revealed in its fractography. The fibrous structure of the cortex is clearly seen only on the lateral surfaces of dry step fractures. The cuticle cleaves as though it were a homogeneous sleeve; its imbricated cells do not slide over each other nor is delamination detectable except in high magnification views of some wet fractures.

This is in marked contrast to the behavior of cotton as reported by Hearle and Sparrow (11). Dry fractures of cotton are complex and elongated; wet fractures are even more elongated and their resemblance to the fracture of a yarn was taken as an indication that water weakens the interfibrillar matter.

A similar weakening might have been expected in the case of hair in view of its pronounced swelling in water, but from our data it would appear that the intercellular and interfibrillar material in both wet and dry hair is as strong as the keratinous matter in both the cortex and the cuticle. The cuticle–cortex boundary, however, is a zone of intercellular weakness in the wet state and this weakness is markedly aggravated by oxidative bleaching, as shown in Figure 10; cylindrical segments of the entire cuticle have been lost in the process of tensile fracture. This is the only evidence of bleach damage; dry breaks of bleached hair appear to be quite similar to those of virgin hair.

The weakness of this boundary is also revealed in virgin hair in sleeve fractures (Figure 2) and in the related flaring of the cuticle after its tensile failure, as seen in Figure 4. The multiplicity of the cuticle cracks on wet extension indicates that the junction with the cortex fails only locally, probably as a result of the combined forces of axial shear and radial tension generated by the elastic relaxation of torn cuticle to its unstressed length and radius. The flaring in Figure 4c is about 30% of the fiber diameter as would be expected for relaxation from 70% extension at constant volume (assuming a Poisson ratio of 0.5 throughout).

The effect of age on hair fracture is quite different from that of bleach. Where cuticle is present its bond with the cortex seems unchanged, but the cortex in old hair splits and fibrillates much more than in young hair. With reference to virgin hair, we argued above that intact cuticle is involved in the generation of splitting forces; on the same argument we would expect that loss of cuticle on old hair should lead to less, not more, splitting on tensile fracture. From the fact that the contrary is observed we conclude that the major effect of aging in the cortex as revealed in fractography is a significant decrease in the inherent cohesiveness of this tissue at the intercellular level. Loss of cuticle in vivo, however, leaves the cortex much more vulnerable to other modes of stress and we do not wish to imply that such loss is of no consequence cosmetically; on the contrary, we propose that even in young hair cuticle rupture in the wet state may have significant cosmetic consequences. The evidence of multiple fracture of the cuticle on wet extension (Figures 3 and 4) suggests a mechanism for producing "frizzies" in midshaft. If the detached cuticle were subsequently eroded away from such fracture sites the cortex would be locally exposed to mechanical and chemical attack. In extreme cases this might lead to a condition dermatologists would diagnose as acquired trichorrhexis nodosa (14).

The spongy scales seen in hairs dried in the extended state after wet stretching to cuticle rupture (Figure 4b) are thought to be the remains of cells which have split through the endocuticle layer as proposed by Swift and Bews (15) in reference to similar features on hair which had been subjected to prolonged agitation in water in their cuticle isolation procedure. It seems plausible that if the hair shown in Figure 4 were even mildly scoured in the wet state the scales would slough off and the end result would be a normal-looking hair. This is supported by our observation that after a hair has been broken in water under the optical microscope a considerable amount of scaly, isotropic matter is seen in the bath. It seems reasonable to postulate that such cracking of the swollen endocuticle will occur in hairs under tension since the inclination of the stacked cuticle cells to the fiber axis should give rise to a component of force normal to their surfaces.

This sloughing phenomenon should be studied further, especially with reference to the question of whether it occurs at the much lower extensions involved in ordinary grooming operations (such as setting wet hair on rollers) and also whether it occurs when the entire cycle of extension and relaxation occurs in water. In either case it may make a significant contribution to the gradual loss of cuticle associated with aging.

Hair fractures in dry solvents (glycerin, ethanol and ethyl acetate) look like wet fractures on cursory examination, but the absence of cuticle cracks and the location of sleeve fracture surfaces in the cortex rather than at the base of the cuticle suggest a sequence of events different from those of both wet and dry breaks.

The absence of noticeable response to pH variation and addition of surfactant indicates that the wet fracture dynamics are not very sensitive to either the charge state of the protein or to reduction of interfacial tension with the environment at the fracture site. Removal of accessible lipids with chloroform/methanol was also without noticeable effect on dry or wet fractures.

With reference to Figure 11, the shape of the curves shows that there is not a direct relationship between the plateau-force/break-force ratio and percentage of elongation at break. Nevertheless some interesting features are noted. Compared with the reported decrease in plateau force vs. relative humidity for keratin fibers (16), we find that the plateau-force/break-force ratio decreases more slowly, indicating that a decrease in the break force also occurs with increasing relative humidity. This provides a second, indirect confirmation that wet hair is weaker than dry hair.

The percentage of elongation at break is almost constant at 55 to 60% in the 50 to 79% RH range in which jagged fractures are almost invariably obtained in air. We conclude that, except for highly hydrated hairs, this is the limiting extensibility of the cortex.

It is interesting to note in connection with the difference in hair fracture at intermediate vs. very high humidities that over 60% of the observed radial swelling of wool by water occurs above 70% RH (17), indicating a change in the effect of water at high humidities. Based on our results, we propose that a similar change in hair properties occurs at high humidities. Over 60% of the change in relative rigidity of wool occurs above 65% relative humidity (18). From our data and that on wool it appears that hydration is the dominant variable affecting both the stress/strain behavior and the fracture mechanics, and that the two are interrelated. It seems appropriate to point out that our data on percentage of elongation at high relative humidities follows a trend very similar to the uptake of water by wool in the same range (19). Based on our own data, hair shows the same behavior up to 90% RH, the highest humidity at which water uptake was determined.

SUMMARY

Fracture pattern and stress/strain behavior of hair are interrelated through degree of hydration. The different fracture patterns obtained for wet and dry hair are attributed to an inversion in the relative extensibilities of the cuticle and cortex. The boundary of these two tissues is weak in the wet state and this weakness is aggravated by oxidative bleaching. Aging causes a reduction of cohesiveness in the cortex as well as a loss of cuticle; a new mechanism, not necessarily involving abrasion, is proposed for cuticle loss. Finally, a new demonstration of the lower tensile strength of wet, relative to dry, hair is presented.

ACKNOWLEDGEMENTS

We wish to acknowledge several helpful discussions with Dr. Hans-Dietrich Weigmann of Textile Research Institute. We also thank Avon Products, Inc., for encouraging this research.

REFERENCES

(1) R. Caputo and B. Ceccarelli, Study of normal hair and of some malformation with a scanning electron microscope, *Arch. Klin. Exp. Derm.*, 234, 242 (1969).

(2) A. Tosti, S. Villardita, M. L. Fazzini and R. Scalici, Contribution to the knowledge of dermatophytic invasion of hair, *J. Invest. Dermatol.*, 55, 123 (1970).

(3) E. Wyatt, E. Bottoms and S. Comaish, Abnormal hair shafts in psoriasis on scanning electron microscopy, *Brit. J. Dermatol.*, 87, 368 (1972).

(4) E. Bottoms, E. Wyatt and S. Comaish, Progressive changes in cuticular pattern along the shafts of human hair as seen by scanning electron microscopy, *Brit. J. Dermatol.*, 86, 379 (1972).

(5) R. P. Ayer and J. A. Thompson, Scanning electron microscopy and other new approaches to hair spray evaluation, *J. Soc. Cosmet. Chem.*, 23, 617 (1972).

(6) S. P. DiBianca, Innovative scanning electron microscopic techniques for evaluating hair care products, *J. Soc. Cosmet. Chem.*, 24, 609 (1973).

(7) A. C. Brown and J. A. Swift, Hair breakage: the scanning electron microscope as a diagnostic tool, *J. Soc. Cosmet. Chem.*, 26, 289 (1975).

(8) E. Bernstein, *Dynamic Experiments on Hair in the Scanning Electron Microscope,* in "The First Human Hair Symposium," A. C. Brown, Medcom Press, New York, New York, 1974, pp 317–331.

(9) N. A. Lange, "Handbook of Chemistry," 10th ed, McGraw-Hill Publishing Company, New York, New York, 1956, pp 1420–1421.

(10) J. W. S. Hearle and S. C. Simmens, Electron microscope studies of textile fibres and materials, *Polymer*, 14, 273 (1973).

(11) J. W. S. Hearle and J. T. Sparrow, The fractography of cotton fibers, *Text. Res. J.*, 41, 736 (1971).

(12) E. Lehmann, Mikroskopische untersuchungen über chemische und physikalische vorgänge an Pelztierhaaren, *Melliand Textilber.*, 22, 145 (1941).

(13) J. H. Bradbury and G. V. Chapman, An investigation by light microscopy of the swelling of wool fibers, *Text. Res. J.*, 33, 666 (1963).

(14) M. E. Chernosky, *Acquired Trichorrhexis nodosa.* in "The First Human Hair Symposium," A. C. Brown, Medcom Press, New York, New York, 1974, pp 36–49.

(15) J. A. Swift and B. Bews, The chemistry of human hair cuticle-I: a new method for the physical isolation of cuticle, *J. Soc. Cosmet. Chem.*, 25, 13 (1974).

(16) Encyclopedia of Polymer Science & Technology, Wiley, New York, New York, 8 (1968), p 22.

(17) Ibid., p 30.

(18) Ibid., p 28.

(19) Ibid., p 37.

J. Soc. Cosmet. Chem., 29, 469–485 (August 1978)

Stiffness of human hair fibers

G. V. SCOTT and C. R. ROBBINS *Colgate-Palmolive Research Center, 909 River Road, Piscataway, NJ 08854.*

Received November 3, 1977. Presented at Annual Scientific Meeting, Society of Cosmetic Chemists, December 1977, New York, New York.

Synopsis

The STIFFNESS of COMPONENT FIBERS is known to be important to the behavior of a fiber mass, but measurements are lacking in the cosmetic literature probably because of experimental difficulties with published methods. Recognizing this, we devised a simple method to compare fibers for stiffness.

A fiber with a small weight on each end is draped over a wire and the distance ("D") between the vertical legs is measured. Fibers with a wide range of thicknesses clearly showed that values of "D" relate linearly to cross-sectional areas, as expected of "stiffness." This prompted a theoretical study which yielded equations in terms of "D" for calculating, e.g., elastic bending moduli and shapes of hanging fibers.

Empirical and theoretical guides are given for selection of wire diameter and fiber weights. The average elastic modulus for bending fibers, assumed round in cross section, is approximately equal to that for stretching the same fibers. Fiber stiffness is affected by humidity and chemical treatments but is relatively unaffected by shampoos.

INTRODUCTION

The stiffness or resistance to bending of individual fibers unquestionably plays an important role in determining the behavior of any assembly of fibers. Textile literature (1–7) recognizes this importance in attempts to relate fiber stiffness to such fabric properties as flexibility, drape, handle, crease resistance and wear. Although changes in fiber stiffness must likewise affect manageability, body, combing, wave retention and handle of human hair (8, 9), the few hair measurements reported are mainly found in wool research literature (4, 10, 11). Several reasons may account for the lack of hair research in this area.

Measurement of fiber stiffness has been an experimentally difficult task. Our need for measurements arose during an investigation of effects on hair produced by polymerization within the fibers. Appreciable tensile increases were achieved, but we wished to directly measure changes in fiber stiffness. Sophisticated methods, each with appropriate theory, were reviewed in the textile literature. Many articles depended on deflection of very short fiber segments treated as cantilever beams, either end-loaded (3–5, 7, 12, 13) or center-loaded (2, 6). We tried the end-loading approach with only partial success. A "loop deformation" method (1, 6, 12) was rejected because fiber rings had to be very carefully made round, in one plane and small, 1 to 2 cm in diameter. Both beam and loop methods required precise measurement of very small deflections and forces. A dynamic procedure using short lengths of fibers as vibrating reeds (3, 6, 10, 11, 14) seemed experimentally more attractive, but we preferred a static or quasi-static (10) method for relating to hair behavior. No other methods reviewed offered better prospects for routine screening of hair treatment effects.

Changes in fiber strength are conveniently monitored by conventional tensile measurements which presumably serve as indirect measures of fiber stiffness. Controversy exists, however, as to the equivalence of elastic moduli calculated from stretching and from bending keratin fibers (3–5, 11). Unlike stretching, fiber bending involves both extension and compression with greatest strains near peripheral points of the fiber cross section. As a consequence, if fiber strength is affected chiefly in outer portions of a fiber, treatment effects may be detected more readily by stiffness than by tensile measurements.

Aside from means for estimating stiffness, a question remains as to the extent to which hair fiber stiffness can be altered by practicable hair treatments. Few current hair products of the nondamaging variety can be expected to produce more than superficial effects on stiffness. With a convenient measuring means available, however, perhaps this can be changed.

Essential working details of a simple method for measuring hair fiber stiffness were first disclosed in a very brief communication (15). The present paper describes the complete method giving information which includes a theoretical basis for equations, experimental data obtained on hair fibers and how these data relate to other measured properties of the same fibers. For easier reading, theoretical equations are derived in the Appendix with appropriate equations brought forward where needed in the text. The Appendix also contains a glossary of symbols used in this paper.

EXPERIMENTAL MATERIALS AND METHODS

Hair fibers used were from a 15-year-old Caucasian female (H), a 12-year-old Caucasian female (L) and from purchased South Korean hair (A. Klugman Inc., New York, New York). Unless otherwise specified, the fibers were equilibrated and measured in a room maintained at 60% RH, 75°F.

STIFFNESS DETERMINATION (D)

The procedure used for determining stiffness is as follows: weights are attached to each end of a fiber by threading the end through a short length of plastic tubing and inserting a tapered metal pin in the tubing to wedge the fiber. The weights of pin plus tubing on each fiber end are equal and known exactly.

The fiber is carefully draped over a wire hook and a separately hung guide bar is brought into light contact with the fiber legs to hold the fiber plane perpendicular to the optical axis of a horizontal cathetometer. The distance between the two vertical legs is measured several times by moving the distal end upwards, sliding the fiber to different contact points on the hook. The average distance in centimeters is expressed as the stiffness index (D) for that fiber.

For most human hair fibers, a recommended weight of pin and tubing is 0.1 g with a hook wire diameter of 0.75 mm.

LINEAR DENSITY DETERMINATION (L)

The fiber is measured for length to the nearest millimeter and is weighed to the nearest 0.01 mg using a Roller Smith® 3-mg Precision Balance (Federal Pacific Electric Co., Newark, New Jersey). Results are conveniently expressed as micrograms per cm (L) of fiber.

TENSILE DETERMINATION (H)

A fiber of 5-cm gauge length is extended at a rate of 0.1 in./min using an Instron® Model TM with Tension Cell A set at 10 g full scale. From the linear portion of the charted trace, the Hookean or elastic slope is estimated as g per mm extension (H) of the 5-cm fiber.

RESULTS AND DISCUSSION

Although fiber stiffness is important for overall hair performance, no convenient method for measurement of single fibers appeared to be available. Several approaches were tried in an effort to develop an empirical procedure which might be applied for evaluating hair treatment effects. Instron measurement of the work required to draw large hair loops taut between pegs was encouraging but suggested the simpler method described in this paper.

A fiber, weighted on each end, is draped over a fine wire and the distance (D) between the vertical legs is measured. The test proved useful on an empirical basis and became more acceptable with development of theory, outlined in the Appendix. The test is referred to below as the "Balanced Fiber" method and the distance between legs as the "Stiffness Index."

FIBER SHAPE

A fiber was hung in the usual way and photographed. Before theory was developed, attempts were made to shape-fit enlargements with simple curves that might empirically characterize the hanging fiber. Our lack of success here is readily explained by the complexity of the theoretical equation for fiber shape (Appendix, eq 5).

The equation was tested by measuring the enlargement for a D value and calculating values of y at assigned x values. The points coincide with the fiber shape as shown in Figure 1, confirming the theoretical treatment.

In another photo, not shown, a pronounced short-length bend just above the vertical part of the fiber had apparently no effect on the otherwise smooth inverted-U shape. A technique of comparing theoretical and photographed fiber shapes may be useful for examining individual fibers for eccentricities. For this purpose, calculations have been simplified by providing computed factors (Appendix—Fiber Shape). The distance from the hook to any point along the fiber may also be calculated by applying similar computations to eq 6, Appendix.

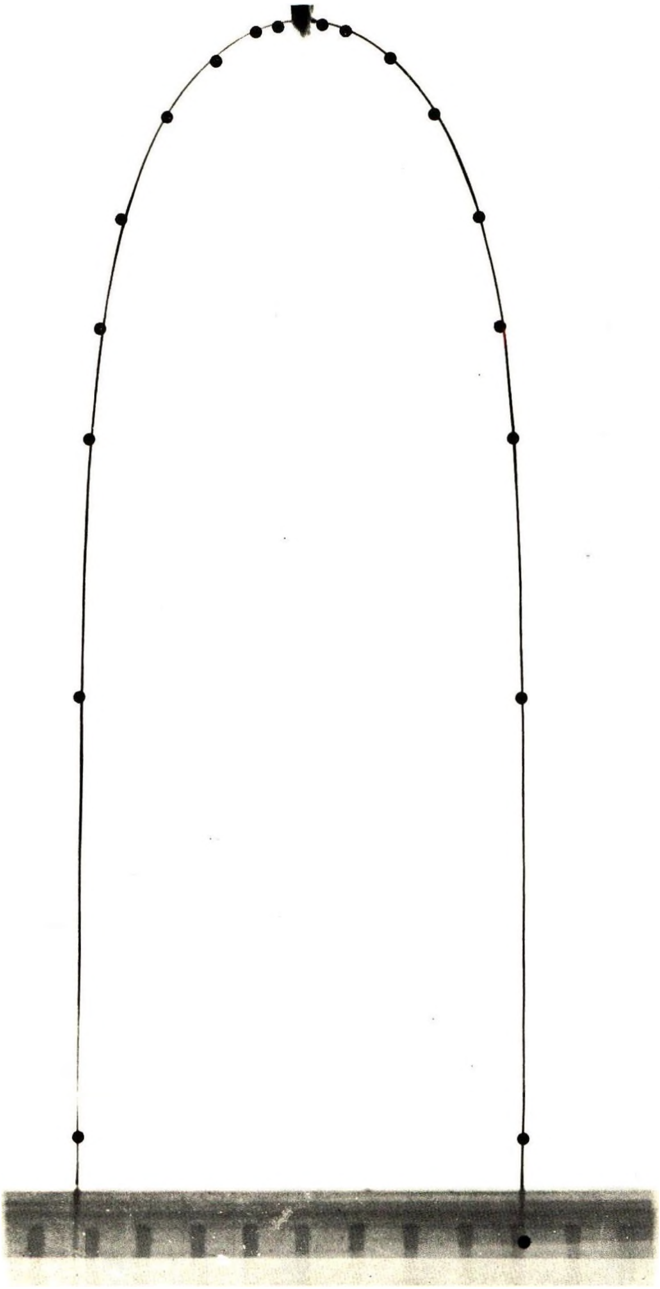

Figure 1. Photograph of a balanced fiber with calculated points superimposed

The closest analogy to the Balanced Fiber method appears to be a method developed by D. Sinclair (16). A long glass fiber is twisted slightly to form a loop which is gradually drawn tight by moving one free end of the fiber. Force is measured as a function of the distance the end is moved.

The procedure may not be suitable for hair fibers, but the same force and reaction considerations apply for a segment of the looped fiber as apply for our balanced fiber. In confirmation, we succeeded in transforming eq 5 in the Appendix into an equation identical with that derived for the looped fiber.

RELATION TO LINEAR DENSITY (L)

In developing a stiffness test a test of accuracy is required since satisfactory materials or methods are not available for reference. Fibers of larger cross-sectional area (A) were therefore assumed to be stiffer. This assumption has deficiencies, however, since fibers with the same area values may differ in stiffness because of shape or composition. For example, flat fibers bend more easily than cylindrical fibers. Nevertheless, this assumption provided a good, first test of accuracy.

Actual measurement of fiber diameters is difficult and linear densities, determined for each fiber, were considered to be proportional to cross-sectional areas of unaltered fibers. Area values may be estimated by dividing these measurements, expressed as g/cm, by 1.31 g/cm^3, the bulk density found for wool fibers (17, 18) and assumed (11, 19) appropriate for hair.

The data plotted in Figure 2 represent 24 fibers from three sources measured at 60% RH, 75°F. The only basis for selection of fibers from two individuals and Korean hair was to cover a broad range of linear densities.

Each point represents an average of four stiffness values taken at random along the fiber length. A Bartlett test (20) indicates that standard deviations for the point-to-point measurements on each of the fibers are homogeneous with a 3.7% pooled standard deviation.

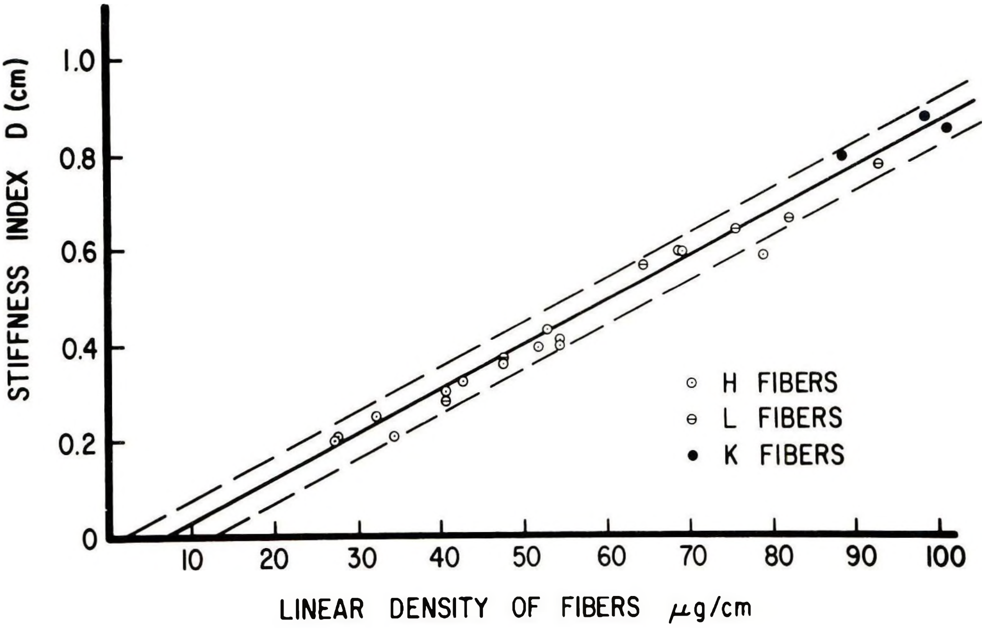

Figure 2. Effect of linear density on the stiffness index

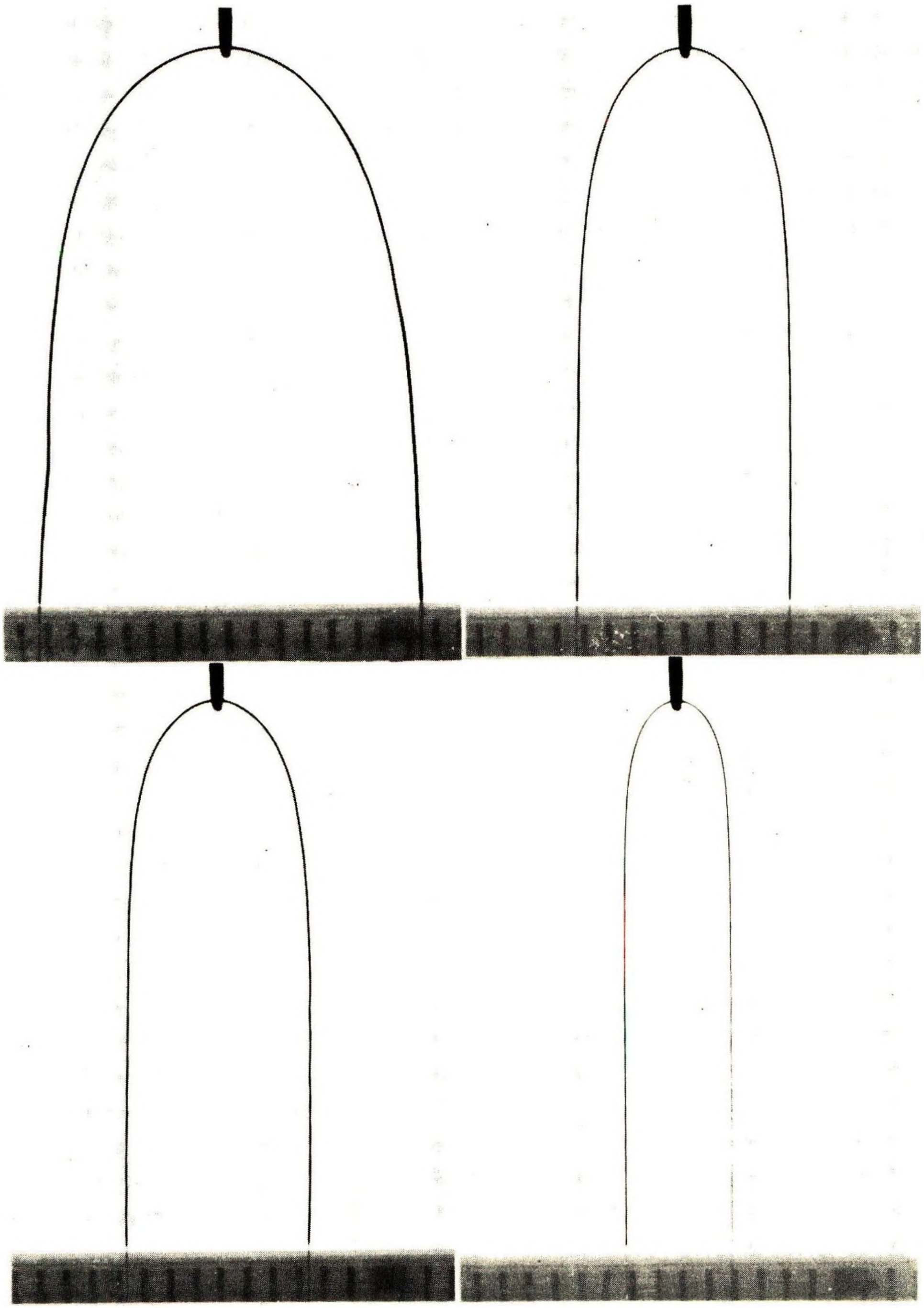

Figure 3. Photographs of balanced fibers having linear densities of 118, 71, 55 and 32 $\mu g/cm$

The straight-line relationship in Figure 2 of stiffness index to linear density and hence to approximate cross-sectional area is anticipated from eq 7 in the Appendix since the bending modulus should be nearly a constant. The scatter of points within the 95% confidence limits in Figure 2 is attributed mainly to shape differences among fibers with flatter fibers giving low and rounder fibers high stiffness values. Slight inelastic yielding of thinner fibers during measurement may account for the intercept not passing through the graph origin in Figure 2.

To more graphically illustrate the variation in stiffness from fine to coarse fibers, the photographs in Figure 3 were taken of four fibers weighted equally and with the proximal or root ends at the left of the hook. The linear densities correspond approximately to fiber diameters of 107, 83, 73 and 55 μ. It is apparent that the weight must be increased for the thickest fiber if the stiffness index D is to be measured.

EFFECT OF ATTACHED WEIGHTS

Stiffness indices were determined for three fibers with different weights attached to the fiber ends. In accordance with eq 7 and 9 in the Appendix, the stiffness index squared is plotted against the reciprocal of the attached weight for each fiber. Results in Figure 4 show linearity in agreement with theoretical prediction.

When fibers such as those shown in Figure 3 are not all measurable at the same weight, stiffness results are more conveniently compared in terms of stiffness coefficients (see

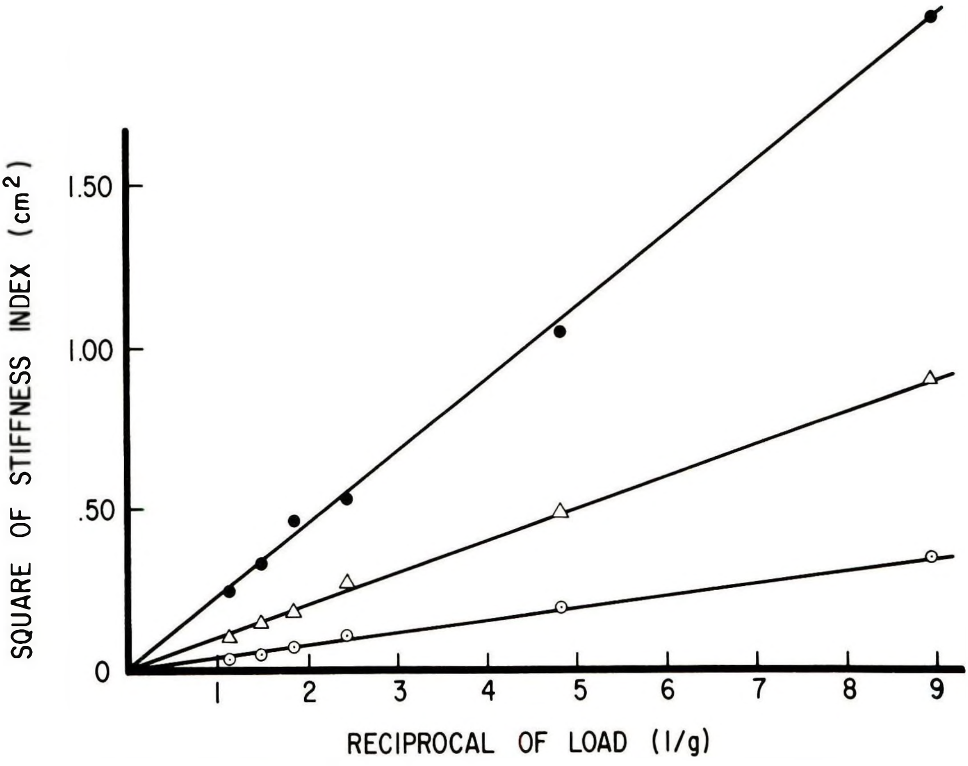

Figure 4. Effect of load on the stiffness index using functions indicated by eq 3

Appendix eq 9), which compensate for different weight loadings. Weights should be large enough to produce vertical hang without imparting a set to the fiber. As a precaution, fibers should be examined after measurement for signs of imparted set.

The effect of weight change on the stiffness index and on bending moments at the hook are derived in the Appendix. Briefly, increasing weights fourfold will double the bending moment and halve the distance between fiber legs.

EFFECT OF HOOK WIRE DIAMETER (W)

The diameter of wire used to suspend fibers was varied from 0.19 to 3.16 mm to test effects on the "D" measurement. Results in Table I show that D values are independent of wire size for most of the range covered. Careful handling of fibers is especially important with the fine wire sizes. At the largest wire size, the D measurement increases for all but the stiffest fiber.

Empirically we learned that wire size is too large if the fiber tends to orient on the support wire in a plane perpendicular to the wire. On the other hand, if a fiber tends to swivel freely, the support wire has an acceptable diameter.

An explanation of this behavior involves the problem of point and arc contacts between fiber and substrate, which is of considerable interest also for frictional studies (21, 22) using capstan methods.

With fine wires, curvature of the wire surface is greater than that of the bent fiber and theoretically contact exists only at a "point." As wire size becomes larger, curvature of the wire surface will, at some stage, equal the curvature of the bent fiber. Beyond this stage, contact between fiber and wire becomes an arc which increases in length as wire size is further increased.

Equal curvature of fiber and wire is achieved when the wire diameter (W) is equal to half the D measurement (see Appendix). "Point" contact thus exists when the ratio D/W is above two and arc contact below two.

The data in Table I provide an interesting empirical test of the D/W criterion. For wire sizes to 1.62 mm, D/W is greater than two and D values do not depend on wire size. For the 3.16-mm wire and all fibers except the stiffest, the D/W ratio is less than two and D measurements change. For the stiffest fiber, D/W = 2.18 (point contact) and the D measurement is unaffected by this wire size.

Table I

Hook Wire Diameter

Wire (cm)	0.019	0.024	0.031	0.038	0.076	0.128	0.162	0.316
Lin. Dens.				"D" Distance				
46.9 μg/cm	0.35	0.35	0.34	0.34	0.33	0.33	0.33	0.45
51.1	0.39	—	—	—	—	—	0.39	0.47
56.7	0.41	0.41	0.41	0.40	0.41	0.41	0.39	0.48
58.0	0.44	—	—	—	—	—	0.44	0.51
63.6	0.48	—	—	—	—	—	0.46	0.52
69.0	0.50	—	—	—	—	—	0.51	0.54
89.8	0.61	—	—	—	—	—	0.60	0.62
89.3	0.68	—	—	—	—	—	0.69	0.69

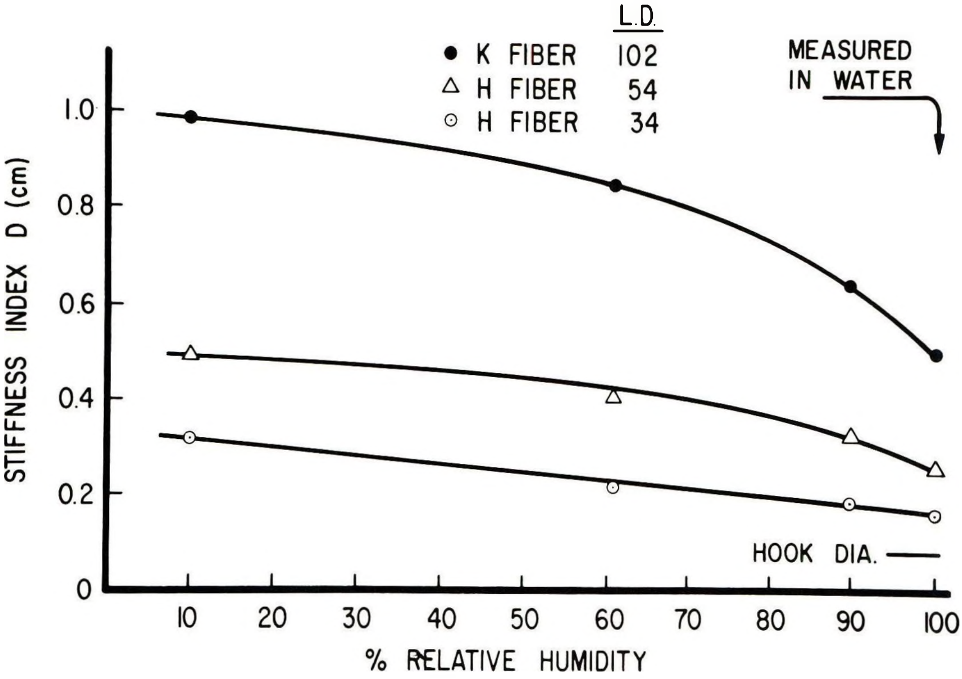

Figure 5. Effect of relative humidity on the stiffness index

EFFECT OF RELATIVE HUMIDITY

The influence of humidity is shown in Figure 5 for three fibers of different thicknesses. At the highest humidity, these fibers were measured without experimental difficulty while immersed in water. The thickest fiber showed greatest sensitivity to humidity changes while the thinnest fiber is limited in the amount of change since the "stiffness index" value in water is less than twice the wire diameter. Immersion testing requires additional study to select optimum conditions. Smaller weights can be used since wet fibers bend more easily and the fiber mass is diminished by buoyancy.

RELATION TO ELASTIC EXTENSION

An objective here was to test the strength of unaltered fibers by bending and by stretching to see how well one measurement predicts the other.

Fourteen fibers were measured for linear density and stiffness index and were then stretched with Instron equipment under conditions suitable for determining the linear or Hookean slope portion of the extension curve. When plotted, the Hookean slope data showed a good, straight-line relationship to linear densities. As expected, strength increased with thickness of fibers.

In Figure 6, stiffness indices and Hookean slopes for the 14 fibers show a satisfactory linear relationship. The prediction equation is approximately $D = 0.0151\ H$ for the dimensions used. Thus, tensile measurements on unaltered fibers may be used, to an extent, to estimate bending strengths.

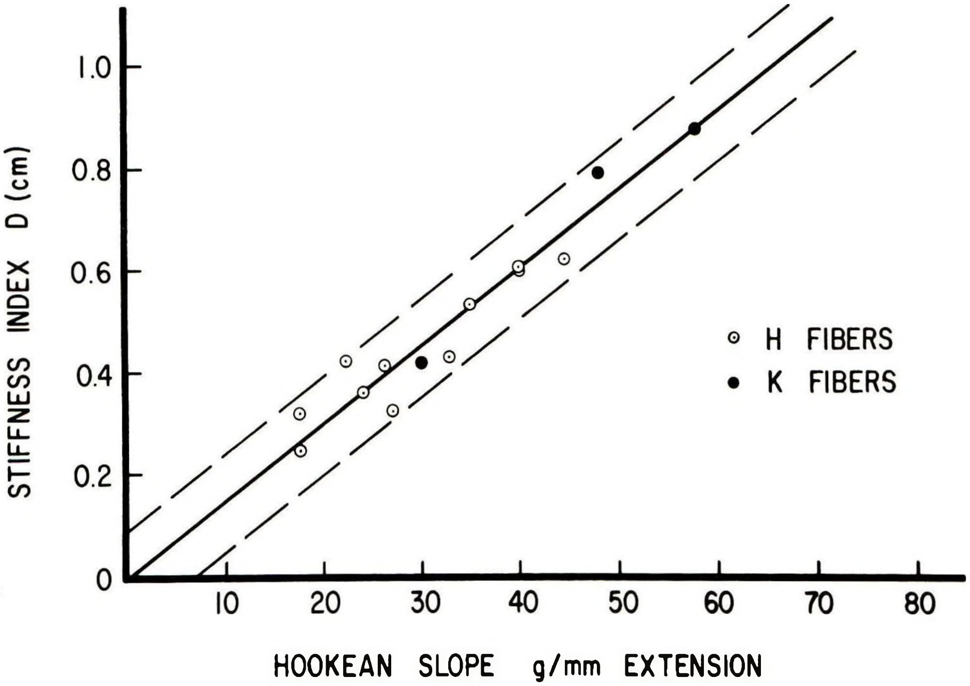

Figure 6. Relation of the stiffness index to the Hookean slope

ELASTIC MODULI

During bending, one side of a fiber is extended and the other side is compressed. For homogeneous elastic fibers with perfectly round cross sections, bending and tensile moduli would be identical and predict each other. For natural fibers such as wool or hair, however, the degree to which this identity holds is a matter of controversy (2–6, 11, 13). This is not surprising since hair fibers are oil-containing, viscoelastic, anisotropic materials which are nonuniform in cross-sectional shape and of variable thickness along their length.

Results are shown in Table II for fibers, measured at 60% RH, 75°F, and arranged according to linear densities (approximate thicknesses). The elastic moduli for bending (E_B) are calculated from eq 7 and those for stretching (E_S) from eq 8. For both calculations, the fibers are assumed to be round in cross section.

The larger spread of values for bending moduli is ascribed to greater dependence on shape factors. It is interesting that the averages for E_B and E_S are approximately equal even though the E_B/E_S ratio varies widely for the individual fibers.

The modulus values in Table II are calculated by assuming all fiber cross sections are circular. Correction for shape would increase E_B values since, in the Balanced Fiber method, bending occurs preferentially across the flattest cross section. Higher E_B values may therefore more closely represent circular fibers and truer E_B values. Accordingly, the data favors an hypothesis (4, 6) that the bending modulus is greater than the stretching modulus. The logic is that outer layers of a fiber are stiffer and play a greater role in bending than in stretching.

Table II
Elastic Moduli[a]

Fiber	Lin. Dens. μg/cm	$E_B \cdot 10^{-10}$	$E_S \cdot 10^{-10}$	E_B/E_S
K	99.5	4.23	3.68	1.15
L	94.9	3.54	3.82	0.93
K	89.2	4.29	3.43	1.25
L	71.8	4.25	3.83	1.11
H	69.2	4.11	3.75	1.10
L	67.7	3.35	3.96	0.85
L	54.6	3.60	4.12	0.88
L	52.9	4.69	3.98	1.18
H	52.6	3.74	4.03	0.93
H	42.3	3.23	4.21	0.77
L	34.4	2.89	4.33	0.67
H	31.3	3.58	3.59	1.00
Aver.	63.4	3.79	3.89	0.97
% SD	—	13.9	6.7	—

[a] Expressed as dynes/cm².

In stiffness studies of various natural and synthetic fibers, textile researchers occasionally include human hair fibers. Results reported for hair are shown in Table III for comparison with balanced fiber results.

Although test fibers were carefully selected and prepared, fiber-to-fiber variation in E_B for the other methods is appreciably greater than for the Balanced Fiber method. The average E_S values show much better agreement in Table III than the E_B values.

With wool fibers, the Balanced Fiber method may generally not be applicable because of insufficient fiber length. A Vibrating Reed Method (11) gave a low, fiber-to-fiber variation (12% S.D.) for wool but the E_B value of 8×10^{10} appears relatively high, presumably because of frequencies used. E_B/E_S ratios reported for wool (3–5, 11) vary from 0.4 to 3.4, possibly because of differences and difficulties in the methods.

APPLICATIONS OF THE METHOD

Although additional study is suggested, a few experiments involving dry stiffness measurements are briefly indicated below to illustrate usefulness of the method.

Table III
Elastic Moduli

Ref.	$E_B \cdot 10^{-10}$	% S.D.	$E_S \cdot 10^{-10}$	% S.D.	E_B/E_S
(4)	1.95[a]	40.9	3.57	16.8	0.55
(11)	5.35[b]	22.4	3.68	7.7	1.45
(10)	4.9[b]	—	—	—	—
(19)	—	—	3.60	—	—
S&R	3.79[c]	13.9	3.89	6.7	0.97

[a] Cantilever Beam Method.
[b] Vibrating Reed Method.
[c] Balanced Fiber Method.

A well known product with hair conditioning claims was applied to fibers in a variety of ways. A decrease in fiber stiffness resulted but the original values were restored following use of a commercially available shampoo (23).

Permanent waving of hair with a personal use product caused fiber stiffness to progressively decrease as time allowed for the reduction step was increased (23). Polymerization within fibers is also generally accomplished with an initial reduction step which weakens fibers. Nevertheless, overall increases in stiffness are achieved by proper selection of monomers and reaction conditions (23).

Proximal and distal halves of four long fibers from each of three individuals were compared for stiffness in an attempt to detect normal wear and aging effects. Unexpectedly, *distal* sections of nine fibers were stiffer and stiffness averaged 2% higher for distal halves of all fibers. Moreover, linear density was greater for distal halves of six fibers.

Bleached and untreated fibers from the same individual could not be distinguished when stiffness and linear density results were graphed. Measurement of *same* fibers before and after bleaching should be more discriminating.

Dry fiber stiffness is mainly discussed in the present paper because of its important influence on a person's hair behavior. However other experiments show that wet stiffness is generally a more sensitive measure of fiber strength changes caused by hair treatments.

CONCLUSIONS

The Balanced Fiber method for measuring fiber stiffness offers simplicity in experimental setup, avoids need for fiber clamping and allows replicate measurements on single fibers. The measuring instrument may be as simple as a ruler or as complex as a traveling microscope. Fibers are not affected by stiffness measurements and can be measured for other physical properties or for changes caused by fiber treatments. The method appears readily adaptable for other materials in filament or sheet forms.

Hair fibers can be routinely compared for stiffness using only the distance measurement. However this parameter has theoretical significance which qualifies the method for use in research programs.

ACKNOWLEDGEMENT

Appreciation is expressed to Messrs. E. J. Gibbons and J. C. Jervert for useful discussions and to Ms. P. Redman for obtaining much of the experimental data.

APPENDIX

LIST OF SYMBOLS

A.	Average cross-sectional area of fiber, cm^2
D.	Stiffness index, cm
E_B.	Elastic modulus for bending
G.	Stiffness coefficient
H.	Hookean slope for extension of a 5-cm fiber, g/m
I.	Moment of inertia of the fiber cross-sectional area
L.	Linear density of fiber, $\mu g/cm$

M.	Bending moment
r.	Average radius of a fiber, cm
R.	Radius of curvature
T.	Tension applied to each fiber end, dynes
W.	Diameter of wire used as support, cm
Z.	Fiber length, cm
e.	Tensile strain on fiber
p.	Bulk density of fiber, g/cm^3
σ.	Tensile stress in fiber

FIBER SHAPE

Physics and engineering texts (24) commonly show equations derived for cantilever beams having very small beam deflections and such equations are often used as a basis for stiffness measurements on fibers. The restriction to small-beam deflections simplifies the derivation steps but, for the fiber hanging over a wire, infinite beam lengths and deflections must be considered in developing suitable theory.

Referring to Figure 1, the right half of the fiber suffices for derivation purposes and fiber weight is assumed negligible compared to the attached weight.

At any point on the fiber, the bending or clockwise moment, $T(D/2 - x)$, will oppose and at equilibrium will equal the restoring or counterclockwise moment, $E_B\, I/R$ where E_B is the elastic modulus for bending, I is the moment of inertia of the cross-sectional area and R is the radius of curvature of the bent fiber. Replacing R with the differential expression (24) for the radius of curvature of an arc, and collecting terms, we obtain

$$\frac{dp}{(1 + p^2)^{3/2}} = \frac{T}{E_B\, I}\left(\frac{D}{2} - x\right) dx \tag{1}$$

where $p = dy/dx$. This is a standard form of differential which integrates to give

$$\frac{p}{(1 + p^2)^{1/2}} = \frac{T}{E_B\, I}\left(\frac{Dx}{2} - \frac{x^2}{2}\right) \tag{2}$$

The integration constant is zero since at the hook x and p equal zero. At the weighted end of the fiber $x = D/2$, p is infinitely large and therefore from eq 2

$$\frac{T}{E_B\, I} = \frac{8}{D^2} \tag{3}$$

Substituting $8/D^2$ for $T/E_B\, I$ in eq 2 and dy/dx for p gives

$$dy = \frac{\left(\frac{4x}{D} - \frac{4x^2}{D^2}\right) dx}{\left[1 - \left(\frac{4x}{D} - \frac{4x^2}{D^2}\right)^2\right]^{1/2}} \tag{4}$$

An integrated expression is obtained from eq 4 by substituting $\cos\theta$ for $4x/D - 4x^2/D^2$ and integrating "by parts."

$$y = \frac{D}{\sqrt{2}} F - \frac{D}{4\sqrt{2}} \log_e \frac{1 + F}{1 - F} + C \tag{5}$$

where

$$F = \left(\frac{1}{2} + \frac{2x}{D} - \frac{2x^2}{D^2}\right)^{1/2}$$

and the constant

$$C = \frac{-D}{2} + \frac{D}{4\sqrt{2}} \log_e \frac{\sqrt{2}+1}{\sqrt{2}-1}$$

For us, the integration of eq 4 was an exercise requiring 40 steps and no effort was made to find a shorter route. Copies of the detailed integration are available for interested persons.

Equation 5 defines the shape taken by an ideal fiber when weighted at the ends and hung from a fine wire. Only distance D must be known to calculate y values at assigned values of x from zero to D/2.

When eq 5 is divided through by D, y/D is expressed as a function of x/D and y/D has a numerical value at each assigned x/D value. A computer print-out of these quantities is provided below. For any D measurements, x and y values along the fiber are readily obtained. Using negative x values, points are obtained for the left half of the fiber.

Factors for Computing Fiber Shape

x/D	−y/D
0.001	0.000002
0.002	0.000008
0.0025	0.000012
0.004	0.000032
0.005	0.000050
0.008	0.000127
0.010	0.000199
0.025	0.001232
0.050	0.004878
0.100	0.019335
0.200	0.079170
0.300	0.194416
0.400	0.423225
0.450	0.664291
0.475	0.908362
0.500	

FIBER LENGTH

The length z of fiber from the wire to any point along the fiber may also be expressed as a function of the D parameter. Using the differential expression for the length of an arc (25) and substituting the value for dy/dx from eq 4, we obtain

$$\frac{dz}{dx} = \left[1 - \left(\frac{4x}{D} - \frac{4x^2}{D^2}\right)^2\right]^{-1/2}$$

This expression may be integrated by trigonometric substitution to give

$$z = \frac{-D}{4\sqrt{2}} \log_e \frac{1 + F}{1 - F} + C' \tag{6}$$

where F is defined as for eq 5 and the integration constant

$$C' = \frac{D}{4\sqrt{2}} \log_e \frac{\sqrt{2} + 1}{\sqrt{2} - 1}$$

ELASTIC MODULI

The elastic bending modulus E_B is expressed in eq 3 as a function of parameters, known experimentally except for I, the moment of inertia of the fiber cross section. In order to calculate E_B, the cross-sectional shape is assumed to be circular and hence $A^2/4\pi$ can be substituted for I to give

$$E_B = \frac{\pi T D^2}{2A^2} \tag{7}$$

The area A is estimated for each fiber by dividing linear density determinations in g/cm units by an assumed 1.31 g/cm^3 bulk density (11, 19).

The elastic stretch or tensile modulus E_S is calculated from

$$E_S = H\,g\,1/A\,\Delta \tag{8}$$

where the Hookean slope H is determined as described in the Experimental Section and the cross-sectional area A is estimated as for the bending modulus. The fiber length 1 is 5.0 cm, the fiber extension Δ is 0.1 cm and g is the gravitational constant.

STIFFNESS COEFFICIENT

The stiffness coefficient G may be preferred over the stiffness index for expression of results if different weights are needed to cover wide ranges of fiber stiffness. The index would require correction to a standard weight basis using the relation $D_1^2 = w_2 D_2^2 / w_1$ where w_1 is the standard g weight and w_2 is the g weight used for the D measurement.

The coefficient is defined (26) as the ratio of an applied force to the displacement from equilibrium and equals E_B I. From eq 3 therefore

$$G = \frac{TD^2}{8} \tag{9}$$

where T is the applied force in dynes. The stiffness coefficient is more useful for practical comparisons than the bending modulus since the actual bending resistance of a fiber is represented without need to estimate fiber diameters and shapes.

FORCES ON THE FIBER

Bending stress and strain for a balanced fiber are greatest at the cross section above the wire where the radius of curvature R is a minimum. As shown earlier, at x = o, E_B

I/R = TD/2 and, from eq 3, EB I = $TD^2/8$. Combining the equations to eliminate E_B I, R = D/4. Strain e is equal to r/R, where r is the radius of the fiber, and hence e = 4r/D. Since the elastic modulus is the ratio of stress to strain, the maximum stress $\sigma = e E_B$. Substituting 4r/D for e and the value of E_B from eq 3 and since $I = \pi r^4/4$, we have for the maximum fiber stress

$$\sigma = \frac{2\,TD}{\pi r^3} \tag{10}$$

Theoretically and empirically, D is proportional to A or r^2 and consequently the maximum stress is inversely proportional to r. Thus, thin fibers undergo greater stresses than thick fibers and require more care in handling during measurements.

The stiffness index value and the maximum bending moment are affected by changes in the applied force T. Since $TD^2 = 8 E_B I$ = a constant, a change from T to kT changes D to $D/\sqrt{k}$. The maximum bending moment M = TD/2. When T is changed to kT, D changes to $D/\sqrt{k}$ and, to maintain the equality 2M = TD, the maximum bending moment changes to $M\sqrt{k}$.

CONTACT OF FIBER WITH WIRE

Acceptable stiffness measurements require that contact between fiber and wire be minimal, theoretically a point contact. For a given bending force and fiber stiffness, this places a limit on wire diameter that may be used.

As shown above, the radius of curvature of the bent fiber R = D/4. For equal radius of curvature of wire and bent fiber, R must equal the wire radius or half its diameter. Replacing R with W/2 gives 2W = D. Accordingly, for "point" contact, wire diameter should be less than half the distance D. At larger wire sizes, contact between fiber and wire assumes an arc shape.

REFERENCES

(1) P. W. Carlene, The relation between fiber and yarn flexural rigidity in continuous filament viscose yarns, *J. Text. Inst.*, 41, T159 (1950).

(2) P. W. Carlene, The measurement of the bending modulus of monofils, *J. Text. Inst.*, 38, T38 (1947).

(3) J. C. Guthrie, D. H. Morton and P. H. Oliver, An investigation into bending and torsional rigidities of some fibers, *J. Text. Inst.*, 45, T912 (1954).

(4) R. M. Khayatt and N. H. Chamberlain, The bending modulus of animal fibers, *J. Text. Inst.*, 39, T185 (1948).

(5) N. E. King, Comparison of Young's modulus for bending and extension of single mohair and kemp fibers, *Text. Res. J.*, 37, 204 (1967).

(6) W. E. Morton and J. W. S. Hearle, "Physical Properties of Textile Fibers," Butterworth and Co., Ltd., London, England, 1962, p 376–383.

(7) K. R. Sen, The elastic properties of single jute filaments, *J. Text. Inst.*, 39, T339 (1948).

(8) C. R. Robbins and G. V. Scott, Prediction of hair assembly characteristics from single fiber properties, submitted for publication, August 1977.

(9) P. S. Hough, J. E. Huey and W. S. Tolgyesi, Hair body, *J. Soc. Cosmet. Chem.*, 27, 571 (1976).

(10) E. M. Karrholm and B. Schroder, Bending modulus of fibers measured with the resonance frequency method, *Text. Res. J.*, 23, 207 (1953).

(11) W. S. Simpson, A comparison of methods of measurement of Young's modulus for keratin fibers, *J. Text. Inst.*, 56, T675 (1965).

(12) R. Meredith and J. W. S. Hearle, "Physical Methods of Investigating Textiles," Interscience Publishers, Inc., New York, New York, 1959, p 235.
(13) T. W. Mitchell and M. Feughelman, The bending of wool fibers, *Text. Res. J.*, **35**, 311 (1965).
(14) J. W. Ballou and J. C. Smith, Dynamic measurements of polymer physical properties, *J. Appl. Phys.*, **20**, 493 (1949).
(15) G. V. Scott and C. R. Robbins, A convenient method for measuring fiber stiffness, *Text. Res. J.*, **39**, 975 (1969).
(16) D. Sinclair, A bending method for measurement of the tensile strength and Young's modulus of glass fibers, *J. Appl. Phys.*, **21**, 380 (1950).
(17) P. Larose, The density of wool in hydrocarbons, *Text. Res. J.*, **34**, 80 (1964).
(18) P. Alexander, R. F. Hudson and C. Earland, "Wool," Chapman and Hall Ltd., London, England, 1963, pp 88–89.
(19) M. Chaikin and N. H. Chamberlain, The propagation of longitudinal stress pulses in textile fibers, *J. Text. Inst.*, **46**, T44 (1955).
(20) W. J. Dixon and F. J. Massey, "Introduction to Statistical Analysis," McGraw-Hill Book Co., Inc., New York, New York, 1957, p 179.
(21) P. Grosberg and D. Plate, Capstan friction for polymer monofilaments with rigidity, *J. Text. Inst.*, **60**, 268 (1969).
(22) I. M. Stuart, Capstan equation for strings with rigidity, *Brit. J. Appl. Phys.*, **12**, 559 (1961).
(23) J. H. Nachtigal, private communication.
(24) B. Worsnop and H. Flint, "Advanced Practical Physics for Students," Methuen and Co., Ltd., London, England, 1941, p 86.
(25) D. Murray, "Differential Equations," Longmans Green and Co., New York, New York, 1936, p 52.
(26) W. Michels, "The International Dictionary of Physics and Electronics," D. Van Nostrand Co., Inc., New York, New York, 1956.

J. Soc. Cosmet. Chem., **29**, 487–496 (August 1978)

Über die Beeinflussung der anaeroben Bakterienflora im Talgdrüsenausführungsgang durch eine äthyllactat- und äthanolhaltige Filmmaske und eine antimikrobielle Tensidlösung

M. GLOOR, W. WOLF und M. FRANKE [*]

Synopsis — A group of 15 healthy male subjects was treated with a face mask containing 1 % ethyl lactate and 50 % ethanol, while a matched group was treated with an antimicrobial surfactant solution with Aromox DMMCDW and Elfan NS242. The left side of the forehead was used as the test area, and a similar active agent free mask and a non-antimicrobial surfactant solution was applied to the right side of the forehead of each individual. Before the start of the treatment and 24 hours after the treatment the number of saprophytic bacteria in the pilosebaceous ducts was analyzed with the aid of a special anaerobic technique. The mask containing ethyl lactate and ethanol caused a significant reduction in the total bacteria and in the propionibacteria counts. The antimicrobial surfactant solution effected a significant decrease in the total bacteria count but did not alter the propionibacteria count. The results indicate that the test mask is an effective acne treatment. The efficacy of the treatment with the surfactant solution has not yet been determined.

Saprophytäre Bakterien, insbesonders Propionibacterium acnes und Propionibacterium granulosum, sind für die Aufspaltung der Triglyceride des Talgdrüsensekretes im Talgdrüsenausführungsgang verantwortlich (21). Den dabei entstehenden freien Fettsäuren wird eine comedonogene Wirkung zugeschrieben (5, 13, 14, 15). Eine Reduktion dieser Bakterien durch ein antimikrobielles Agens müßte also die Menge der freien Fettsäuren und damit auch die Comedonenbildung bei der Akne vermindern. Außerdem wird diesen Bakterien auf einem anderen Weg (z. B. durch andere Ektofermente als Lipasen, Chemotoxine oder immunologische Reaktionen) eine Schlüsselrolle für die Entstehung der entzünd-

---

[*] Aus der Universitäts-Hautklinik Heidelberg (Geschäftsf. ärztl. Direktor: Prof. Dr. U. W. Schnyder), Abteilung Dermatologie I (Schwerpunkt: Allgemeine Dermatologie und Venerologie) mit Poliklinik (Ärztl. Direktor: Prof. Dr. U. W. Schnyder).

lichen Reaktionen in der Akneeffloreszenz zugeschrieben, so daß eine Reduktion dieser Keime durch ein antimikrobielles Agens auch zu einer Besserung der entzündlichen Reaktion führen müßte (1, 8, 9, 18). Die Bedeutung der Propionibakterien wird bei beiden pathogenetischen Vorgängen für wichtiger gehalten als die Rolle der anderen saprophytären Keime (23).

Aus diesem Grund werden antimikrobielle Pharmaka in großem Stil in der Aknetherapie angewendet. Neben antimikrobiellen Wirkstoffen, die in Akneexterna vor allem wegen ihrer gleichzeitig vorliegenden keratolytischen Wirkung eingesetzt werden (Salicylsäure, Schwefel, Benzoylperoxyd), haben sich die systemische und in jüngster Zeit auch die topische Antibioticatherapie durchgesetzt (2). Außerdem werden Maskenrezepturen, die Äthyllactat und Äthanol als Wirkstoffe enthalten und antimikrobielle Tensidlösungen eingesetzt. Die vorliegenden Untersuchungen bezwecken, die Wirkung einer derartigen Maskenrezeptur und einer antimikrobiellen Tensidkombination auf die Bakterienflora im Talgdrüsenausführungsgang zu überprüfen.

Material und Methodik

a) Versuchsaufbau

15 gesunde männliche Versuchspersonen im Alter von 17 - 19 Jahren (Kollektiv I) wurden 10 mal an der linken Stirnseite mit einer Filmmaske, die 50 % Äthanol und 1 % Äthyllactat enthält, behandelt. Die Filmmaske wird flüssig auf die Haut aufgetragen. Innerhalb weniger Minuten bildet sich ein Film, der nach Ende der Einwirkungszeit, die 20 Minuten beträgt, mühelos von der Haut abzuziehen ist. Auf der rechten Stirnseite wurde die gleiche Behandlung mit einer Maskenrezeptur durchgeführt, die kein Äthyllactat enthielt und bei der Äthanol durch Wasser ersetzt war. Im übrigen war diese Maske mit der wirkstoffhaltigen identisch[1]. 15 andere gesunde männliche Versuchspersonen im gleichen Alter (Kollektiv II) erhielten ebenfalls 10 mal an der linken Stirnseite eine Behandlung mit einer antimikrobiellen Tensidlösung[2] und an der rechten Stirnseite eine entsprechende Behandlung mit einer

---

[1] Die wirkstoffhaltige Maske ist als „Jade Pickel Maske mit Alkohol" (Hersteller: Curta & Co. GmbH, Frankfurt/M) im Handel; wir danken dem Hersteller für die Sonderanfertigung der wirkstofffreien Maske.

[2] Dimethylkokosfett-Aminoxyd Zwischenfraktion (AROMOX DMMCD/W 30 %ig) 3,5, Triäthanolaminlaurylsulfat (ELFAN 240 TS 40 %ig) 30,0, NaCl 0,5, Wasser ad 100,0; Hersteller beider Tenside: Akzo Chemie Düren BRD. Beide Tenside sind nach Auskunft der Hersteller frei von Konservierungsmitteln.

nicht antimikrobiellen Tensidlösung[3]. Die Behandlungen erfolgten jeweils täglich von Mittwoch bis Samstag und vom darauffolgenden Montag bis Freitag. An dem dazwischenliegenden Sonntag wurde aus technischen Gründen keine Behandlung durchgeführt. Bakteriologische Untersuchungen wurden unmittelbar vor Behandlungsbeginn und 24 Stunden nach der letzten Applikation vorgenommen. Alle Versuchspersonen vermieden während des gesamten Versuchs jede zusätzliche Einwirkung auf die Gesichtshaut durch Externa. Da die Beeinflussung der Bakterienflora im Talgdrüsenausführungsgang vor Entstehung eines Comedo überprüft werden sollte, war es nicht notwendig, Aknepatienten als Versuchspersonen zu verwenden.

b) Methoden

Es wurden isoliert die Bakterien aus dem Talgdrüsenausführungsgang nach der von HOLLAND et al (11) angegebenen Methode gewonnen. Dabei wird ein mit einem Tropfen Cyanoacrylatgel[4] beschichteter aufgerauhter Stempel solange auf die Haut aufgedrückt, bis sich das Gel verfestigt hat. Dann wird der Stempel ruckweise entfernt. An der Stempelunterfläche hängen dann Teile der Haarfollikel und Talgdrüsenausführungsgänge. Da das Gel bactericid ist, werden superficielle Keime nicht miterfaßt. Die an den Follikelanteilen hängenden Bakterien werden mit einer speziellen Vorrichtung in 12,5 ml Reinforced Clostridial Medium (RCM) [5] mit einem Zusatz von 1 % Tween 80 [6] verteilt. Methodische Details finden sich in den Publikationen von HOLLAND et al (11) sowie ROBERTS (19). 0,1 ml RCM werden unverdünnt und in Verdünnungen bis zu 10^{-3} auf Reinforced Clostridial Agar[5] aufgebracht. Nach anaerober Kultur (7 Tage, 37° C) Auszählung der Keimzahl in der üblichen Weise. Dabei werden die aus zwei unmittelbar hintereinander aufgelegten Stempeln gewonnenen Keimzahlen addiert, um die Keimzahl in dem Untersuchungsareal zu ermitteln. Für die Differenzierung der Bakterien waren Kolonieform und -farbe, gramgefärbte Ausstriche und der Ausfall des Caseintests maßgebend. So ist es möglich zu unterscheiden zwischen P. acnes, P. granulosum, grampositiven Kokken und Sarcinen. Die Kokken wurden nicht weiter differenziert. Für die Angrenzung von P. acnes und P. granulosum ist der Caseintest ein zuverlässiges Kriterium. P. avidum kommt an der Stirn extrem selten vor.

---

[3] Polyaethylenglycollauryläthersulfat, Natriumsalz (ELFAN NS 242), Konzentration 6 %, bezogen auf die waschaktive Substanz; Hersteller: Akzo Chemie Düren BRD.

[4] Permabound Contact Cement; Hersteller: Staident Labor, Staines, Middlesex, England.

[5] Hersteller: Oxoid Deutschland GmbH, Wesel BRD.

Es zeigt ähnlich wie P. acnes eine caseinpositive Reaktion und wird bei unserem Vorgehen P. acnes zugezählt. In Einzelfällen bedienten wir uns zusätzlicher biochemischer Parameter (Gelatin-Hydrolyse, Indolproduktion, Nitratreduktion) und des Phagentests, der nach neueren Ergebnissen bei negativem Ausfall nur unsichere Aussagen auf das Vorliegen von P. granulosum erlaubt (12) und dem deshalb nur relativ wenig Bedeutung beigemessen wurde. Methodische Details zu allen genannten Methoden finden sich bei MARPLES und MC GINLEY (16) sowie ROBERTS (19).

Bakteriologische Keimzahlbestimmungen ergeben logarithmische Verteilungen, deshalb wurden die ermittelten Keimzahlen logarithmisch transformiert. Um die logarithmische Transformation der 0-Werte zu ermöglichen, wurde zu den in 2 x 0,1 ml unverdünnten RCM ermittelten Keimzahlen jeweils der Wert 1 hinzugezählt Die so gewonnenen Zahlen wurden der statistischen Berechnung zugrunde gelegt. Bewertet wurden Gesamtkeimzahl und Zahl der Propionibakterien (P. acnes und P. granulosum zusammengenommen). Es wurden jeweils die Differenzen der logarithmisch transformierten Werte über den WILCOXON-Test für Paardifferenzen mit dem hypothetischen Mittelwert 0 verglichen. Als Signifikanzniveau wurde 1 % vorgegeben. Zur Ermittlung der Bakterienzahl/cm^2 ist es notwendig, die Keimzahl in 2 x 0,1 ml unverdünntem RCM durch Delogarithmieren und Reduktion des erhaltenen Wertes um 1 zu ermitteln und diese Zahl mit 80 zu multiplizieren.

Ergebnisse

Da P. granulosum nur beim kleineren Teil der Fälle gefunden wurde, sind in den Tabellen 1 und 2 P. acnes und P. granulosum zusammengefaßt. P. granulosum war bei Kollektiv I nur einmal vor Behandlungsbeginn (Keimzahl 1250 / 2 x 0,1 ml RCM) und nach Behandlung mit der wirkstofffreien Maske (Keimzahl 50 / 2 x 0,1 ml RCM) nachweisbar. Bei Kollektiv II fand sich P. granulosum nur zweimal bei den Ausgangsuntersuchungen (Keimzahl 90 bzw. 1000 / 2 x 0,1 ml RCM). Die Differenz zwischen Gesamtkeimzahl und Propionibakterien besteht im wesentlichen aus grampositiven Kokken. Sarcinen waren nur ausnahmsweise vorhanden (Keimzahl maximal 1400 / 2 x 0,1 ml RCM).

Gesamtkeimzahl und Zahl der Propionibakterien vor und nach Anwendung der Masken sind in Tabelle 1 gegenübergestellt. Die wirkstoff-

---

6) Hersteller: Sigma Chemie, Neubiberg BRD.

Gesamtkeimzahl (anaerobe Kultur)			
	vor Behandlung	nach Behandlung mit der wirkstofffreien Maske	nach Behandlung mit der wirkstoffhaltigen Maske
N	15	15	15
M	2,8903	2,6712	2,0997
S	1,0457	1,0778	1,2653

Propionibakterien (P. acnes und P. granulosum zusammengenommen)			
	vor Behandlung	nach Behandlung mit der wirkstofffreien Maske	nach Behandlung mit der wirkstoffhaltigen Maske
N	15	15	15
M	2,2688	2,1607	1,5487
S	1,5403	1,4464	1,5000

Tabelle 1

Mittelwerte und Standardabweichungen der dekadischen Logarithmen der um die Zahl 1 vermehrten Gesamtkeimzahl (bei anaerober Kultur) und der um die Zahl 1 vermehrten Zahl der Propionibakterien (P. acnes und P. granulosum zusammengenommen) bezogen auf 2 x 0,1 ml unverdünntes RCM vor Behandlung, nach Behandlung mit der wirkstofffreien Maske und nach Behandlung mit der wirkstoffhaltigen Maske. Das geometrische Mittel der Keimzahlen bezogen auf 1 cm^2 erhält man durch Delogarthmieren des Mittelwertes der Logarithmen, Reduktion dieses Wertes um die Zahl 1 und anschließende Multiplikation mit 80.

haltige Maske reduziert die Keimzahl signifikant, gleichgültig ob die Gesamtkeimzahl oder nur die Zahl der Propionibakterien bewertet werden. Das gilt nicht nur für den Wert vor der Behandlung verglichen mit dem nach der Behandlung sondern auch für den Wert nach Behandlung mit der wirkstofffreien Maske. Eine geringe jedoch signifikante Reduktion der Gesamtkeimzahl ist durch die wirkstofffreie Maske nachweisbar.

Die Untersuchungsergebnisse nach Anwendung der Tensidlösungen sind in Tabelle 2 gegenübergestellt. Die antimikrobielle Tensidlösung reduziert die Gesamtkeimzahl signifikant, gleichgültig ob der Wert nach

Gesamtkeimzahl (anaerobe Kultur)

	vor Behandlung	nach Behandlung mit der nicht antimikrobiellen Tensidlösung	nach Behandlung mit der antimikrobiellen Tensidlösung
N	15	15	15
M	2,8576	2,6944	2,1069
S	0,9080	0,7404	0,9459

Propionibakterien (P. acnes und P. granulosum zusammengenommen)

	vor Behandlung	nach Behandlung mit der nicht antimikrobiellen Tensidlösung	nach Behandlung mit der antimikrobiellen Tensidlösung
N	15	15	15
M	2,0704	1,6527	1,6001
S	0,9070	0,7404	0,9459

Tabelle 2

Mittelwerte und Standardabweichungen der dekadischen Logarithmen der um die Zahl 1 vermehrten Gesamtkeimzahl (bei anaerober Kultur) und der um die Zahl 1 vermehrten Zahl der Propionibakterien (P. acnes und P. granulosum zusammengenommen) bezogen auf 2 x 0,1 ml unverdünntes RCM vor Behandlung, nach Behandlung mit der nicht antimikrobiellen Tensidlösung und nach Behandlung mit der antimikrobiellen Tensidlösung. Das geometrische Mittel der Keimzahlen bezogen auf 1 cm^2 erhält man durch Delogarithmieren des Mittelwertes der Logarithmen, Reduktion dieses Wertes um die Zahl 1 und anschließende Multiplikation mit 80.

Behandlung mit der nicht antimikrobiellen Lösung oder der Ausgangswert als Vergleich herangezogen werden. Ein solcher Nachweis läßt sich nicht bei den Propionibakterien führen. Vielmehr finden sich nach Anwendung der antimikrobiellen Lösung nahezu identische Werte wie nach Anwendung der nicht antimikrobiellen Tensidlösung. Der antimikrobielle Effekt der Tensidlösung scheint sich somit in erster Linie auf die grampositiven Kokken zu beziehen.

Die Ergebnisse bei den einzelnen Versuchspersonen sind im Detail in der Inauguraldissertation WOLF (24) aufgeführt.

Diskussion

SWANBECK (22) hat als erster gezeigt, daß Äthyllactat in einer alkoholischen Lösung unter Okklusivbedingungen eine Verminderung der freien Fettsäuren in den Hautoberflächenlipiden bewirkt. GLOOR et al (7) konnten später deutlich machen, daß dieser Effekt nur zum kleinen Teil dem Wirkstoff Äthyllactat und zum weit größeren Teil der Grundlage Äthylalkohol zukommt. Außerdem konnten diese Autoren zeigen, daß die Anwendung unter Maskenbedingungen der in der Aknebehandlung unpraktikablen Okklusivbehandlung mit Folien ebenbürtig ist. Ein klinischer Wirkungsnachweis für die Äthyllactatbehandlung in einer alkoholischen Grundlage unter Okklusivfolien bei Akne findet sich bei SWANBECK (22). Für die in den vorliegenden Untersuchungen verwendete 50 % Äthanol und 1 % Äthyllactat enthaltende Maske wurde ebenfalls ein klinischer Wirkungsnachweis erbracht (3).

Zur definitiven Klärung des Wirkungseffektes ist es notwendig, den Nachweis zu erbringen, daß die applizierten antimikrobiellen Agentien in die Talgdrüsenausführungsgänge penetrieren und dort zu einer Reduktion der Keimflora insbesondere der Propionibakterien führen. Die vorliegenden Untersuchungen zeigen: Die äthyllactat- und äthanolhaltige Maske reduziert signifikant die Gesamtkeimzahl und die Propionibakterien im Talgdrüsenausführungsgang. Die auf Grund des Nachweises einer Reduktion der freien Fettsäuren in den Hautoberflächenlipiden und des klinischen Wirkungsnachweises bestehende Vermutung, daß es sich bei dieser Therapie um eine effektive Lokalbehandlung der Akne handelt, wird durch die vorliegenden Ergebnisse bestärkt. Zu einem kleinen Teil dürfte nach den vorliegenden Befunden dieser Effekt durch das Maskenmaterial selbst bedingt sein, zum größeren Teil kommt es den Wirkstoffen Äthyllactat und Äthanol zu, wobei Äthanol nach eigenen früheren dünnschichtchromatographischen Ergebnissen (7) das wichtigste Agens sein dürfte.

Waschlösungen werden seit langer Zeit in der Aknetherapie eingesetzt. In erster Linie erwartet man bei deren Verwendung, daß Lipide im Talgdrüsenausführungsgang bzw. im Comedo emulgiert werden (20). Dieser Auffassung wird in jüngerer Zeit entgegengehalten, daß die Tenside nur auf der Hautoberfläche und nicht im Talgdrüsenausführungsgang wirksam werden und daß somit die Tensidbehandlung der Akne nutzlos sei (17). Bei diesen Diskussionen blieb unberücksichtigt, daß Tenside z. T. antimikrobiell wirken. Einen Hinweis auf eine Reduktion der mikrobiellen Lipolyse auf behaarter bzw. unbehaarter Haut durch antimikrobielle Tensidlösungen (ELFAN 240 TS / AROMOX DMMCD / W bzw. TEXAPON TH / SOFTIGEN 767) haben eigene Untersuchungen ergeben. Bezüglich der unbehaarten Haut ist einschränkend hinzuzufügen, daß die Untersuchungen nicht geklärt haben, ob sich dieser Effekt nur auf die Hautoberfläche oder auch auf die Talgdrüsenausführungsgänge erstreckt (4,6).

Die vorliegenden Ergebnisse zeigen, daß das verwendete Tensidgemisch im Talgdrüsenausführungsgang antimikrobiell wirksam ist. Es beeinflußt aber offenbar in erster Linie die grampositiven Kokken. Da — wie bereits oben ausgeführt — wahrscheinlich den Propionibakterien und nicht den grampositiven Kokken die Hauptbedeutung in der Pathogenese der Akne zukommt, erscheint es als fragwürdig, ob mit einer solchen Therapie ein klinischer Erfolg bei der Akne erzielt werden kann. Die Ergebnisse zeigen außerdem, daß die dünnschichtchromatographischen Analysen des Verhältnisses freie Fettsäuren / Triglyceride nicht ausreichen, um den Wert einer antimikrobiellen Therapie bei der Akne definitiv zu beurteilen. Als positives Ergebnis läßt sich ableiten, daß die Anwendung von antimikrobiellen Tensiden ein erfolgversprechender Weg der Aknetherapie sein könnte, wenn es gelänge, Tenside zu finden, die auch die Propionibakterien in hinreichender Weise hemmen.

Zusammenfassung

Je 15 gesunde männliche Versuchspersonen wurden 10 mal mit einer Filmmaske, die 1 % Äthyllactat und 50 % Äthanol als Wirkstoff enthielt, bzw. mit einer antimikrobiellen Tensidlösung (AROMOX DMMCD W / ELFAN 240 TS) behandelt. Versuchsstelle war die linke Stirnhälfte. Auf der rechten Stirnhälfte kam eine analoge wirkstofffreie Maske bzw. eine nicht antimikrobielle Tensidlösung (ELFAN NS 242) zur Anwendung. Vor Behandlungsbeginn und 24 Std. nach Abschluß der Behandlung wurden mit einer speziellen Methode die unter anaeroben Bedingungen wachsenden saprophytären Keime in den Talgdrüsenausführungsgängen analysiert. Die äthyllactat- und äthanolhaltige Maske reduziert die Gesamtkeimzahl und die Propionibakterien signifikant. Die antimikrobielle Tensidlösung führt zwar zu einer signifikanten Verminderung der Gesamtkeimzahl jedoch nicht der Propionibakterien. Die Ergebnisse lassen annehmen, daß die Maskenrezeptur eine effektive Aknetherapie darstellt. Ob dies auch für die Behandlung mit der verwendeten Tensidlösung gilt, muß offen bleiben.

Literatur

(1) Edwards, J. C., Williams, S., Tan, S., Holland, K. T., Roberts, C. D., Cunliffe, W. J., Physiology of C. acnes exoenzymes: lipase, protease, hyaluronidase, a comparison. J. invest. Derm. 64, 290 (1976).

(2) Gloor, M., Zur Therapie der Acne vulgaris mit antimikrobiellen Pharmaka. Zbl. Haut-Geschl. Kr. 138, 1 - 12 (1977).

(3) Gloor, M., Über die Reduktion der freien Fettsäuren in den Hautoberflächenlipiden als Kriterium für die therapeutische Wirksamkeit antimikrobieller Aknetherapeutika. Arzneimittel Forsch. 27, 2179-2181 (1977).

(4) Gloor, M., Döring, W. J., Kümpel, D., Über den Einfluß synthetischer Tenside auf die Zusammensetzung der Hautoberflächenlipide. Fette-Seifen-Anstrichmittel 78, 40-43 (1976).

(5) Gloor, M., Habedank, W. D., Zur Pathogenese der Acne vulgaris. Münch. med. Wschr. 118, 649-652 (1976).

(6) Gloor, M., Jäger, B., Baldes, G., Wirkungseffekt waschaktiver Substanzen in Kopfwaschmitteln. Hautarzt 28, 404-406 (1977).

(7) Gloor, M., Mendel, R., Baumann, C., Friederich, H. C., Untersuchungen zur Äthyllactat-Therapie der Akne vulgaris. Einfluß von Wirkstoff und alkoholischer Grundlage auf die Hautoberflächenlipide. Hautarzt 26, 149-152 (1975).

(8) Gould, D. J., Cunliffe, W. J., Holland, K. T., Chemotaxis and acne. Annual Meeting Europ. Soc. Derm. Res. 2.-4. 5. 1977 Amsterdam.

(9) Hägele, W., Schäfer, H., Stüttgen, G., Über die Bedeutung der Triglyceridspaltung durch Corynebacterium acnes für die Acne vulgaris. Arch. Derm. Forsch. 246, 328-334 (1973).

(10) Holland, K. T., Cunliffe, W. J., Roberts, C. D., Acne vulgaris: an investigation into the number of anaerobic diphteroids and members of the micrococcaceae in normal and acne skin. Brit. J. Derm. 96, 623-626 (1977).

(11) Holland, K. T., Roberts, C. D., Cunliffe, W. J., Williams, M., A technique for sampling microorganisms from the pilo-sebaceous ducts. J. appl. Bact. 37, 289-296 (1974).

(12) Jong, E. C., Ko, H. L., Pulverer, G., Studies in bacteriophages of propionibacterium acnes. Med. Microbiol. Immunol. 261, 263-271 (1975).

(13) Kanaar, P., Follicular-keratogenic properties of fatty acids in the external ear canal of the rabbit. Dermatologica (Basel) 142, 14-22 (1971).

(14) Kligman, A. M., Wheatley, V. R., Mills, O. H., Comedonogenicity of human sebum. Arch. Derm. 102, 267-275 (1970).

(15) Lorincz, A., Krizek, H., Brown, S., Follicular hyperkeratinization induced in the rabbit ear by human skin surface lipids. 13. Int. Congr. Derm. München 2, 1016-1017. Springer-Verlag; Berlin-Heidelberg-New York 1968.

(16) Marples, R. R., Mc Ginley, K. J., Corynebacterium acnes and other anaerobic diphteroids from human skin. J. med. Microbiol. 7, 349-357 (1974).

(17) Plewig, G., Kligman, A. M., Acne. Morphogenesis and treatment. Springer-Verlag Berlin; Berlin-Heidelberg-New York 1975.

(18) Puhvel, S. M., The possible relationship of corynebacterium acnes (propionibacterium acnes) to the pathogenesis of acne vulgaris. J. Amer. med. Wom. Ass. 24, 321-325 (1969).

(19) Roberts, C. D., The role of bacteria in acne vulgaris. PhD Thesis, Leeds 1975.

(20) Schneider, W., Erfahrungen mit einer neuen Aknetherapie. Ein Beispiel für die Bedeutung der sog. Grundlagen in der modernen externen Therapie. Dtsch. med. Wschr. 91, 2017-2022 (1966).

(21) Shalita, A., Genesis of free fatty acids. J. invest. Derm. 62, 332-335 (1974).
(22) Swanbeck, G., A new principle for the treatment of acne. Acta derm.-venereol. (Stockh.) 52, 406-410 (1972).
(23) Voss, J. G., A microbial etiology of acne. Cutis 17, 487-496 (1976).
(24) Wolf, W., Über die Beeinflussung der anaeroben Bakterienflora im Talgdrüsenausführungsgang durch eine äthyllactat- und äthanolhaltige Filmmaske und eine antimikrobielle Tensidlösung. Inauguraldissertation Heidelberg 1978.

Wir danken der Deutschen Forschungsgemeinschaft für die Unterstützung der Untersuchungen.

Wir danken Herrn Dr. K. T. Holland (Department of Microbiology, University of Leeds) und Herrn Dr. G. Scheurlen (Institut für Medizinische Dokumentation, Statistik und Datenverarbeitung der Universität Heidelberg) für ihre Unterstützung bei der Durchführung der Untersuchungen.

J. Soc. Cosmet. Chem., 29, 497–521 (August 1978)

Cosmetic properties and structure of fine-particle synthetic precipitated silicas

S. K. WASON *J. M. Huber Corporation, Chemicals Division,*
P.O. Box 310, Havre de Grace, MD 21078.

Received September 30, 1977. Presented at Annual Scientific Meeting,
Society of Cosmetic Chemists, December 1977, New York, New York.

Synopsis

Submicron-fine particle, synthetic silicas are of three types: fumed silicas, silica gels and precipitated silicas. Recent research has led to the synthesis of a wide variety of new controlled-structure, functional-precipitated silicas which exhibit unique cosmetic and dentifrice properties. The end-use applications of the precipitated silicas can be controlled by controlling their structure. It is now possible to make predictions regarding the thickening, viscosity building, humectant demand index, dentifrice abrasive and polishing characteristics of the new class of synthetic, precipitated products. The methods of preparation, the chemistry, the structure and the new cosmetic applications of the precipitated products are discussed.

I. INTRODUCTION

Fine-particle, synthetic silicas are amorphous, submicron size, white powders. In the literature, these products have often been referred to interchangeably as silicas, hydrated silicas, silicon dioxide, silicic acid, fillers, silica pigments, xerogels, aerogels, amorphous silicas, etc. The discussions which will be presented here will hopefully clarify and distinguish between the various types of silicas.

Silicas can be categorized into two major classes: natural silicas and synthetic silicas. Since the natural silicas are mined from the ground and are quite different in structure, properties and functions than the synthetic silicas, we have excluded these products from our discussion here.

Synthetic silicas are of three types: fumed silicas, silica gels and precipitated silicas—and are prepared either by a vapor phase process or by a liquid phase process. Products which are synthesized by the vapor process are called fumed silicas. The products which are derived from the liquid process or wet process are further categorized as silica gels or precipitated silicas. In the CTFA (Cosmetic, Toiletry and Fragrance Association) cosmetic ingredient dictionary (1) the adopted name for the precipitated silicas and silica gels is hydrated silica; the fumed silicas are referred to as silicas.

For the present discussion we will first review the key properties of the three types of silicas. Then we will discuss the results of our recent research investigation in which we have learned more about the chemistry, structure and properties of the precipitated products. We have learned that the properties of the precipitated silicas can be fixed by controlling their structure during precipitation. We have synthesized precipitated silicas with diverse combinations of properties, and we will discuss how their silica structure can be correlated to key properties and functional performance.

II. OVERALL VIEW OF SYNTHETIC SILICAS

A. METHOD OF PREPARATION

As mentioned earlier, the known synthetic silicas are prepared either by the vapor phase or by the liquid phase process. *Fumed silicas* are prepared by the hydrolysis of silicon tetrachloride vapor in a flame of hydrogen and oxygen at an elevated temperature (2, 3). The reaction conditions are shown in Figure 1. *Silica gels and precipitated silicas* are prepared by the acidulation of aqueous sodium silicate solution (4) with an acidification agent, such as sulfuric acid (see Figure 1). In the case of silica gels, the reaction is generally conducted under acid conditions. The precipitated silicas are produced under alkaline reaction conditions.

PREPARATION OF SILICAS

FUMED SILICAS (VAPOR PROCESS)

Prepared By Steam Hydrolysis Of Silicon Tetrachloride At High Temperatures.

$$2H_2 + O_2 \longrightarrow 2\,H_2O$$

$$SiCl_4 + 2\,H_2O \longrightarrow SiO_2 + 4\,HCl$$

or

$$2\,H_2 + O_2 + SiCl_4 \xrightarrow{1000^\circ C} SiO_2 + 4\,HCl$$

SILICA GELS AND PRECIPITATED SILICAS (LIQUID PROCESS)

$$\underset{\text{SODIUM SILICATE}}{Na_2O \; x \; SiO_2} + H_2SO_4 \longrightarrow x\,SiO_2 + Na_2SO_4 + H_2O$$

SILICA GEL: **Produced Under Acid Conditions.**

PRECIPITATED SILICA: **Produced Under Alkaline Reaction Conditions.**

Figure 1. Preparation of silicas

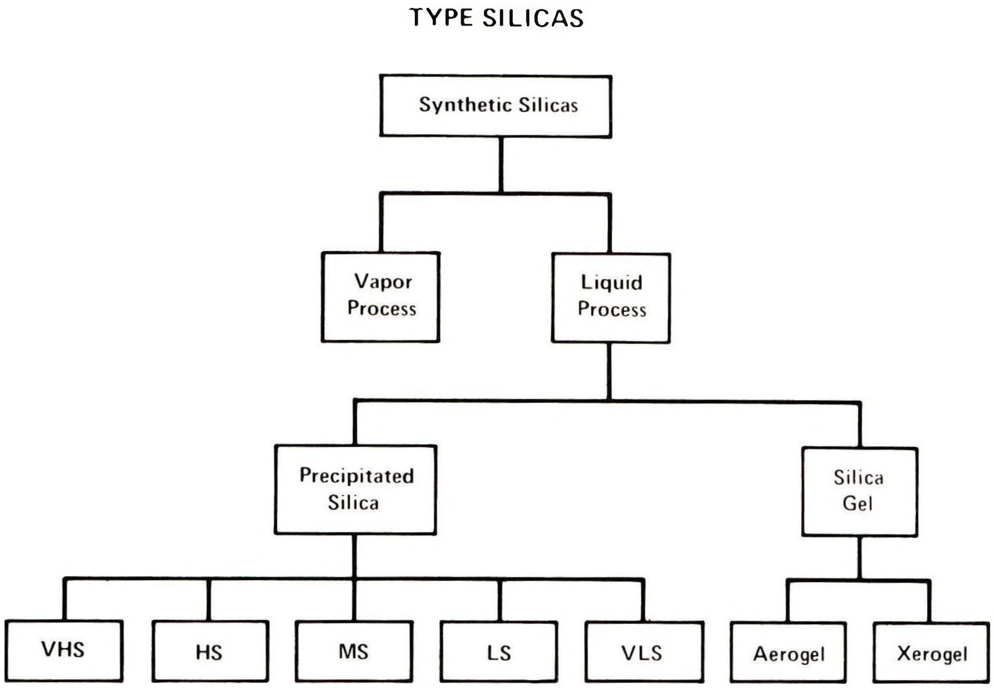

Figure 2. Type silicas

B. TYPES OF SILICAS

A system for classifying the various types of synthetic silicas is found in Figure 2. It is shown in Figure 2 that silica gels are of two types, xerogels and aerogels. During the manufacture of silica gels first a hydrosol, then a hydrogel is formed. When a hydrogel is washed and then dried from an organic medium without the shrinkage of structure (4), it is called an aerogel. Otherwise, it is called a xerogel.

Development of new, controlled-structure silicas has created the need for further classifying the precipitated silicas into five classes (see Figure 2): VHS—Very High Structure, HS—High Structure, MS—Medium Structure, LS—Low Structure and VLS—Very Low Structure.

The end-use properties of a precipitated silica are related to its structure, its particle size and its surface silanol group density. The definitions of the VHS to VLS are discussed later in the text under Section III-B.

C. COMPARATIVE PROPERTIES OF SYNTHETIC SILICAS

The properties of the fumed silicas (prepared via the vapor process) have been studied by many workers (5–7) and their properties have been found to be similar in some respects to the silicas prepared by the liquid phase or wet process. This is understandable in that the properties of the fine-particle synthetic silicas, regardless of their method of preparation, must be related to the following key parameters: BET surface area, particle size and silanol group density.

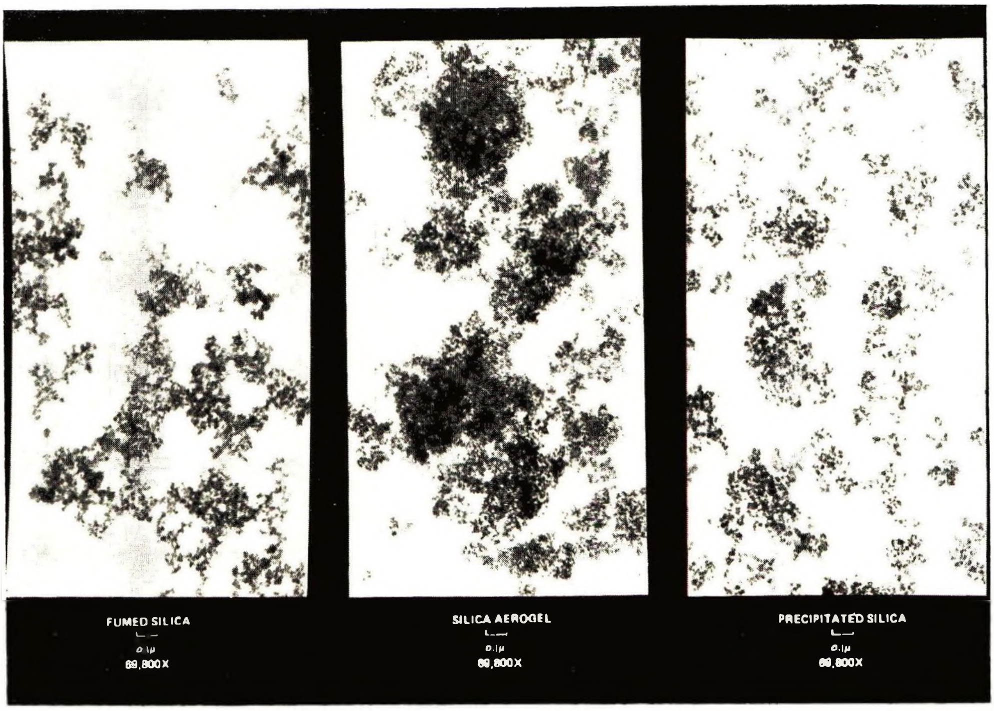

Figure 3. Electron photomicrographs of three types of synthetic silicas

From BET surface area measurement, one can calculate the primary particle diameter of synthetic silicas assuming spherical particles. In real life, these primary particles do not exist in the silica powder as such, but are further aggregated to exhibit the secondary particle structure (3). The secondary particles further aggregate during the manufacturing process to form the tertiary structure called the "agglomerates." Thus in synthetic silicas one can envision the following three types of particle size structure: primary particles (also called ultimate particles), secondary particles (also called aggregates) and tertiary particles (also called agglomerates). Primary particles are easy to recognize in fumed silicas and somewhat more difficult to recognize in precipitated silicas. The existence of primary particles in silica gels is purely hypothetical (8).

We have compared the electron micrographs of a typical fumed silica, a silica aerogel and a precipitated silica in Figure 3 at the same magnification of 69,800X. From the examination of Figure 3, one can clearly recognize the primary particles of the fumed silica. These primary particles exhibit a chain-type structure or secondary structure. In the electron micrograph of the precipitated silica one can recognize the primary structure in which the primary particles form irregular-shaped secondary structure of varying sizes.

In the electron micrograph of the typical silica aerogel one does not see the primary particles; instead, one sees a secondary, three dimensional mesh that is supposedly responsible for the very high internal surface area in silica gels (8).

In Table I we have listed the comparative physical properties of the three types of silicas. Silica gels exhibit very high BET surface area due to internal porosity. Fumed

Table I
Comparative Properties of Three Types of Silicas

PROPERTY	FUMED	SILICA GEL	PRECIPITATED
Surface Area (m^2/g)	200-400	300-1000	60-300
Type Surface Area	External	Internal	External
Porosity	Non-porous	Porous	Both
Bulk Density, g/l	32-64	96-160	160-192
5% pH	3-4.2	4-7.5	6.5-7.5
Silanol Groups/nm^2	2-4	4-8	8-10
Ave. Particle Diameter (nm)	14	--	18
% SiO_2 (Ignited Basis)	99.8 (Min.)	99.5	98.0

silicas and precipitated silicas exhibit relatively lower surface areas in comparison to the silica gels. Both the fumed silicas and precipitated silica are generally nonporous, but it is easy to create microporosity in the precipitated silicas during the process of manufacture.

The surface properties of synthetic silicas, such as viscosity building, thickening, adsorption and rheological properties, are related to the silanol group density of the silica surface and the extent of hydration. The surface properties of silica powders have been reviewed by Hockey (9) and Hair (10). It is generally recognized that there are three types (9, 11–13) of surface hydroxyl groups present on the surface of synthetic silicas: isolated, vicinal (on adjacent silicon atoms) and geminal (two silanols on same silicon atom) silanol groups.

The silanol group density is maximum in the precipitated silicas and eight to ten silanol group/nm^2 have been reported widely in the literature for the precipitated silicas. Since fumed silicas are prepared in a water-deficient reaction condition, it is not too surprising that they have extremely lower silanol group density/nm^2 than do precipitated silicas. It is believed that due to the very high reaction temperature used in the fumed silica process, initially almost all the silanol groups condense to form siloxane groups. But the presence of water vapor and lower temperature during the final stages of the manufacturing process result in rehydroxylation which increases the silanol group content in the fumed silicas to a final value of two to four OH group/nm^2.

Silica gels exhibit silanol group density intermediate between the extreme exhibited by the fumed and the precipitated silicas.

III. NEW CONTROLLED-STRUCTURE PRECIPITATED SILICAS

A. PROCESS VARIABLES

Precipitated silicas are produced by the acidulation of sodium silicate solutions with a mineral acid. The product properties can be controlled by controlling the key process variables. The key process variables and the manufacturing steps used in producing the precipitated silicas are depicted in Figure 4.

As an illustration, a low-structure precipitated silica is prepared (14 a, b, c) by first adding a fraction of the theoretical silicate needed for the reaction to a heated, stirred

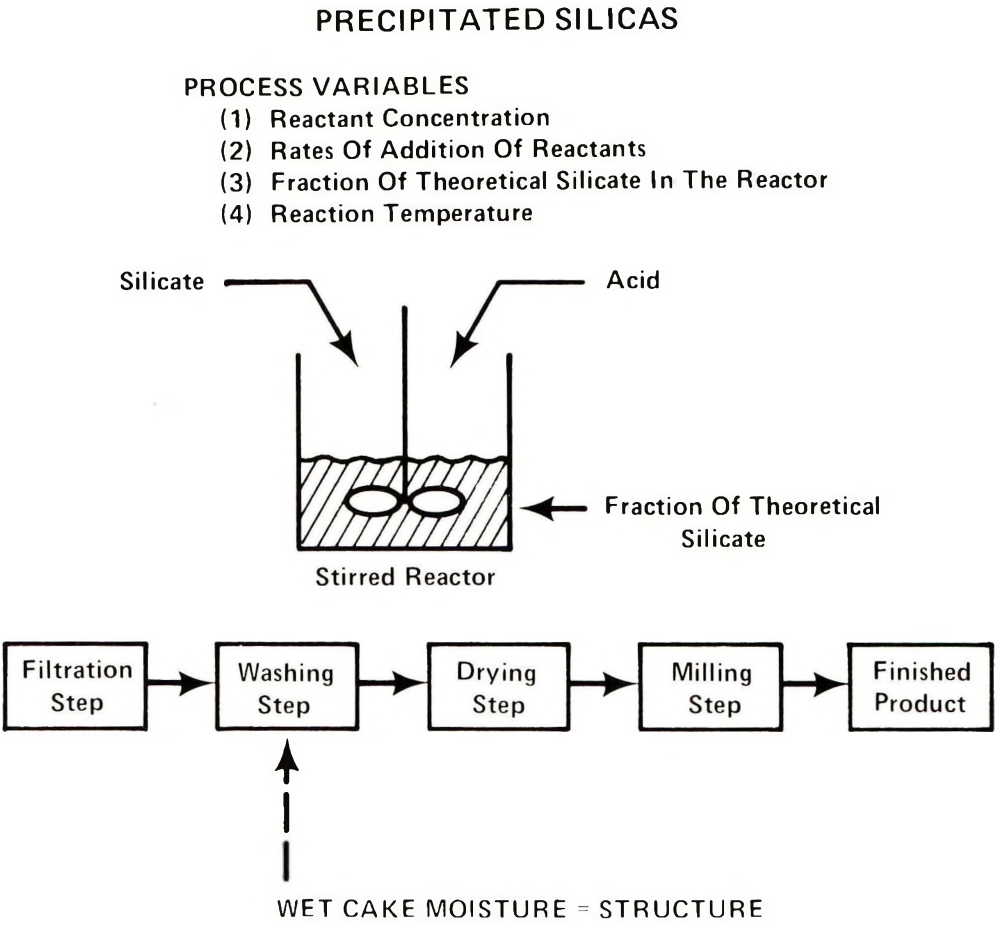

Figure 4. Precipitated silica manufacturing steps

reactor and then simultaneously adding the acidulating agent and the remaining silicate at predetermined rates until the silica precipitation is completed. At this point the precipitate is filtered, washed to remove the sodium sulfate by-product, dried and milled to the desired degree of fineness.

It turns out that the amount of water associated with the washed silica precipitate is the structural water, and it is a very important property which "tags" the product properties of the resulting dry finished product. This property is referred to as the % wet cake moisture (WCM). Under a given set of manufacturing and process conditions, % WCM will vary with the structure level of the dry product. A product with a very high % WCM content is defined as a high-structure silica and a product with a relatively low water content is defined as a low-structure silica. In this context, we will use % WCM or structure synonymously.

B. WET CAKE MOISTURE VERSUS STRUCTURE INDEX

As mentioned above, the water content of the precipitated product prior to drying is an important property. This water is present between the particles and inside the parti-

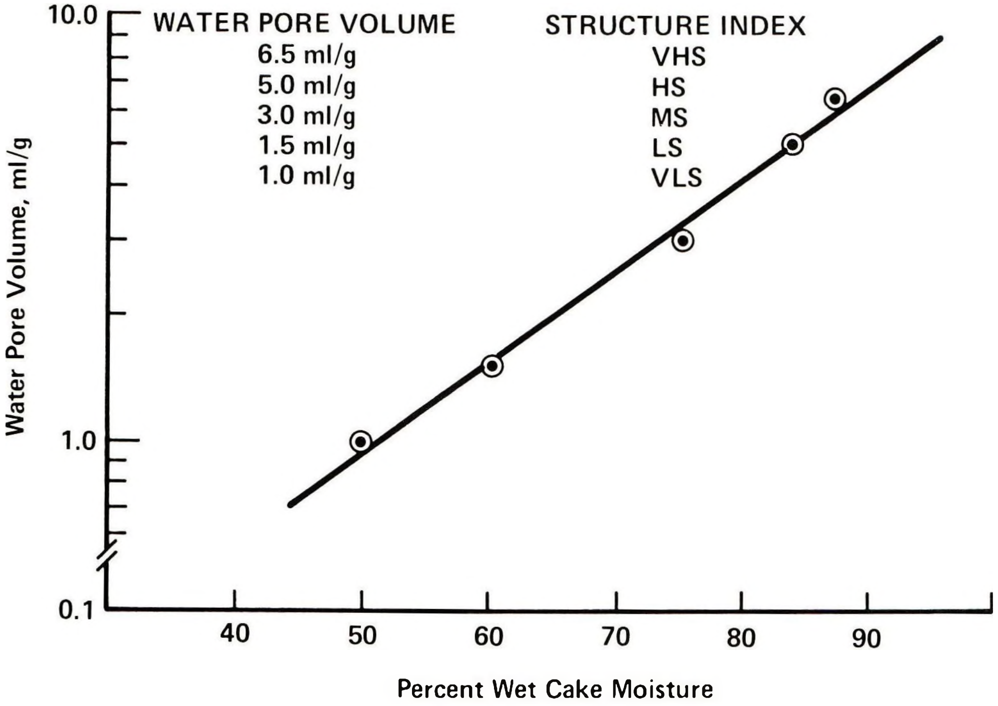

Figure 5. Plot of water pore volume versus WET cake moisture

cles. Therefore, at a fixed set of reaction conditions, the water associated with the precipitate or the filter cake is called the structural water. The amount of water associated with one part of the dry, recoverable product is defined as the water pore volume. The amount of water associated with 100 parts of the dry recoverable product is defined as Structure Index (SI) (15 a, b). Thus the water pore volume (PV) and SI are related to the % WCM by the following equation.

$$PV = \left(\frac{\%\ \mathrm{WCM}}{100 - \%\ \mathrm{WCM}} \right) \qquad (1)$$

$$SI = \left(\frac{\%\ \mathrm{WCM}}{100 - \%\ \mathrm{WCM}} \right) \times 100 \qquad (2)$$

A plot of water pore volume versus the % WCM is shown in Figure 5. Thus a product with water pore volume above 6.5 or SI values above 650 is arbitrarily defined as a VHS (very high structure silica). A low structure silica (LS) is one which exhibits a water pore volume above 1.5 or SI values above 150. These definitions are clearly explained in Figure 5. It must be pointed out that the log of the water pore volume or the log SI is linearly related to the % WCM. The SI values of products between the % WCM values of 80 to 85 are given in Table II (15).

C. STRUCTURE CONTROL

One of the key variables which can be used for controlling the properties and the structure of silica is the fraction of the theoretical silicate which is added to the reaction me-

Table II
WET Cake Moisture (WCM) Versus Structure Index (SI)

% WCM	SI
80	400.0
81	426.3
82	455.5
83	488.2
84	525.0
85	566.7

dium prior to the acidulation. Figure 6 shows how the silica structure increases as the fraction of the theoretical silicate in the reaction medium increases.

D. ELECTRON PHOTOMICROGRAPHS OF CONTROLLED STRUCTURE SILICAS

The electron photomicrographs of VHS (very high structure) and HS (high structure) silicas are shown in Figure 7. The comparative photomicrographs of MS (medium structure) and LS (low structure) silicas are shown in Figure 8. In Table III we have compared the particle size of the VHS to LS silicas. Examination of Table III clearly points to the fact that the primary particle size increases as the silica structure level decreases. Thus the control of particle size via controlling the silica structure provides an important tool for producing silicas for diverse specialty and cosmetic applications.

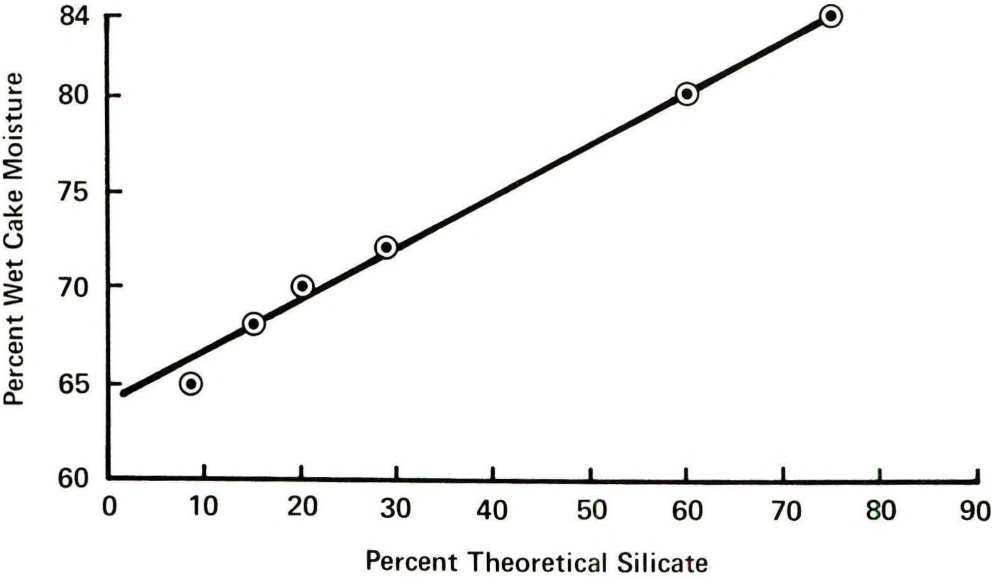

Figure 6. Method of controlling the silica structure

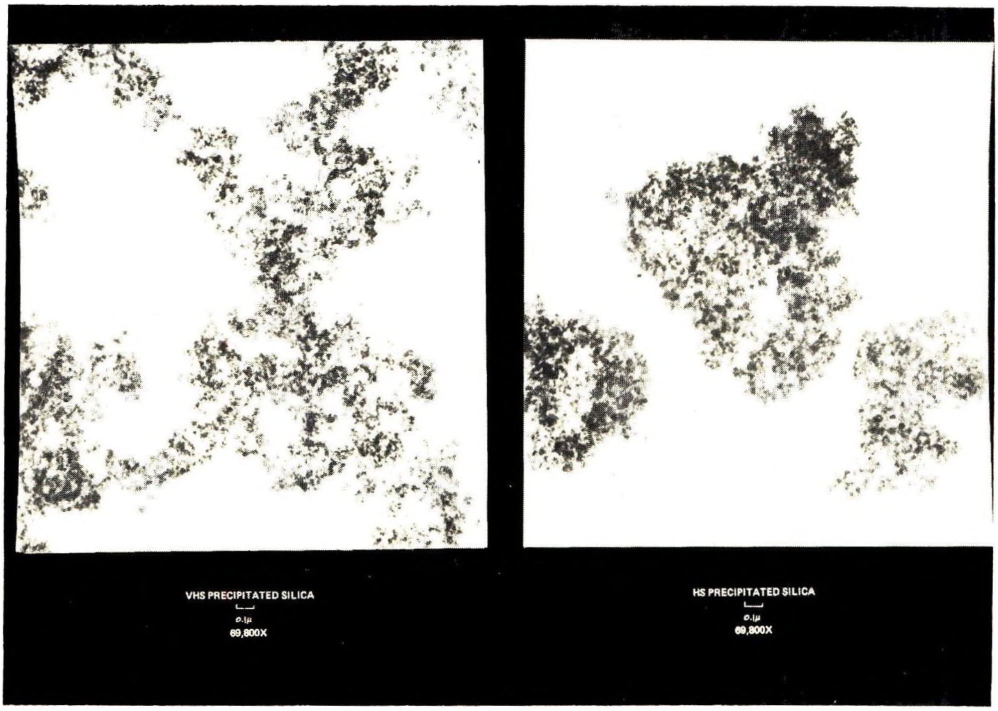

Figure 7. Electron photomicrographs of VHS and HS silicas

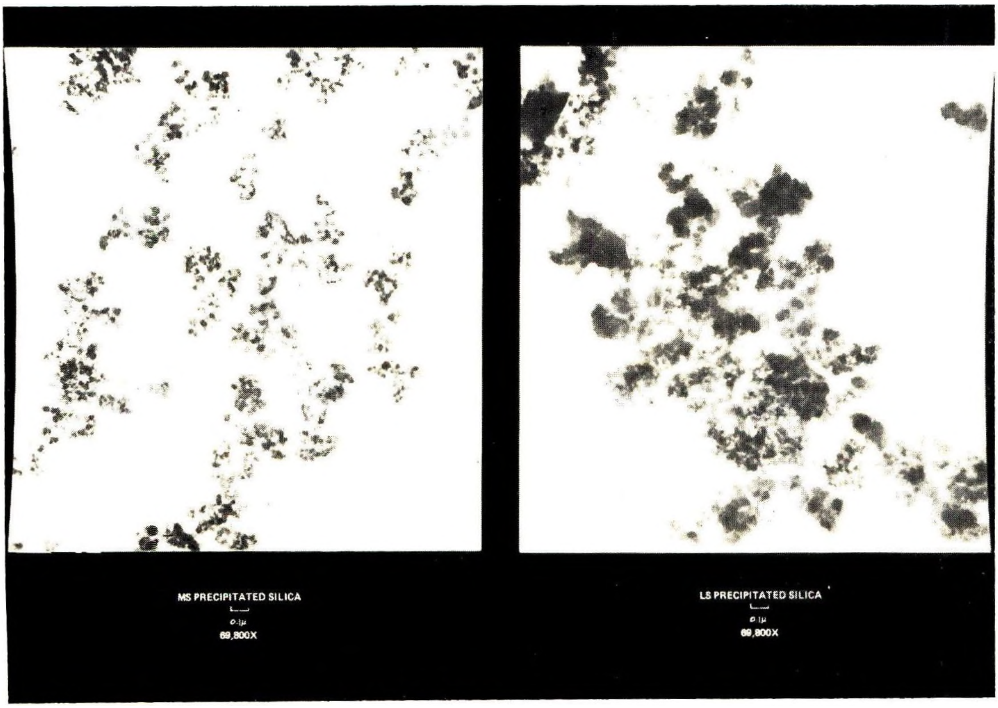

Figure 8. Electron photomicrographs of MS and LS silicas

Table III
Particle Size of Precipitated Silicas

STRUCTURE	EMSA m²/g	PARTICLE DIAMETERS, nm MEAN PARTICLE DIAMETER	MINI-MUM	MAXI-MUM
VHS	250	12	5	20
HS	175	17	5	30
MS	145	20	5	25
LS	60	51	5	300

IV. RESULTS AND DISCUSSIONS

A. METHOD OF EVALUATION AND PROPERTIES OF PRECIPITATED SILICAS

Six controlled-structure silicas (structure level from VHS to VLS) were prepared similar to the method illustrated in Figure 6. All the precipitated samples were washed, dried and air micronized to produce micron-size silicas. These six samples were designated as A, B, C, D, E and F. The finished samples were characterized by the various physical properties, such as oil absorption (OA), glycerine absorption (GA), mineral oil absorption (MA), sorbitol absorption (SA), BET surface area (BET), average particle size (APS), porosity by mercury intrusion (HGI), glycerine demand index (GDI), mineral oil demand index (MDI), sorbitol demand index (SDI), % wet cake moisture (WCM) and structure index (SI). The data are summarized in Tables IV and V. The oil absorption of silicas was determined by the ASTM rub-out method (16). This test is based on the principle of mixing linseed oil with a silica by rubbing with a spatula on a smooth surface until a stiff putty-like paste is formed. By measuring the quantity of oil required to produce a very stiff, putty-like paste, which will not break or separate when it is cut with the spatula, one can measure the oil absorption of silica—a value which represents the volume of oil required per unit weight of silica to saturate the silica sorptive capacity. The oil absorption value is calculated by the following eq 3.

$$\text{Oil Absorption} = \frac{\text{ml oil absorption} \times 100}{\text{weight of silica sample, gram}} \tag{3}$$

$$= \text{ml oil}/100\text{ g silica}$$

The ASTM method was modified in that the linseed oil was replaced by glycerine, mineral oil (saybolt viscosity 340 to 350) or sorbitol (70% solution) when running the respective humectant and mineral oil absorption values.

Surface area was determined by the nitrogen adsorption method (17) of Brunauer, Emmett and Teller (BET) while the average particle size (secondary particle size) was determined by the Coulter Counter method (18) using Model TAII.

The void volume of silicas was determined by the Aminco-Winslow Porosimeter (19). This instrument is a completely hydraulic machine used to measure the void structure of various materials. The mercury is forced into the voids as a function of pressure and the volume of mercury intruded per gram of sample is calculated at each pressure setting. Increments in volume (cc/g) at each pressure setting are plotted against the void size corresponding to the pressure setting increments. We have listed in Table IV the total intruded volume of mercury in cc Hg/g of silica.

Table IV
Properties of Precipitated Controlled Structure Silica Samples (A-F)

PROPERTIES/PRODUCT	A	B	C	D	E	F
STRUCTURE CODE	VHS	HS	MS	MS	LS	VLS
% WET CAKE MOISTURE	86	84	80	75	60	55
STRUCTURE INDEX	614.3	525.0	400.0	300.0	150.0	122.0
OIL ABSORPTION, ml/100g	210	196	177	153	92	72
GLYCERINE ABSORPTION, ml/100g	163	140	136	119	113	72
SORBITOL ABSORPTION, ml/100g	196	189	158	148	120	75
MINERAL OIL ABSORPTION, ml/100g	205	199	175	161	99	90
BET SURFACE AREA, m^2/g	200	140	125	85	65	50
AVG. PARTICLE DIAMETER, μm	3.0	3.2	4.2	6.4	8.0	9.6
MERCURY INTRUSION POROSITY, ccHg/g	6.32	5.39	4.66	3.94	1.84	1.58

Glycerine demand index (GDI), mineral oil demand index (MDI) and sorbitol demand index (SDI) values (listed in Table V) were determined by converting the respective liquid into free-flowing powders by the addition of silica for ease of handling and blending into dry formulations. Silica was mixed with a known weight of liquid until a free-flowing powder was obtained. The humectant demand index (HDI) or the drying-up capacity was calculated as the weight of the liquid dried up by 100 g of silica until a free-flowing powder was obtained.

The % WCM values of the precipitated silicas were determined by drying 100 g of the washed precipitate or the filter cake at 150°C until a constant weight of dry silica was obtained. The % WCM value is obtained by subtracting the dry weight of silica from 100 (the gross weight of the precipitate).

The SI values were calculated by using eq 2.

B. CORRELATION OF PROPERTIES VERSUS SILICA STRUCTURE

The experimental data listed in Tables IV and V were evaluated by a computer program using multilinear regression eq 4

$$\bar{Y} = \sum_{i=1}^{n} a_i \bar{x}_i + b \qquad (4)$$

where $\bar{Y}$ is the dependent variable such as % WCM or SI, $\bar{x}$ the independent variable and "a" is a multilinear regression coefficient.

Table V
Humectant Demand Index (Drying-up Capacity) Versus Precipitated Silica Structure

PROPERTY/PRODUCT	A	B	C	D	E	F
% WET CAKE MOISTURE	86	84	80	75	60	55
STRUCTURE INDEX	614.3	525.0	400.0	300.0	150.0	122.0
STRUCTURE CODE	VHS	HS	MS	MS	LS	VLS
GLYCERINE DEMAND INDEX, g/100g	265.0	242.5	233.3	212.5	100.0	92.1
MINERAL OIL DEMAND INDEX, g/100g	233.3	203.0	194.1	150.0	81.8	73.3
SORBITOL DEMAND INDEX, g/100g	257.1	244.8	233.3	185.7	98.0	88.7

Table VI

Correlations Between Precipitated Silica Structure (% WCM and SI) and its Physical Properties

STRUCTURE PARAMETER	PROPERTIES	CORRELATION COEFFICIENT	STRUCTURE PARAMETER	PROPERTIES	CORRELATION COEFFICIENT
% WCM	OIL ABSORPTION	0.998	LOG STRUCTURE INDEX	OIL ABSORPTION	0.999
	GLYCERINE ABSORPTION	0.920		GLYCERINE ABSORPTION	0.925
	SORBITOL ABSORPTION	0.967		SORBITOL ABSORPTION	0.970
	MINERAL OIL ABSORPTION	0.996		MINERAL OIL ABSORPTION	0.997
	BET SURFACE AREA	0.895		BET SURFACE AREA	0.926
	AVG. PARTICLE DIAMETER	0.981		AVG. PARTICLE DIAMETER	0.986
	MERCURY INTRUSION POROSITY	0.985		MERCURY INTRUSION POROSITY	0.995
	GLYCERINE DEMAND INDEX	0.991		GLYCERINE DEMAND INDEX	0.984
	MINERAL OIL DEMAND INDEX	0.986		MINERAL OIL DEMAND INDEX	0.993
	SORBITOL DEMAND INDEX	0.993		SORBITOL DEMAND INDEX	0.992

The calculations were carried out by the computer in which a correlation matrix is determined first. Then the program introduces the independent variable one by one. In step one, the variable $\overline{x}$ is introduced which has the strongest correlation with $\overline{Y}$. At each consecutive step the independent variable is introduced by the program which has the best correlation coefficient. Table VI gives the correlation coefficient results when the silica % WCM and log structure index (dependent variables) were correlated with the various physical properties listed in Tables IV and V. Note in Table VI that the % WCM and log structure index parameters of silicas correlate very well with the physical properties of silicas samples A through F. The various mathematical equations relating the silica structure with its physical properties are listed in Table VII. These equations suggest that there is a very high degree of correlations between the silica structure and its physical properties.

C. OIL ABSORPTION VERSUS STRUCTURE INDEX

The structure (% WCM) of silica correlates very well with the oil absorption. Therefore the oil absorption value can be used for predicting the end-use properties of the precipitated silicas. A plot of log SI versus oil absorption is shown in Figure 9.

Table VII

Mathematical Relationship Between the Precipitated Silica Structure and Its Physical Properties

% WCM (SILICA STRUCTURE) = 0.23 (OIL ABSORPTION) + 39.0
LOG SI (STRUCTURE INDEX) = 0.012 (OIL ABSORPTION) + 3.93

% WCM (SILICA STRUCTURE) = 0.38 (GLYCERINE ABSORPTION) + 25.7
LOG SI (STRUCTURE INDEX) = 0.019 (GLYCERINE ABSORPTION) + 3.24

% WCM (SILICA STRUCTURE) 0.26 (MINERAL OIL ABSORPTION) + 33.0
LOG SI (STRUCTURE INDEX) = 0.013 (MINERAL OIL ABSORPTION) + 3.63

%WCM (SILICA STRUCTURE) = 0.28 (SORBITOL ABSORPTION) + 32.4
LOG SI (STRUCTURE INDEX) = 0.014 (SORBITOL ABSORPTION) + 3.59

% WCM (STRUCTURE) = 0.21 (SURFACE AREA) + 50.3
LOG SI (STRUCTURE INDEX) = 0.011 (SURFACE AREA) + 4.47

% WCM (STRUCTURE) = -4.7 (AVG. PARTICLE SIZE) + 100.1
LOG SI (STRUCTURE INDEX) = -0.24 (AVG. PARTICLE SIZE) + 7.08

% WCM (STRUCTURE) = 6.7 (MERCURY INTRUSION POROSITY) + 47.0
LOG SI (STRUCTURE INDEX) = 0.34 (MERCURY INTRUSION POROSITY) + 4.33

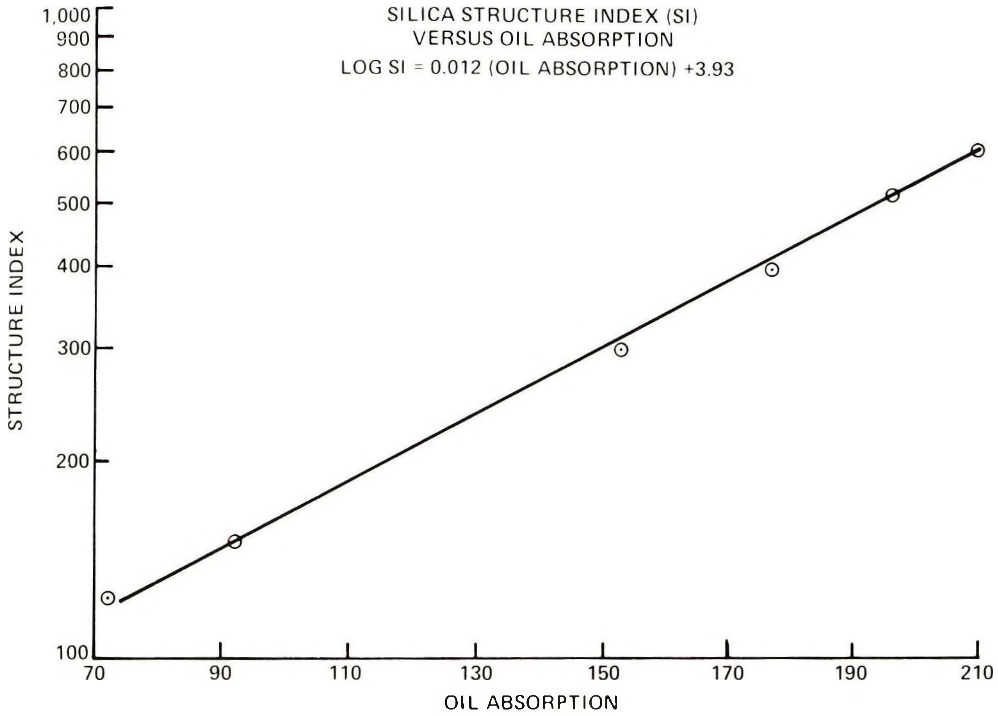

Figure 9. Plot of silica structure versus oil absorption

Experience of producing a wide variety of precipitated silicas has led us to the conclusion that VHS silicas exhibit oil absorption values above 200 ml oil/100 g silicas. The precipitated silicas between the oil absorption range of 125 to 175 ml/100 g silica are classified as MS silicas. Products with oil values below 200 and above 175 are called HS silicas. Products below 75 ml oil/100 g silica are called VLS silicas and the LS silicas range between the values 75 to 125 ml oil/100 g silica. Note that in Table IV we have referred to the product "C" as MS silica due to its WCM and SI values even though its oil absorption is slightly above the 175 ml oil/100 g silica cut-off range for the MS structure silica.

D. GLYCERINE, MINERAL OIL AND SORBITOL ABSORPTION VERSUS THE SILICA STRUCTURE

Figure 10 shows the relationship between the % WCM of silica samples and their corresponding mineral oil absorptions. Figure 11 is a plot of log SI versus the humectant absorption values of the various controlled-structure silicas. The mineral oil absorption values are relatively higher than the glycerine/sorbitol absorptions obtained with the same silica samples (see Table IV). This may be due to the nonhydrogen-bonding nature of the mineral oil. Note, also that the sorbitol absorption values are higher than the corresponding glycerine absorption values. The mathematical relationships between the silica structure and various liquid absorption values are predicted by the regression program. These equations are listed in Table VII as well as in Figures 10 and 11.

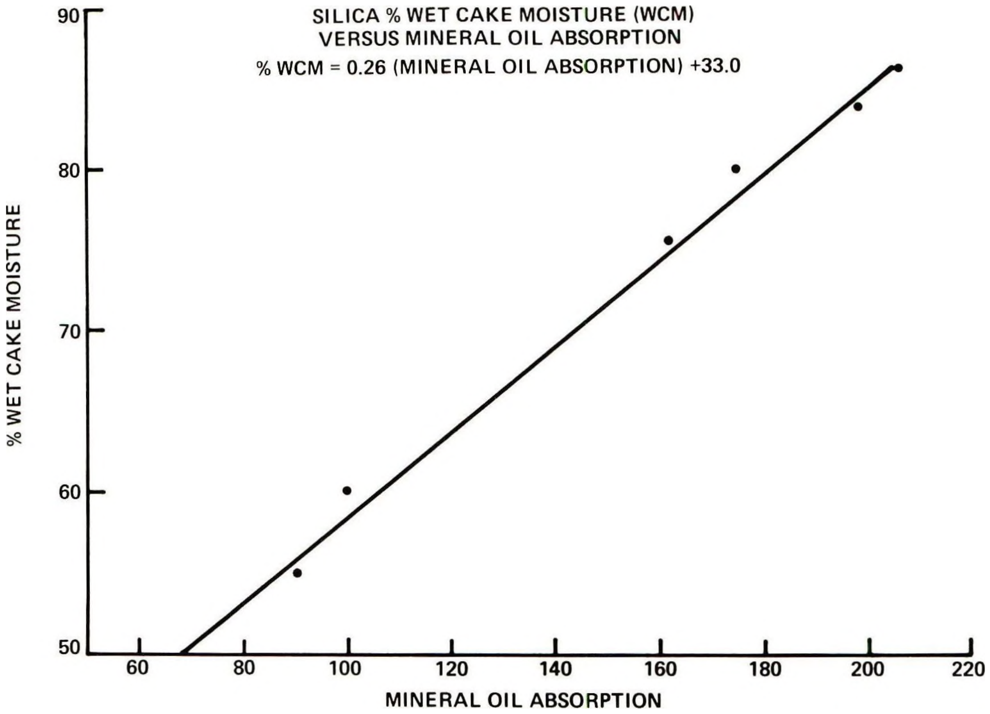

Figure 10. Plot of silica structure versus mineral oil absorption

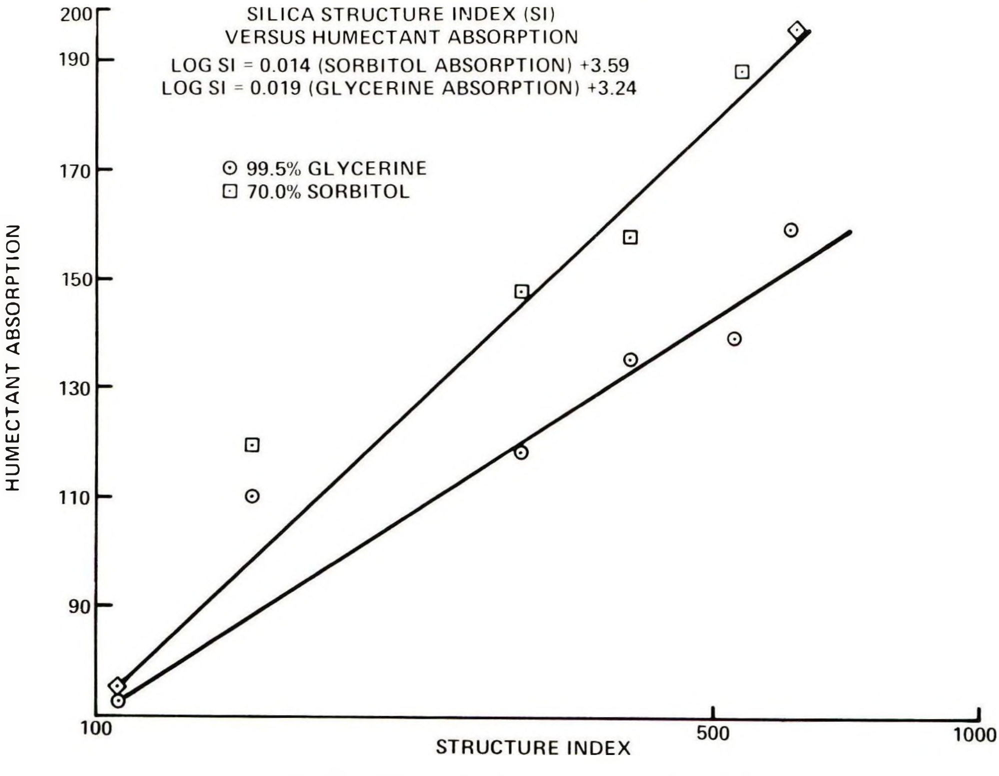

Figure 11. Plot of silica structure versus humectant absorption

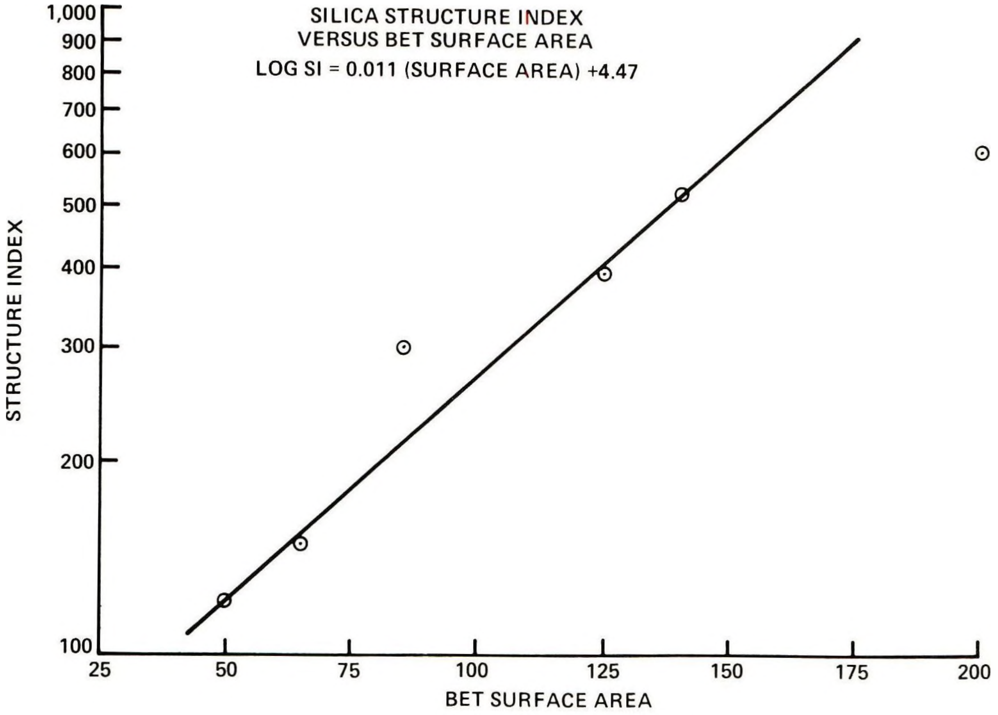

Figure 12. Plot of structure index versus BET surface area

E. SILICA STRUCTURE VERSUS THE BET SURFACE AREA

The BET surface area of the various controlled-structure silicas was correlated with the silica structure. A plot of log SI versus the BET surface area of the six controlled-structure silicas of Table IV is depicted in Figure 12.

F. AVERAGE PARTICLE SIZE VERSUS THE SILICA STRUCTURE

A good correlation was obtained between the various structurally different silica samples and their corresponding average particle size (secondary particle size). A plot of % WCM and APS (average particle size) is shown in Figure 13. Thus it is clear that as the silica structure decreases, the particle size correspondingly increases (see also Tables IV and VII).

G. VOID VOLUME VERSUS THE SILICA STRUCTURE

The relationship between the void volume of silica as determined by the mercury intrusion method and its silica structure is shown in Figure 14. A low-structure silica exhibits low-void volume and as the silica structure increases, the void volume of silica correspondingly increases. This is shown mathematically by regression equations in Table VII as well as in Figure 14.

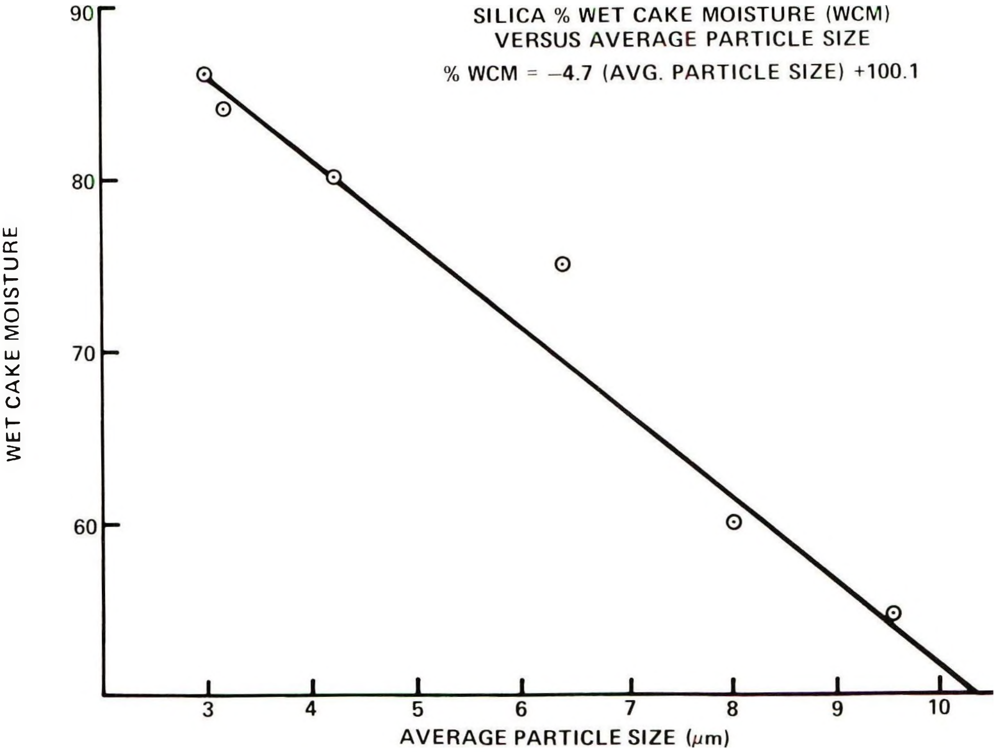

Figure 13. Plot of silica structure versus average particle size

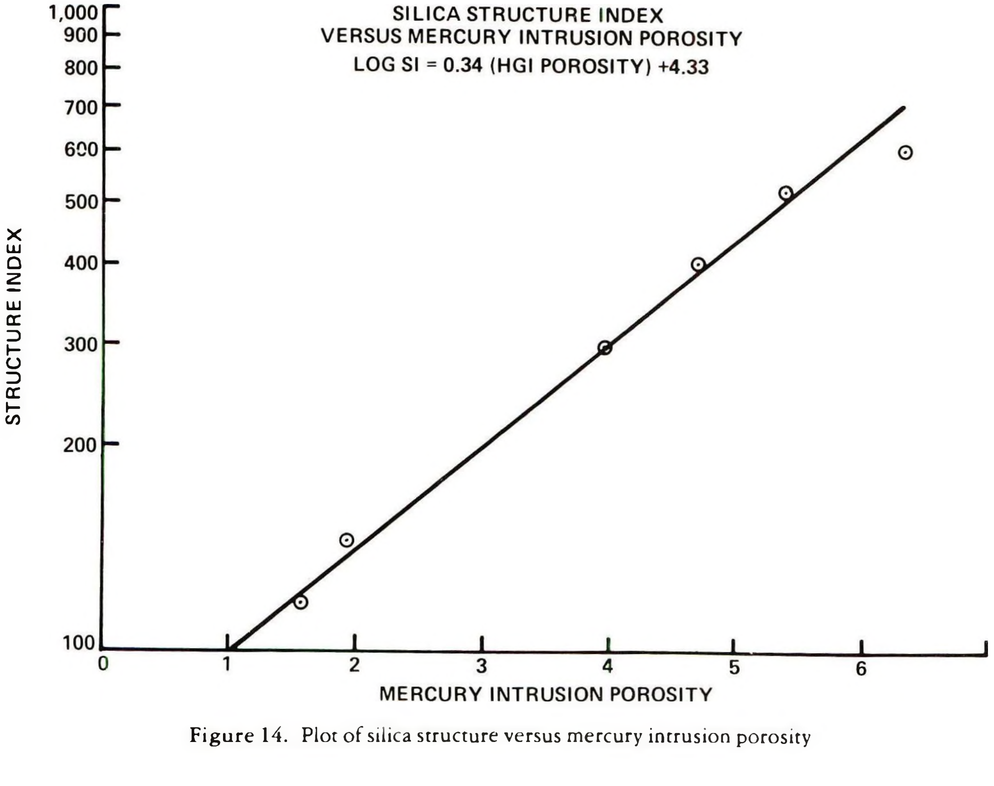

Figure 14. Plot of silica structure versus mercury intrusion porosity

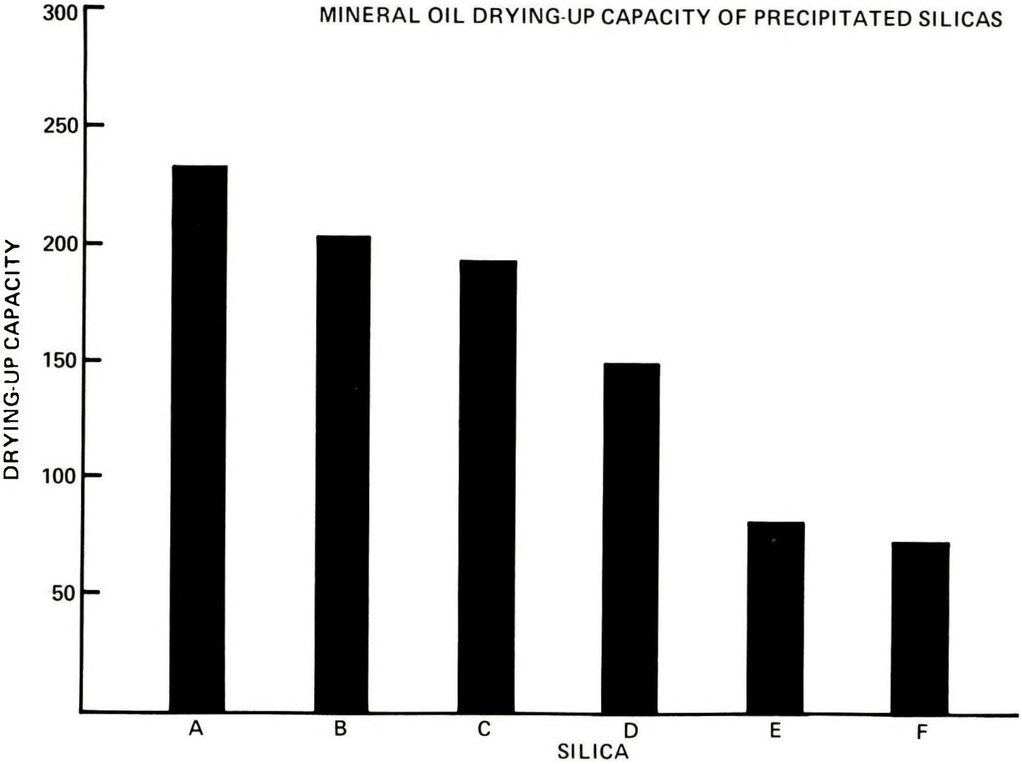

Figure 15. Mineral oil drying-up capacity of precipitated silicas

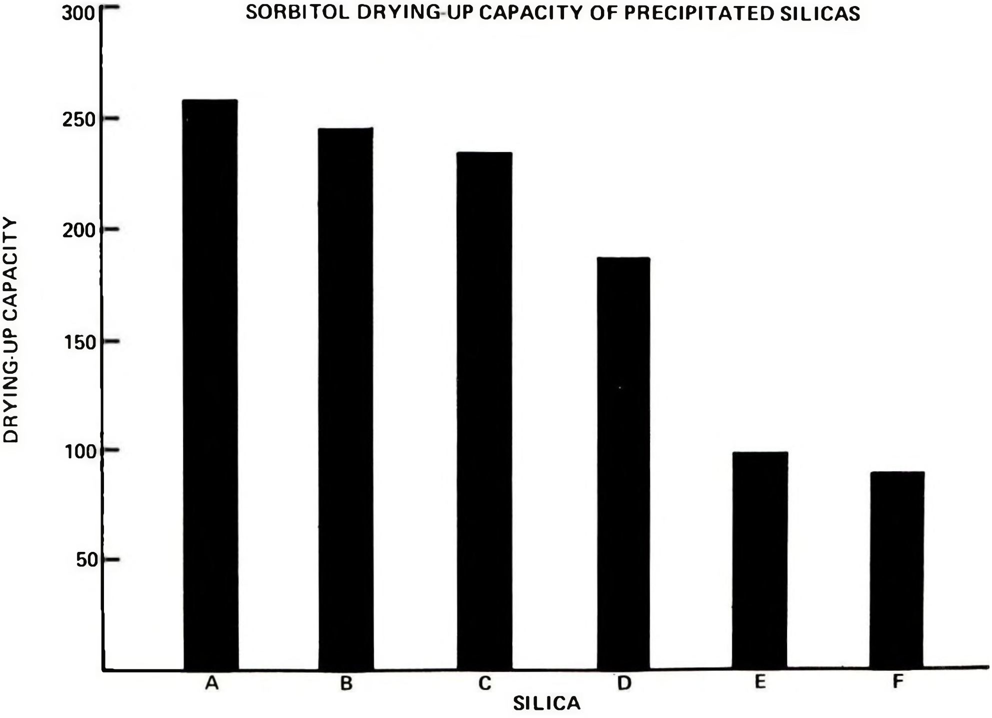

Figure 16. Sorbitol drying-up capacity of precipitated silicas

H. GLYCERINE, SORBITOL AND MINERAL OIL DEMAND INDEX VERSUS SILICA STRUCTURE

Precipitated silicas are used for converting the liquids into dry, free-flowing powders. This technique is used for ease of handling and dry blending "liquids" into many formulations. The drying-up capacity of precipitated silicas increases with the increase in the silica structure level. This is shown in Figures 15–17 and data are listed in Table V.

V. DENTIFRICE PROPERTIES OF CONTROLLED-STRUCTURE PRECIPITATED SILICAS

A. THICKENING AND VISCOSITY BUILDING PROPERTIES

The thickening and viscosity building properties of the six controlled-structure silica samples (for physical properties of silica, see Table IV) were studied in a nonhydrogen-bonding liquid (mineral oil), as well as a hydrogen-bonding liquid, such as glycerine (poly functional alcohol). The effect of silica concentration on the viscosity of mineral oil and glycerine is shown in Figures 18 and 19, respectively.

The thickening and viscosity building properties of the precipitated silicas are influenced by the following factors: 1) nature of the liquid medium, 2) structure of the precipitated silica, 3) concentration of the silica, 4) particle size and surface area of the silica, 5) silanol group density, 6) degree of dispersion, 7) nature of additives, if any, and 8) pH of the system.

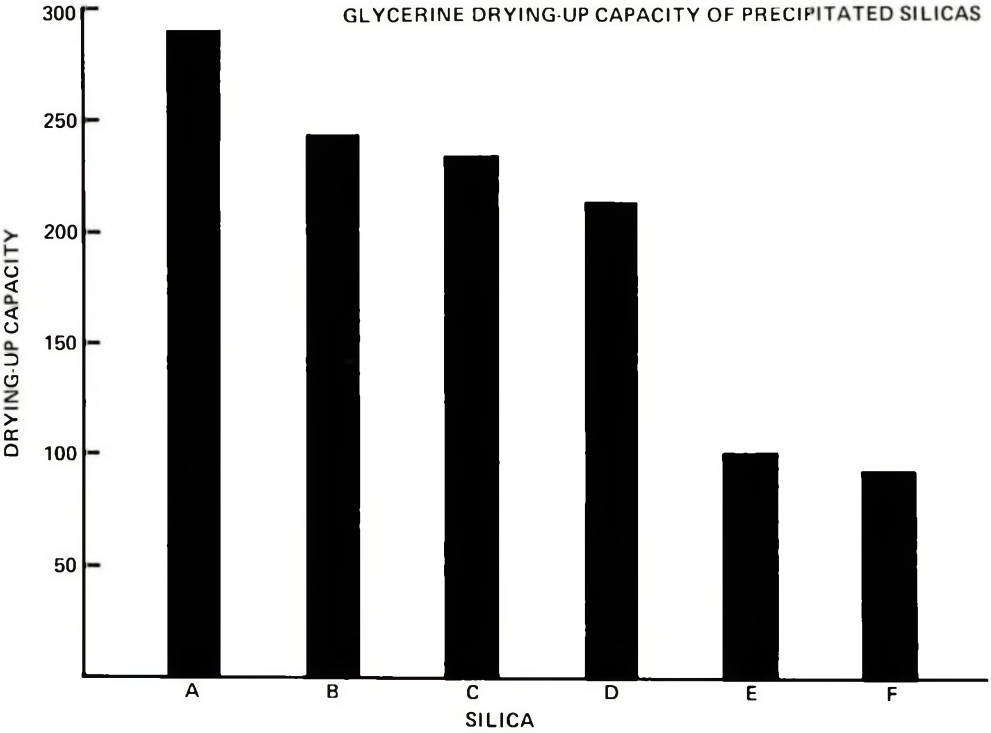

Figure 17. Glycerine drying-up capacity of precipitated silicas

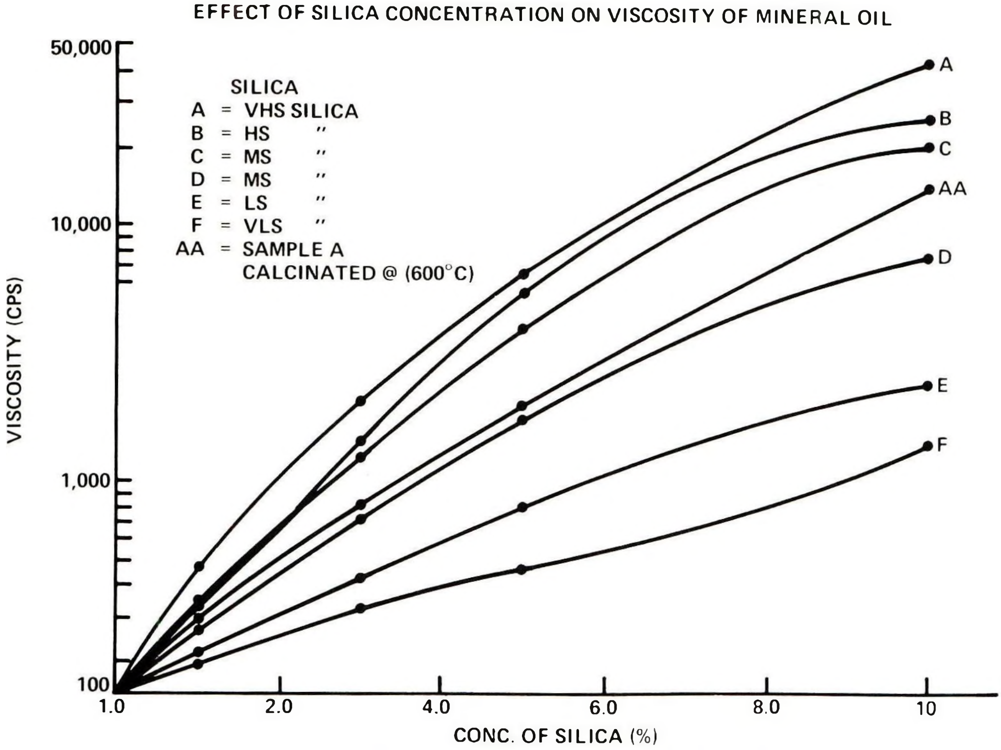

Figure 18. Effect of silica concentration on viscosity of mineral oil

From Figure 18, it is clear that only 3 to 6% of VHS silica (Sample A) is extremely effective in increasing the viscosity of mineral oil. At the same level of concentration (3 to 6%) the viscosity increase produced by the VHS silica (Sample A) is much lower in the glycerine medium.

This result is explained by the fact that the precipitated silicas produce a much higher viscosity increase when added to the nonhydrogen-bonding liquid system (mineral oil). In the nonhydrogen-bonding systems, the hydroxyl groups of the precipitated silicas have a greater tendency to hydrogen bond with each other because there is no competition for hydrogen bonding in the liquid medium. This situation is reversed when the silica is added to a hydrogen-bonding liquid system such as glycerine. The hydrogen-bonding liquid system competes for the silanol group of silicas thereby reducing the ability of the silica-silanol groups to hydrogen bond with each other. This explains the lower viscosity increase observed when silicas are added to the hydrogen-bonding liquid system.

The viscosity of a liquid system would increase when the silica structure level increases, the particle size decreases, the BET surface area increases and the silica concentration or use level increases.

It appears that the silanol group density of silicas also influences the viscosity of liquid systems. To prove this concept, a VHS silica, Sample A, was calcined for 2 hr at 600°C to partially remove the silanol groups. This calcined silica material, AA, was added to mineral oil to study the viscosity effects. From Figure 18, it is clear that the viscosity increase contributed by Sample AA (calcined VHS silica) is much lower than the vis-

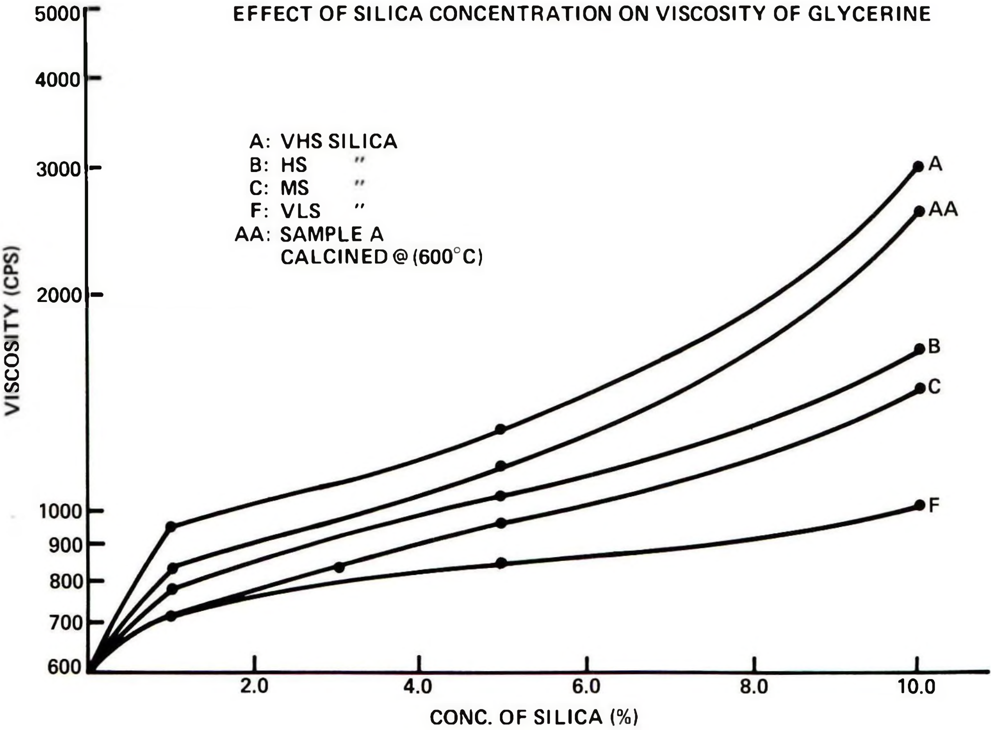

Figure 19. Effect of silica concentration on viscosity of glycerine

cosity increase obtained with the regular Sample A. This substantiates the fact that silica thickener efficiency is reduced when silanol groups are partially removed.

Additives have an effect on the viscosity behavior of silicas in various systems. In general, addition of 1 to 2% by weight (based on total weight of system) of a hydrogen-bonding additive (ethylene glycol, amines, etc.) to precipitated silica in a nonhydrogen-bonding or slightly polar system will increase viscosity because addition of the additive will increase the probability of silanol—silanol group interactions by acting as bridging groups. Large addition of additives (5 to 10%) of hydrogen-bonding additive would tend to decrease the viscosity of nonhydrogen-bonding, liquid-silica system.

It has been observed that the most favorable pH range for thickening liquid systems capable of hydrogen bonding is between 4 to 8; the maximum viscosity is obtained with silica close to pH 7.

In summarizing, for cosmetic applications one needs to choose a very high structure silica with the highest BET surface area and the finest particle size to obtain the maximum viscosity increase in a given system.

B. DENTIFRICE SILICA ABRASIVES VERSUS RDA

Dentifrice compositions contain an abrasive, liquid humectant, thickener, sudsing agent, flavor and minor amounts of other optional ingredients. Extensive studies have been undertaken by many workers concerning the cleaning, polishing and abrasivity of dentifrices. It is generally recognized in the literature that abrasivity and cleaning properties are more or less directly related, i.e., the higher the abrasivity, the greater the cleaning efficiency (20, 21).

It is well recognized that a dentifrice should contain some abrasive agent (21–23), but there has been concern expressed over the possible deleterious effects of excessive abrasiveness (20, 24, 25). The Council on Dental Therapeutics (24) cautions that a dentifrice should be no more abrasive than is necessary to keep teeth free of accessible plaque, debris and superficial stain.

We have undertaken extensive research and developed methods by which we can control the abrasivity of precipitated silicas (14, 15). Ideally, dentifrice abrasive should provide maximum cleaning and polishing with minimum abrasion to enamel, dentin and cementum. To do an effective job in a dentifrice, we believe the silica abrasive should exhibit the following properties: lowest humectant demand, controlled abrasivity, controlled particle size and shape, good fluoride compatibility, good cleaning properties and acceptable surface properties and compatibility behavior.

In a series of tests, we have found that low-structure precipitated silicas can be used effectively in dentifrices to provide an acceptable cleaning at low abrasion. The RDA (26) (radioactive dentin abrasion) of precipitated silica abrasives is related to silica structure (15). A plot of silica abrasive RDA versus its oil absorption is shown in Figure 20.

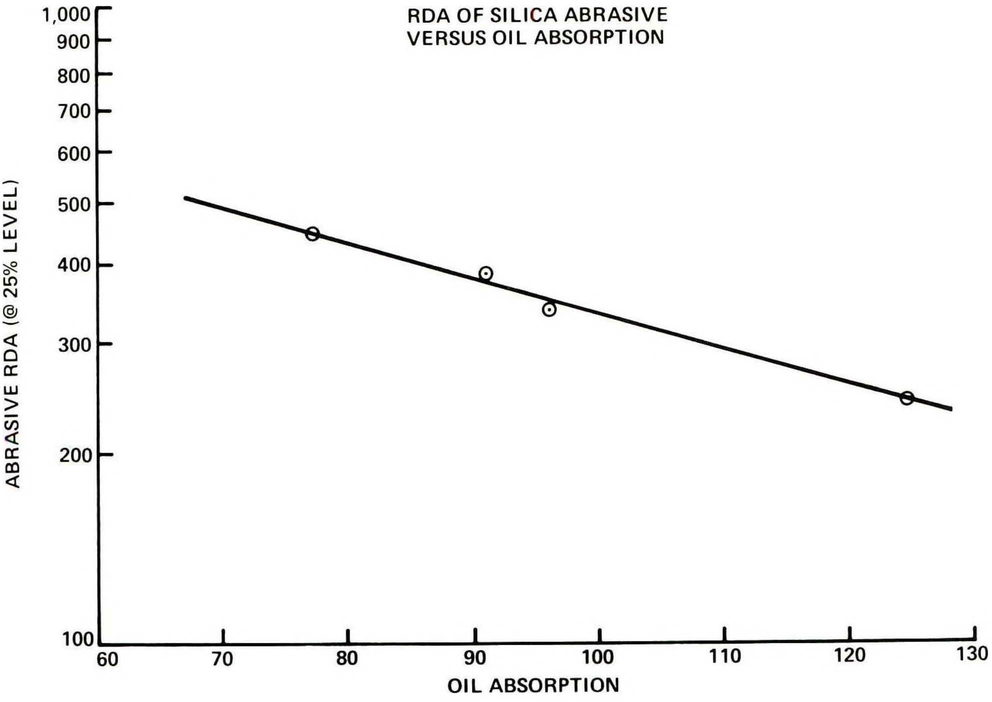

Figure 20. Plot of silica RDA versus oil absorption

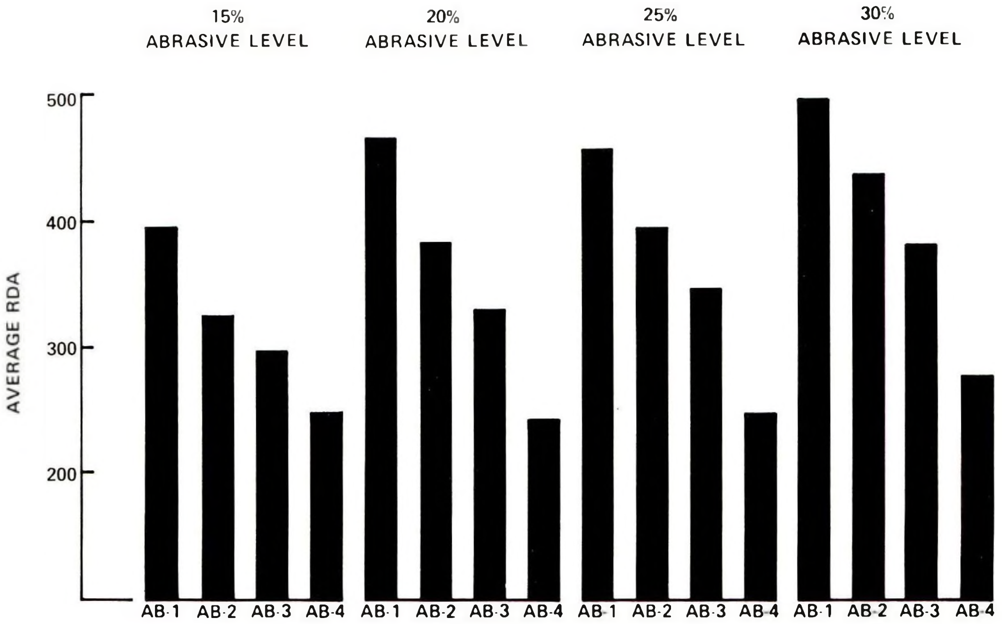

Figure 21. Effect of silica concentration on RDA

C. RDA VERSUS ABRASIVE LEVEL

A series of low-structure precipitated silica abrasives was prepared and evaluated for RDA at various levels of concentration. Figure 21 shows the effect of silica concentration on its RDA values; silica abrasive can be used at about 25% level in a dentifrice matrix to produce the acceptable RDA values. The RDA values of silica abrasives do not proportionately increase with the abrasive level. This gives the cosmetic chemist tremendous flexibility in formulating an acceptable dentifrice by controlling the level of silica abrasive in the dentifrice formulation.

The RDA of precipitated silica abrasive can be calculated by using eq 5

$$\text{RDA} = -4.17\,(\text{Oil Absorption}) + 5.3\,(\%\ \text{Abrasive Level}) + 640.8 \qquad (5)$$

VI. COSMETIC APPLICATIONS

The synthetic silicas are inert, nontoxic, chemically pure, white powders which are acceptable under the FDA regulations for use in food and cosmetic formulations. Typical properties of synthetic silicas are listed in Table VIII and are discussed below.

A. DRYING-UP LIQUIDS

For many food, cosmetic and pharmaceutical applications it is essential to dry up the active ingredients on an inert, nontoxic carrier. Synthetic silicas are widely used in such applications for drying up liquids into powders. Since the drying-up capacity of silica is related to its structure, a cosmetic chemist should choose a VHS or HS silica for this type of application.

Table VIII
Cosmetic Application of Silicas

PROPERTY	APPLICATION	SILICA STRUCTURE
DRYING-UP LIQUIDS	FOODS, COSMETICS, PHARMACEUTICALS	VHS, HS
ANTI-CAKING	FOODS, COSMETICS, HOUSEHOLD PRODUCTS	VHS, HS
CONDITIONING AGENT	PERSONAL CARE, SPECIALTY	VHS
SUSPENSION	HAIR CARE, DEODORANTS, COSMETICS, LIQUIDS	VHS
THICKENING	TOOTHPASTE, LIQUIDS, SPECIALTY	VHS, MS
TABLETTING AID	PHARMACEUTICALS, COSMETICS	VHS, MS
ABRASIVES AND POLISHING AGENT	TOOTHPASTE	LS, VLS
ADSORBENT	POLYOLS	LS, VLS
VISCOSITY CONTROL	NAIL POLISHES, COSMETICS	VHS
GLOSS REDUCTION	SPECIALTY	VHS, MS

B. ANTI-CAKING

Many cosmetic, food and pharmaceutical preparations tend to cake up in the container or the box in which they are packaged. Due to the fine particle size and very high absorption capacity of VHS or HS silica, these silicas are widely used to make cosmetic and specialty formulations free-flowing.

C. CONDITIONING

Some cosmetic and specialty powder formulations are difficult to flow due to moisture pick-up by one or several ingredients of the formulations. The flow properties and angle of repose of these powder formulations can be improved in such situations by the addition of 1 to 2% by weight of synthetic silica.

D. SUSPENSION AID

In many cosmetic formulations, such as in aerosol and antiperspirant formulations, a very small amount of silica is needed to provide suspension characteristics to the active ingredients of the formulation. A VHS or HS silica of high absorption capacity and surface area is used in this type of application.

E. THICKENING AGENT

The addition of 6 to 16% VHS or HS silicas to dentifrice formulations, aqueous or oil systems, would convert them to gels or pastes. The superior thickening efficiency of a precipitated silica depends upon its structure, particle size, surface area and nature of additives.

F. TABLETTING AID

Precipitated silicas serve as binders, eliminate sticking and act as tabletting aids in pharmaceutical and specialty applications.

G. ABRASIVE AND POLISHING AGENT

Due to mild abrasivity and controlled structure, precipitated silicas are used as mild abrasives and polishing agents in toothpaste formulations. LS and VLS silicas are ideally used because of their low humectant demand and acceptable compatibility features with other toothpaste formula ingredients.

H. ADSORBENT

Controlled-structure precipitated silicas are used to purify polyols and to remove traces of impurities from many liquids and effluents. The choice of proper silica would depend upon the nature and concentration of the impurity present in the liquid.

I. VISCOSITY CONTROL

A relatively small amount of VHS silicas increases the viscosity of creams, lotions, ointments, acne preparations and other specialty products enabling the cosmetic chemist to control the viscosity characteristics of his finished product.

J. GLOSS REDUCTION

Synthetic silicas are widely used as de-lustering agents to reduce the gloss of varnishes, lacquers and other surface coatings.

VII. CONCLUSIONS

We have presented here the structure, chemistry and preparation of controlled-structure precipitated silicas. We have correlated the properties and the end-use applications of silicas to their structure. The variety of cosmetic applications in which synthetic silicas are currently being used is already phenomenal. Further insight into surface chemistry and silica structure is needed to further explore the future cosmetic properties of synthetic silicas.

REFERENCES

(1) CTFA Cosmetic Ingredient Dictionary, Bulletin No. 3 (March 1974), published by the Cosmetic, Toiletry and Fragrance Association, Washington, D.C.
(2) E. Wagner and H. Brunner, *Angew. Chem.*, **72**, 744 (1960).
(3) R. Bode, H. Ferch and H. Fratzscher, *Kaut. Gummi Kunstst.*, **20**, 578 (1967).
(4) R. K. Iler, "The Colloid Chemistry of Silica and Silicates," The Cornell University Press, Ithaca, New York, 1955, Chapter VI.
(5) A. V. Kiselev, "The Structure and Properties of Porous Materials," Butterworths Scientific Publications, London, England, 1958, p 158.
(6) J. A. Hockey and B. A. Pethica, Surface hydration of silicas, *Trans. Faraday Soc.*, **57**, 2247 (1961).
(7) J. A. Hockey, "The Nature of the Silica Surface," Ph.D. Thesis, Manchester University, Manchester, England, 1960.
(8) F. Kindervater, Concerning the structure of silica fillers, *Kaut. Gummi Kunstst.*, **26**, 7 (1973).
(9) J. A. Hockey, The surface properties of the silica powder, *Chem. Ind. (London)*, **January**, 57 (1965).
(10) M. L. Hair, "Infrared Spectroscopy in Surface Chemistry," Marcel Dekker, Inc., New York, New York, 1967, Chapter 4.

(11) J. J. Fripiat, M. C. Gastucke and R. Brichard, Surface heterogeneity in silica gel from kinetics of isotopic exchange OH-OD, *J. Phys. Chem.*, **66**, 805 (1962).

(12) C. G. Armistead, A. H. Typer, F. H. Hambleton, S. A. Mitchell and J. A. Hockey, The surface hydroxylation of silica, *J. Phys. Chem.*, **73**, 3947 (1969).

(13) F. H. Van Cauwelaert, P. A. Jacobs and J. B. Uytterhoeven, Identification of the A-type hydroxyls on silica surfaces, *J. Phys. Chem.*, **76**, 1434 (1972).

(14) (a) S. K. Wason (to J. M. Huber Corp.) U.S. Patent 3893840 (1975).
(b) S. K. Wason (to J. M. Huber Corp.) U.S. Patent 4040858 (1977).
(c) S. K. Wason and R. K. Mays (to J. M. Huber Corp.) U.S. Patent 4067746 (1978).

(15) (a) S. K. Wason (to J. M. Huber Corp.) U.S. Patent 3988162 (1976).
(b) S. K. Wason (to J. M. Huber Corp.) U.S. Patent 4015966 (1977).

(16) Determination of Oil Absorption, *Amer. Soc. Test. Mater. Stand.*, **D**, 281.

(17) S. Brunauer, P. H. Emmett and E. Teller, Adsorption of gases in multimolecular layers, *J. Amer. Chem. Soc.*, **60**, 309 (1938).

(18) Coulter Electronics, Inc., 590 West Twentieth Street, Hialeah, FL 33010.

(19) N. M. Winslow and J. J. Shapiro, An instrument for the measurement of pore size distribution by mercury penetration, A.S.T.M. Bulletin, February 1959, (Aminco Reprint No. 105).

(20) G. K. Stookey and J. C. Muhler, Laboratory studies concerning the enamel and dentin abrasion properties of common dentifrice polishing agents, *J. of Dent. Res.*, **47**, 524 (1968).

(21) P. C. Kitchin and H. B. G. Robinson, How abrasive need a dentifrice be?, *J. of Dent. Res.*, **27**, 501 (1948).

(22) N. J. Dudding, L. O. Dahl and J. C. Muhler, Patient reactions to brushing teeth with water, dentifrice, or salt and soda, *J. Periodontol.*, **31**, 386 (1960).

(23) H. B. McCauley, M. J. Sheehey, D. B. Scott, P. H. Keyes, S. J. Fanale and P. P. Dale, Clinical efficacy of powder and paste dentifrices, *J. Amer. Dent. Ass.*, **33**, 993 (1946).

(24) Council on Dental Therapeutics, Reports of Council and Bureaus: Abrasivity of current dentifrices, *J. Amer. Dent. Ass.*, **81**, 1177 (1970).

(25) P. C. Kitchin, The prevalence of toothroot exposure, and the relation of the extent of such exposure to the degrees of abrasion in different age classes, *J. of Dent. Res.*, **20**, 565 (1941).

(26) R. J. Grabenstetter, R. W. Broze, F. L. Jackson and A. W. Radike, The measurement of the abrasion of human teeth by dentifrice abrasives: a test utilizing radioactive teeth, *J. of Dent. Res.*, **37**, 1060 (1958).

Book Review

CHARACTERIZATION OF POWDER SURFACES, Edited by G. D. Parfitt and K. S. W. Sing, Academic Press Inc., London, England, 1976, x + 464 pages. Price $30.25.

The primary thrust of this excellent book relates to those using powders as pigments and filters in paints, inks, plastics, fibres and equivalent applications. Each of the nine chapters is written by specialists in the areas covered.

The first three are fundamental, surface characterizations—first chemical and then physical, with the trilogy being completed with flow property evaluations. Each of these develops the fundamentals for appropriate evaluation of the cited property. This reviewer found the chapter on flow to be particularly of interest.

The next three are directed to specific pigments—inorganic white, inorganic colored and organic. Each is discussed systematically and, although primarily aimed at the paint and ink industry, these chapters can develop a better comprehension of some of the coated pigments now available for cosmetic use.

The final three chapters cover the specific topics of carbon blacks, silicas and clays. The last two are of special interest, even to those tending to work solely with suspensions and lotions. Unfortunately, the clay chapter is the shortest in the book, only 28 pages.

Each chapter is well referenced and quite current for an edited volume. The index appears to be complete and reasonably detailed. For those actively working in powder technology this should be an excellent addition to their personal libraries. Others with more occasional needs would find this of value in a company or departmental library holding.—JOHN H. WOOD—School of Pharmacy, Virginia Commonwealth University.

Cosmetic Science VOLUME 1

Edited by M. M. BREUER

This and future volumes of *Cosmetic Science* will form a vehicle for authoritative articles reviewing current progress in the field, ranging from the industrial to the theoretical point of view, and drawing upon the expertise of scientists from many different backgrounds and nationalities.

CONTENTS: *G. B. Winter et al.*, Cosmetics and Dental Health. *W. B. Davis*, The Cleaning, Polishing and Abrasion of Teeth by Dental Products. *N. Fukuhara*, Cosmetic Market and Technology in Japan. *E. L. Cussler*, Predicting Skin Feel. *F. Greiter et al.*, Currently Used Sunscreen Materials—Formulation and Testing. *I. D. Rattee*, Colour in Cosmetics. *M. Gloor*, Determination and Analysis of Sebum on Skin and Hairs. *C. Prottery*, The Molecular Basis of Skin Irritation.

1978, 356 pp., $35.25/£18.00 ISBN: 0-12-133001-X

Send payment with order and save postage and handling charges. *Prices subject to change without notice.*

U.S. customers please note: On prepaid orders—payment will be refunded for titles on which shipment is not possible within 120 days.

ACADEMIC PRESS, INC.
A Subsidiary of Harcourt Brace Jovanovich, Publishers
111 FIFTH AVENUE, NEW YORK, N.Y. 10003
24-28 OVAL ROAD, LONDON NW1 7DX

Please send me __copies, Breuer: *Cosmetic Science, Volume 1*

Check enclosed__ Bill me__

NAME____________________
ADDRESS____________________
CITY/STATE/ZIP____________________

New York residents please add sales tax.
Direct all orders to Mr. Paul Negri, Media Dept.
JrnlofSoc.Cosm.Chem/8/78

Please Advise

CHANGE OF ADDRESS

Notify the Society of Cosmetic Chemists, 50 East 41st Street, New York, N.Y. 10017 of your new address promptly to insure continuous receipt of the Journal and other Society news.

Day by Day, Pound by Pound Inventory Control

When we know we've got it, you can be certain you'll have it...when you want it. That's why each morning at Whittaker, Clark & Daniels we run a full computer print-out on our extensive inventory of minerals, colors and chemicals for the cosmetic industry. Whether it's 55 lbs. of Reckitt's ultramarine blue pigments, or a carload of talc, we can pinpoint its location...in a warehouse, on a loading dock or in a freight car. You get all your answers on-the-spot. We deliver!

Serving the Cosmetic and Drug Industries Since 1890.
Bentonites—U.S.P., bacteria-controlled, albagels
Calcium Carbonate—Precipitated, U.S.P.
Calcium Sulfate
Cosmetic Colors—Certified D&C, purified inorganics, custom blends
Kaolins—Colloidal, N.F., bacteria-controlled
Magnesium Products—Magnesium carbonate, magnesium oxide, magnesium hydroxide—Hydro-Magma®
Mica—Water-ground, bacteria-controlled
Stearates—Aluminum, magnesium, calcium, zinc
Talc—Domestic, imported, U.S.P., bacteria-controlled
Titanium Dioxide—C.T.F.A., U.S.P., N.F., bacteria-controlled
Zinc Oxide—U.S.P.

Exclusive worldwide distributors for:
Clark Colors Inc.
Plus custom blending to exacting specifications.
ESTABLISHED 1890

WHITTAKER
ESTABLISHED 1890

WHITTAKER, CLARK & DANIELS, INC.
1000 Coolidge St., South Plainfield, N.J.
07080 · (201) 561-6100 · Telex 138248

WHITTAKER

DELIVERS!

Next to her skin the most bacteria-free beauty aide should be yours.

Now talcs, colors, starches, brushes, vegetable gums, lashes and many other cosmetic ingredients can be safely and inexpensively treated to eliminate contamination worries.

Microbiologically controlled cosmetics are vital. **VACUGAS®** gas sterilization treatment is the answer. It's safe, sure and inexpensive.

Micro-Biotrol Company maintains seven sterilization facilities in key population centers across the country. Our service is fast and convenient. Since Micro-Biotrol pioneered the development of gas sterilization technology, we can answer any and all the questions you may have.

Call or write today for more information.

MICRO-BIOTROL CO.
A DIVISION OF GRIFFITH LABORATORIES
12200 South Central Ave., Alsip, Illinois 60658
(312) 371-0900
UNION, N. J. • UNION CITY, CALIF.
MEMPHIS, TENN. • ATLANTA, GA.
LEVITTOWN, PA. • CHICAGO, ILL.
LOS ANGELES, CALIF.
743-972

INDEX TO ADVERTISERS

Vol. 29 No. 8

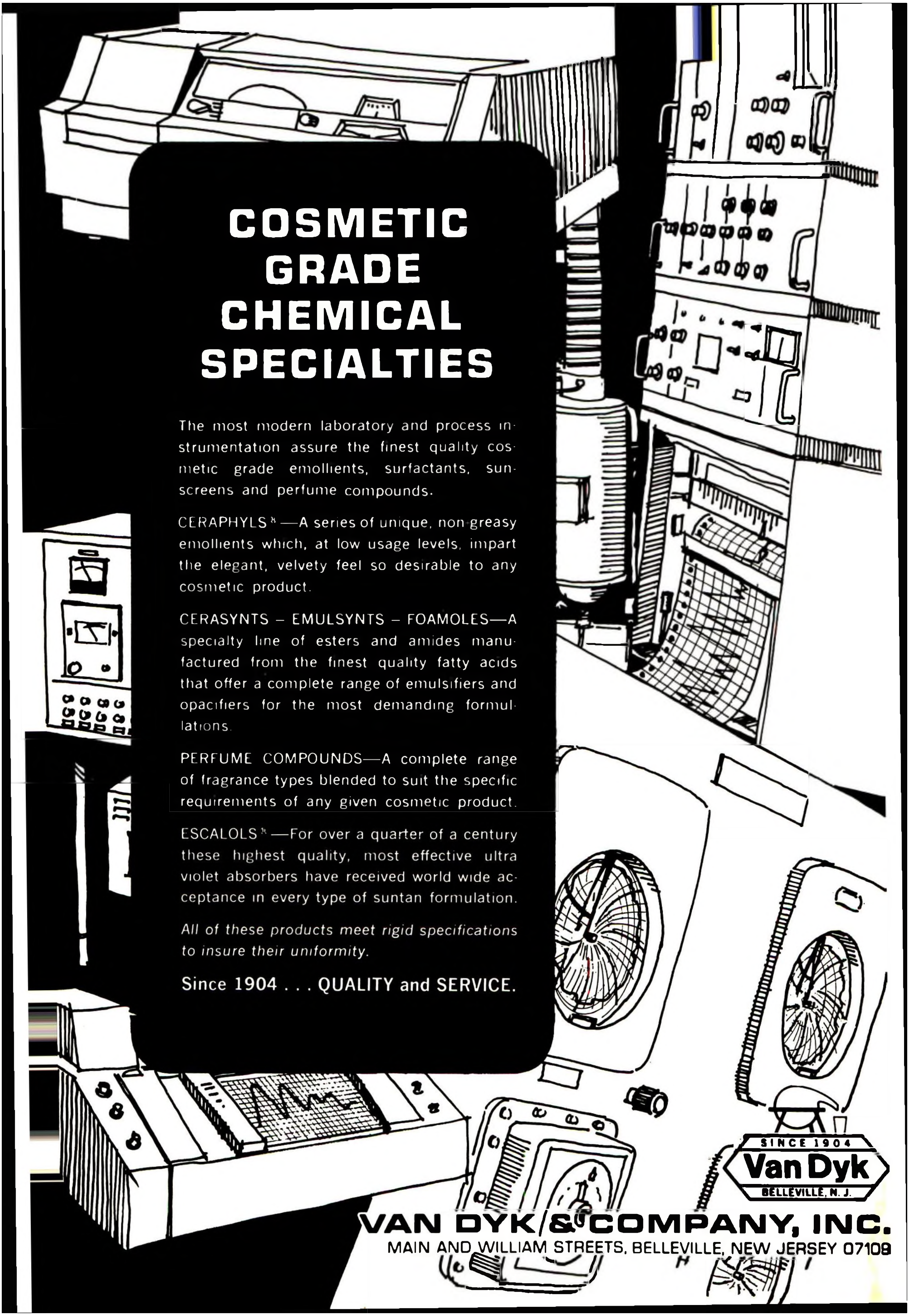

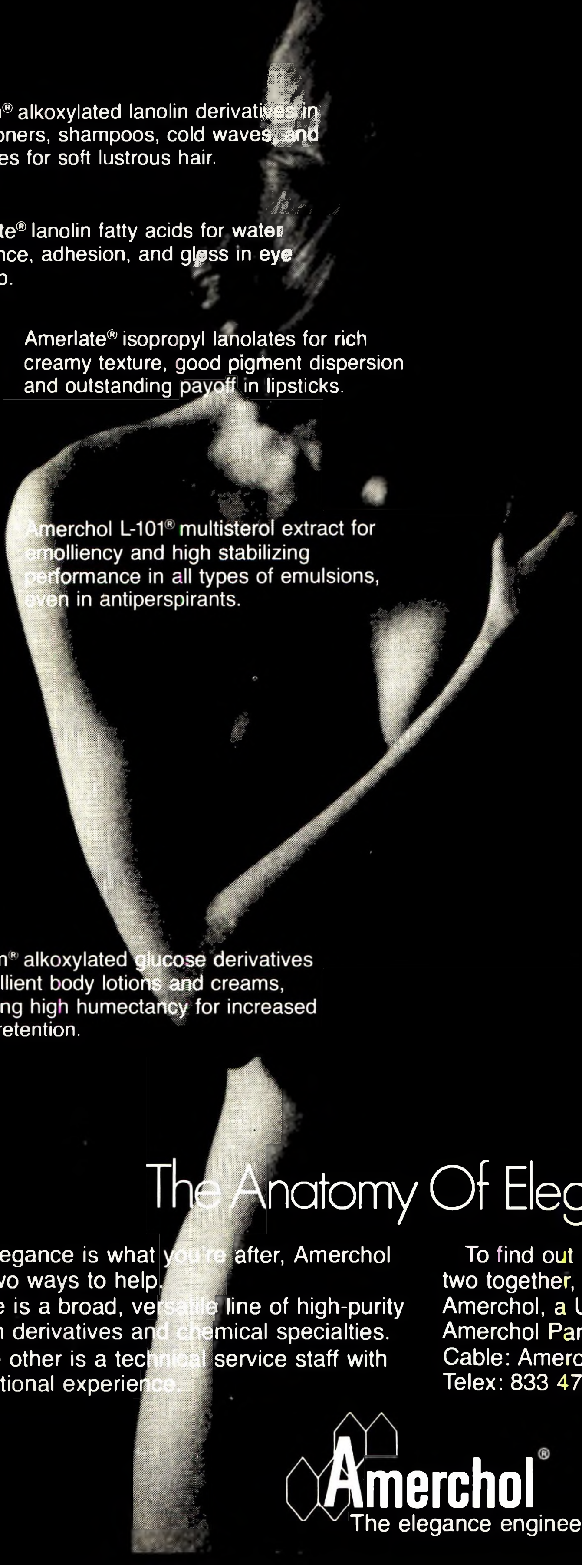

Solulan® alkoxylated lanolin derivatives in conditioners, shampoos, cold waves, and hair dyes for soft lustrous hair.

Amerlate® lanolin fatty acids for water resistance, adhesion, and gloss in eye makeup.

Amerscreen® P u.v. absorber for protecting sensitive facial areas while permitting tanning.

Amerlate® isopropyl lanolates for rich creamy texture, good pigment dispersion and outstanding payoff in lipsticks.

Amerchol L-101® multisterol extract for emolliency and high stabilizing performance in all types of emulsions, even in antiperspirants.

Glucam® alkoxylated glucose derivatives in emollient body lotions and creams, imparting high humectancy for increased water retention.

The Anatomy Of Elegance

If elegance is what you're after, Amerchol has two ways to help.

One is a broad, versatile line of high-purity lanolin derivatives and chemical specialties.

The other is a technical service staff with exceptional experience.

To find out what happens when you put the two together, call (201) 287-1600.

Amerchol, a Unit of CPC International Inc.
Amerchol Park, Edison, New Jersey 08817
Cable: Amerchols.
Telex: 833 472 Amerchol Edin

Amerchol®
The elegance engineers